



CIVIL ENGINEERING STUDIES

Illinois Center for Transportation Series No. 24-011

UILU-ENG-2024-2011

ISSN: 0197-9191

Performance and Design of Continuously Reinforced Concrete Pavements

Prepared By

Apidej Sakulneya

Connor Anderson

Jesus Castro-Perez

Jeffery Roesler, PhD, PE

University of Illinois Urbana-Champaign

Research Report No. FHWA-ICT-24-009

A report of the findings of

ICT PROJECT R27-230

**Performance and Design of Continuously
Reinforced Concrete Pavements**

<https://doi.org/10.36501/0197-9191/24-011>

Illinois Center for Transportation

May 2024

TECHNICAL REPORT DOCUMENTATION PAGE

| | | | | | |
|--|--|---|---|--|-------------------------|
| 1. Report No. FHWA-ICT-24-009 | | 2. Government Accession No. N/A | | 3. Recipient's Catalog No. N/A | |
| 4. Title and Subtitle Performance and Design of Continuously Reinforced Concrete Pavements | | | | 5. Report Date May 2024 | |
| | | | | 6. Performing Organization Code N/A | |
| 7. Authors Apidej Sakulneya, Connor Anderson, Jesus Castro-Perez, Jeffery Roesler (https://orcid.org/0000-0001-6194-269X) | | | | 8. Performing Organization Report No. ICT-24-011 UILU-2024-2011 | |
| 9. Performing Organization Name and Address Illinois Center for Transportation Department of Civil and Environmental Engineering University of Illinois at Urbana-Champaign 205 North Mathews Avenue, MC-250 Urbana, IL 61801 | | | | 10. Work Unit No. N/A | |
| | | | | 11. Contract or Grant No. R27-230 | |
| 12. Sponsoring Agency Name and Address Illinois Department of Transportation (SPR) Bureau of Research 126 East Ash Street Springfield, IL 62704 | | | | 13. Type of Report and Period Covered Final Report 5/16/21–5/31/24 | |
| | | | | 14. Sponsoring Agency Code | |
| 15. Supplementary Notes Conducted in cooperation with the U.S. Department of Transportation, Federal Highway Administration. https://doi.org/10.36501/0197-9191/24-011 | | | | | |
| 16. Abstract This report focuses on the calibration of a design framework for continuously reinforced concrete pavement (CRCP) developed in 2009 by using the most recent performance data acquired from existing CRCP sections in Illinois. Field performance data were used to update the fatigue damage to punchout model coefficients in the design framework. A sensitivity analysis was performed on the updated CRCP design program to determine its sensitivity to traffic levels, shoulder type, and support conditions as well as its magnitude relative to jointed plain concrete pavement design curves. Additionally, the new CRCP design charts were compared to AASHTOWare Pavement ME Design predicted CRCP slab thicknesses for the same inputs. Lastly, AASHTOWare Pavement ME Design was run to predict the performance of CRCP overlays in Illinois and compare the performance data of seven unbonded concrete overlays constructed in Illinois. AASHTOWare Pavement ME Design was then used to generate CRCP overlay thickness design tables for different traffic levels, shoulder types, and support conditions. | | | | | |
| 17. Key Words Continuously Reinforced Concrete Pavement, CRCP Overlays, Punchout, Mechanistic-Empirical Pavement Design, Pavement Performance, AASHTOWare | | | 18. Distribution Statement No restrictions. This document is available through the National Technical Information Service, Springfield, VA 22161. | | |
| 19. Security Classif. (of this report) Unclassified | | 20. Security Classif. (of this page) Unclassified | | 21. No. of Pages 70 + appendices | 22. Price N/A |

ACKNOWLEDGMENT, DISCLAIMER, MANUFACTURERS' NAMES

This publication is based on the results of **ICT-R27-230: Performance and Design of Continuously Reinforced Concrete Pavements (CRCP)**. ICT-R27-230 was conducted in cooperation with the Illinois Center for Transportation; the Illinois Department of Transportation; and the U.S. Department of Transportation, Federal Highway Administration.

Members of the Technical Review Panel (TRP) were the following:

- Charles Wienrank, TRP Chair, Illinois Department of Transportation
- Michael Ayers, Illinois Concrete Pavement Association
- Dennis Bachman, Federal Highway Administration
- Dan Gancarz, Illinois Tollway
- James Krstulovich, Illinois Department of Transportation
- Ojas Patel, Illinois Department of Transportation
- Tim Peters, Illinois Department of Transportation
- LaDonna Rowden, Illinois Department of Transportation
- John Senger, Illinois Department of Transportation
- Heather Shoup, Illinois Department of Transportation
- Filiberto Sotelo, Illinois Department of Transportation

The contents of this report reflect the view of the authors, who are responsible for the facts and the accuracy of the data presented herein. The contents do not necessarily reflect the official views or policies of the Illinois Center for Transportation, the Illinois Department of Transportation, or the Federal Highway Administration. This report does not constitute a standard, specification, or regulation.

EXECUTIVE SUMMARY

The objective of this research project was to update the Illinois Department of Transportation's (IDOT's) current empirical design procedure for continuously reinforced concrete pavements (CRCP) to a mechanistic-empirical design procedure and to develop a mechanistic-empirical design method and design charts for unbonded CRCP overlays of intact or rubblized existing concrete pavement. The phases of this project were divided into five separate tasks. The first task was reviewing past research studies by agencies using CRCP, such as Illinois, Texas, California, and Belgium. Of particular importance were performance studies on new CRCP and CRCP overlays that quantified punchouts, crack spacing and widths, and other design features of the pavement such as the support layers and active crack control.

The second task gathered performance data from current CRCP sections in Illinois through the Illinois Roadway Analysis Database System (IROADS). The CRCP data collected included design life, age, cumulative traffic, pavement cross-section details, crack spacing, and the number of punchouts per mile for each CRCP contract. The performance of the 28 CRCP sections reviewed and assessed were used to update the CRCP design framework originally developed in 2009.

This study verified the proposed Excel-based CRCP design framework against the original CRCP version from 2009. After the re-calibration of the 2009 CRCP design framework was performed, a sensitivity analysis was completed that compared the updated framework's predictions with the jointed plain concrete pavement (JPCP) design charts from Chapter 54 of Illinois Department of Transportation's *Bureau of Design and Environment Manual*. The re-calibrated CRCP design framework was then compared to AASHTOWare Pavement ME Design slab thicknesses for the same set of inputs and was found to deviate at lower and higher traffic levels. AASHTOWare design CRCP thicknesses were thinner at lower traffic levels and thicker at higher equivalent single axle load (ESAL) counts relative to the proposed CRCP framework.

The AASHTOWare Pavement ME Design was then compared with the performance of seven CRCP overlay sections in Illinois where section details, traffic, and materials were known. The comparison of the AASHTOWare Pavement ME Design with the Illinois performance data for CRCP overlays demonstrated that AASHTOWare Pavement ME Design would provide reasonable slab thicknesses and punchout prediction to Illinois conditions and inputs. The research further developed CRCP overlay design tables, accommodating traffic levels from 10 to 300 million ESALs, three distinct shoulder types, and varying conditions of existing pavement.

TABLE OF CONTENTS

| | |
|---|-----------|
| CHAPTER 1: INTRODUCTION | 1 |
| RESEARCH OBJECTIVE AND SCOPE | 1 |
| CHAPTER 2: BACKGROUND REVIEW OF RECENT CRCP FINDINGS | 2 |
| OVERVIEW OF CRCP DESIGN FEATURES AND CRITERIA..... | 2 |
| CRACKING PATTERNS AND DISTRESSES ON CRCP | 3 |
| Punchouts | 3 |
| Transverse Crack Spalling..... | 4 |
| Y-Cracking..... | 4 |
| Cluster Cracking | 4 |
| Horizontal Cracking..... | 4 |
| Active Crack Control Developments | 5 |
| RECENT CRCP PERFORMANCE STUDIES | 6 |
| Texas Performance Results..... | 6 |
| California Performance Study..... | 7 |
| Oregon Performance Study | 10 |
| Illinois Performance Studies | 11 |
| Belgium Performance Study | 15 |
| CHAPTER 3: CRCP AND CRCP OVERLAY PERFORMANCE DATA FROM ILLINOIS | 17 |
| IMAGE AND VIDEO ASSESSMENT DIFFICULTIES..... | 21 |
| CHAPTER 4: NEW CRCP DESIGN—PUNCHOUT PERFORMANCE MODEL UPDATE..... | 23 |
| REVIEW OF EXISTING CRCP DESIGN SOFTWARE | 23 |
| CRCP Design Framework Sensitivity Analysis | 25 |
| CONCRETE FATIGUE EQUATIONS | 27 |
| Recalibration of Punchout-to-Damage Model..... | 31 |
| Updated CRCP Punchout Prediction Model..... | 33 |
| CHAPTER 5: UPDATED CRCP DESIGN CHARTS FOR ILLINOIS | 38 |
| CRCP DESIGN COMPARISON OF UIUC’S UPDATED CRCP DESIGN FRAMEWORK VS. AASHTOWARE PAVEMENT ME DESIGN | 45 |

| | |
|--|-----------|
| CHAPTER 6: DEVELOPMENT OF CRCP OVERLAY DESIGN PROCESS FOR ILLINOIS..... | 53 |
| CRCP OVERLAY DESIGN TABLES | 60 |
| 20-Year Overlays on Existing CRCP/JPCP/JRCP | 60 |
| 30-Year Overlays on Existing CRCP/JPCP/JRCP | 60 |
| 20-Year Overlay on Rubblized CRCP/JPCP/JRCP | 61 |
| 30-Year Overlay on Rubblized CRCP/JPCP/JRCP | 62 |
| CHAPTER 7: SUMMARY AND CONCLUSION | 66 |
| REFERENCES..... | 68 |
| APPENDIX A: CRCP AND CRCP OVERLAY PERFORMANCE DATA FROM ILLINOIS | 71 |
| AVERAGE DAILY TRAFFIC TO ESALS CALCULATIONS..... | 71 |
| APPENDIX B: CRCP DESIGN FRAMEWORK SENSITIVITY ANALYSIS | 75 |
| CRCP SENSITIVITY ANALYSIS | 75 |
| 20 Year, 0.7% Steel..... | 75 |
| 30 Year, 0.8% Steel..... | 76 |
| APPENDIX C: CONCRETE FATIGUE EQUATIONS | 78 |
| JPCP SENSITIVITY ANALYSIS..... | 78 |
| APPENDIX D: UPDATED CRCP DESIGN CHARTS FOR ILLINOIS | 85 |
| APPENDIX E: CRCP PAVEMENT ME DESIGN COMPARISONS..... | 91 |
| AADTT TO ESAL CORRELATION 20-YEAR TRAFFIC | 91 |
| AADTT TO ESAL CORRELATION 30-YEAR TRAFFIC | 92 |

LIST OF FIGURES

| | |
|--|----|
| Figure 1. Schematic. Types of normal and undesirable cracks and distresses on CRCP. | 3 |
| Figure 2. Schematic. CRCP punchout mechanism. | 4 |
| Figure 3. Photo. Active crack control saw cut notch. | 5 |
| Figure 4. Map. Location and construction year of CRCP projects assessed. | 7 |
| Figure 5. Graph. Transverse crack spacing on Illinois Tollway CRCP test sections. | 13 |
| Figure 6. Graph. Transverse crack width on Illinois Tollway CRCP test sections. | 14 |
| Figure 7. Graph. Percentage of saw cuts with cracks propagating from the saw cut notch in section 3. | 14 |
| Figure 8. Graph. Occurrences of undesirable cracks normalized per 1,000 ft. | 15 |
| Figure 9. Equation. Traffic factor equation used to calculate ESALs. | 17 |
| Figure 10. Image. IROADS image of transverse cracks in right driving lane with light pole, pavement stripes, shoulder grooves, and pavement width as reference distances. | 21 |
| Figure 11. Image. IROADS image of highlighted transverse cracks in right driving lane with light pole, pavement stripes, and shoulder grooves. | 22 |
| Figure 12. Graph. Power function punchout model prediction. | 24 |
| Figure 13. Graph. S-Curve punchout model prediction. | 24 |
| Figure 14. Graph. Power function punchout model prediction, updated Excel. | 25 |
| Figure 15. Graph. S-Curve punchout model prediction, updated Excel. | 25 |
| Figure 16. Graph. CRCP thickness sensitivity to CRCP steel contents and subgrade conditions. | 26 |
| Figure 17. Graph. CRCP slab thickness sensitivity to K-value and shoulder type. | 27 |
| Figure 18. Equation. Zero-maintenance fatigue equations. | 28 |
| Figure 19. Equation. MEPDG (AASHTO Pavement ME) fatigue equations. | 28 |
| Figure 20. Equation. ACPA fatigue equations. | 28 |
| Figure 21. Graph. Comparison of CRCP and IDOT JPCP slab thicknesses for tied concrete shoulder. ... | 30 |
| Figure 22. Graph. CRCP vs IDOT JPCP thicknesses with asphalt shoulders and poor and granular subgrade. | 30 |
| Figure 23. Graph. JPCP tied and untied shoulders on poor and granular subgrade support conditions (poor: K-value = 50 psi/in.; granular: K-value = 200 psi/in.). | 31 |
| Figure 24. Equation. S-Curve punchout prediction model. | 31 |
| Figure 25. Equation. Slab stress ratio equation for top and bottom tensile stresses. | 32 |

Figure 26. Equation. Cumulative fatigue damage calculation..... 33

Figure 27. Graph. 2009 S-curve punchout-to-damage model..... 34

Figure 28. Graph. Accumulated damage versus observed punchout for the 2009 calibration. 34

Figure 29. Graph. Current S-Curve punchout-to-damage model..... 35

Figure 30. Graph. Accumulated damage versus observed punchout from current recalibration. 35

Figure 31. Equation. Punchout equation used in MEPDG..... 36

Figure 32. Graph. Relationship between accumulated damage and punchouts from *Guide for Mechanistic Empirical Design of New and Rehabilitated Pavement Structures*. 36

Figure 33. Graph. Predicted vs observed punchouts for nationwide CRCP calibration database ($R^2= 68\%$).
..... 37

Figure 34. Graph. CRCP slab thickness at 95% reliability, K-value = 50 psi/in., and three shoulder types for a 20-year design. 42

Figure 35. Graph. CRCP slab thickness at 95% reliability, K-value = 100 psi/in., and three shoulder types for a 20-year design. 42

Figure 36. Graph. CRCP slab thickness at 95% reliability, K-value = 200 psi/in., and three shoulder types for a 20-year design. 43

Figure 37. Graph. CRCP slab thickness at 95% reliability, K-value = 50 psi/in., and three shoulder types for a 30-year design..... 43

Figure 38. Graph. CRCP slab thickness at 95% reliability, K-value = 100 psi/in., and three shoulder types for a 30-year design. 44

Figure 39. Graph. CRCP slab thickness at 95% reliability, K-value = 200 psi/in., and three shoulder types for a 30-year design. 44

Figure 40. Graph. Comparison of CRCP thickness between proposed CRCP design framework and AASHTOWare Pavement ME Design (20-year design, K = 50 psi/in., asphalt shoulder). 50

Figure 41. Graph. Comparison of CRCP thickness between proposed CRCP design framework and AASHTOWare Pavement ME Design (20-year design, K = 100 psi/in., asphalt shoulder). 50

Figure 42. Graph. Comparison of CRCP thickness between proposed CRCP design framework and AASHTOWare Pavement ME Design (20-year design, K = 200 psi/in., asphalt shoulder). 50

Figure 43. Graph. Comparison of CRCP thickness between proposed CRCP design framework and AASHTOWare Pavement ME Design (20-year design, K = 50 psi/in., PCC tied separate shoulder)..... 51

Figure 44. Graph. Comparison of CRCP thickness between proposed CRCP design framework and AASHTOWare Pavement ME Design (20-year design, K = 100 psi/in., PCC tied separate shoulder)..... 51

Figure 45. Graph. Comparison of CRCP thickness between proposed CRCP design framework and AASHTOWare Pavement ME Design (20-year design, K = 200 psi/in., PCC tied separate shoulder)..... 51

Figure 46. Graph. Comparison of CRCP thickness between proposed CRCP design framework and AASHTOWare Pavement ME Design (20-year design, K = 50 psi/in., PCC tied monolithic shoulder). .. 52

Figure 47. Graph. Comparison of CRCP thickness between proposed CRCP design framework and AASHTOWare Pavement ME Design (20-year design, K = 100 psi/in., PCC tied monolithic shoulder). 52

Figure 48. Graph. Comparison of CRCP thickness between proposed CRCP design framework and AASHTOWare Pavement ME Design (20-year design, K = 200 psi/in., PCC tied monolithic shoulder). 52

Figure 49. Equation. AASHTOWare fatigue model. 53

Figure 50. Equation. AASHTOWare punchout model. 53

Figure 51. Graph. Comparison of CRCP overlay thickness on intact concrete pavement provided by AASHTOWare Pavement ME Design. 63

Figure 52. Graph. Comparison of CRCP overlay thickness on rubblized concrete pavement provided by AASHTOWare Pavement ME Design. 63

Figure 53. Graph. Comparison of CRCP overlay thickness on intact concrete pavement and rubblized concrete pavement with asphalt shoulder. 64

Figure 54. Graph. Comparison of CRCP overlay thickness on intact concrete pavement and rubblized concrete pavement with PCC separate shoulder. 64

Figure 55. Graph. Comparison of CRCP overlay thickness on intact concrete pavement and rubblized concrete pavement with PCC monolithic shoulder. 65

Figure 56. Equation. Traffic factor equations. 74

Figure 57. Graph. Chart for JPCP slab thickness given granular subgrade (K-value= 200 psi/in.). 79

Figure 58. Graph. Chart for JPCP slab thickness given poor subgrade (K-value = 50 psi/in.)..... 79

Figure 59. Graph. Sensitivity analysis of JPCP slab thickness. 80

Figure 60. Graph. CRCP vs JPCP slab thickness with tied concrete shoulder. 80

Figure 61. Graph. CRCP vs JPCP slab thickness with asphalt shoulder. 81

Figure 62. Graph. CRCP vs JPCP slab thickness on granular support with tied shoulder (k-value = 200 psi/in.)..... 81

Figure 63. Graph. CRCP vs JPCP slab thickness on poor support with tied shoulder (k-value = 50 psi/in.)..... 82

Figure 64. Graph. CRCP vs JPCP slab thickness on granular support with asphalt shoulder (k-value = 200 psi/in.)..... 82

Figure 65. Graph. CRCP vs JPCP slab thickness on poor support with asphalt shoulder (k-value = 50 psi/in.)..... 83

Figure 66. Graph. CRCP sensitivity at 0.8% steel content. 83

Figure 67. Graph. CRCP sensitivity at 0.7% steel content. 84

Figure 68. Graph. AADTT vs ESAL correlation, $y = 7,538.2x+1,275.1$ 91

Figure 69. Graph. AADTT vs ESAL correlation 30-year, $y = 12,627x-210.76$ 92

LIST OF TABLES

| | |
|---|----|
| Table 1. Assessing Concrete Core Material Properties from Texas CRCP Sections..... | 7 |
| Table 2. Comparison of California and FHWA CRCP Design Factors | 9 |
| Table 3. Comparison of Concrete and Construction Requirements for CRCP..... | 9 |
| Table 4. Summary of CRCP Projects with Design Features in California | 10 |
| Table 5. Summary of CRCP Cracking Patterns and Distresses in California | 10 |
| Table 6. Performance Data for Unbonded CRCP Overlays in Oregon | 11 |
| Table 7. Performance of CRCP Overlays in Illinois..... | 12 |
| Table 8. Illinois Tollway Route 390 CRCP Sections | 12 |
| Table 9. Percentage of Cracks Initiated at Notches from Belgium CRCP Study | 16 |
| Table 10. CRCP Overlay Data from IDOT | 18 |
| Table 11. CRCP Section Details in Illinois..... | 19 |
| Table 12. CRCP Section Performance Data in Illinois | 20 |
| Table 13. Sample Inputs for Design Input | 23 |
| Table 14. Inputs for 20- and 30-Year CRCP Design Charts for Updated CRCP Design Framework | 39 |
| Table 15. 20-Year CRCP Design Thicknesses for Updated CRCP Design Framework | 40 |
| Table 16. 30-Year CRCP Design Thicknesses for Updated CRCP Design Framework | 41 |
| Table 17. Layer Inputs for AASHTOWare for Composite K = 200 psi/in..... | 46 |
| Table 18. Layer Inputs for AASHTOWare for Composite K = 100 psi/in..... | 46 |
| Table 19. Layer Inputs for AASHTOWare for Composite K = 50 psi/in..... | 46 |
| Table 20. Comparison of 20- and 30-Year AADTT versus ESALs for AASHTO Traffic Input..... | 46 |
| Table 21. AASHTO Pavement ME Inputs for 20-Year CRCP Designs | 47 |
| Table 22. AASHTO Pavement ME Inputs for 30-Year CRCP Designs | 47 |
| Table 23. AASHTOWare Pavement ME Design versus Proposed CRCP Design Thickness Comparisons for Tied Shoulder and 20-Year Design Life | 48 |
| Table 24. AASHTOWare Pavement ME Design versus Proposed CRCP Design Thickness Comparisons for Tied Shoulder and 30-Year Design Life | 49 |
| Table 25. Values of Coefficients in AASHTOWare Pavement ME Punchout Models | 54 |
| Table 26. Unbonded Concrete Overlays (JPCP and CRCP) in Illinois | 55 |
| Table 27. Unbonded Concrete Overlays Traffic Data in Illinois..... | 55 |

| | |
|---|----|
| Table 28. Summary of Unbonded CRCP Overlays in Illinois | 56 |
| Table 29. AASHTOWare Predicted Unbonded CRCP Overlay Thickness in Illinois..... | 57 |
| Table 30. AASHTO Pavement ME Inputs for Unbonded CRCP Overlays in Illinois | 58 |
| Table 31. Unbonded CRCP Overlay Inputs (Existing PCC Rubbilized) for AASHTOWare in Illinois | 59 |
| Table 32. Slab Thickness for 20-Year Unbonded CRCP Overlays on Existing PCC with Asphalt Shoulder | 60 |
| Table 33. Slab Thickness for 20-Year Unbonded CRCP Overlays on Existing PCC with PCC Tied Separate Concrete Shoulder | 60 |
| Table 34. Slab Thickness for 20-Year Unbonded CRCP Overlays on Existing PCC with Monolithic Tied Concrete Shoulder | 60 |
| Table 35. Slab Thickness for 30-Year Unbonded CRCP Overlays on Existing PCC with Asphalt Shoulder | 60 |
| Table 36. Slab Thickness for 30-Year Unbonded CRCP Overlays on Existing PCC with PCC Tied Separate Concrete Shoulder..... | 61 |
| Table 37. Slab Thickness for 30-Year Unbonded CRCP Overlays on Existing PCC with Monolithic Tied Concrete Shoulder | 61 |
| Table 38. Slab Thickness for 20-Year Unbonded CRCP Overlays on Rubblized PCC with Asphalt Shoulder..... | 61 |
| Table 39. Slab Thickness for 20-Year Unbonded CRCP Overlays on Rubbilized PCC with PCC Tied Separate Concrete Shoulder..... | 61 |
| Table 40. Slab Thickness for 20-Year Unbonded CRCP Overlays on Rubbilized PCC with Monolithic Tied Concrete Shoulder | 62 |
| Table 41. Slab Thickness for 30-Year Unbonded CRCP Overlays on Rubblized PCC with Asphalt Shoulder..... | 62 |
| Table 42. Slab Thickness for 30-Year Unbonded CRCP Overlays on Rubblized PCC with PCC Tied Separate Concrete Shoulder..... | 62 |
| Table 43. Slab Thickness for 30-Year Unbonded CRCP Overlays on Rubblized PCC with Monolithic Tied Concrete Shoulder | 62 |
| Table 44. ESALs Calculated Based on AADT..... | 71 |
| Table 45. CRCP Section Details in Illinois..... | 72 |
| Table 46. CRCP Section Performance Data in Illinois | 73 |
| Table 47. Percent of Traffic in Design Lane | 74 |
| Table 48. Inputs for Sensitivity Analysis | 75 |

| | |
|---|----|
| Table 49. Inputs for Sensitivity Analysis | 76 |
| Table 50. JPCP Sensitivity 20 Year Analysis Inputs and Thicknesses-Tied Shoulders, K value = 50 psi/in. | 78 |
| Table 51. JPCP Sensitivity 20 Year Analysis Inputs and Thicknesses-Untied Shoulders, K value = 50 psi/in. | 78 |
| Table 52. JPCP Sensitivity 20 Year Analysis Inputs and Thicknesses-Tied Shoulders, K value = 200 psi/in. | 78 |
| Table 53. JPCP Sensitivity 20 Year Analysis Inputs and Thicknesses-Untied Shoulders, K value = 200 psi/in. | 78 |
| Table 54. Thickness Difference between 2009 and Proposed Framework, 20 Years, Asphalt Shoulder | 85 |
| Table 55. Thickness Difference between 2009 and Proposed Framework, 20 Years, PCC Tied Separate Shoulder..... | 86 |
| Table 56. Thickness Difference between 2009 and Proposed Framework, 20 Years, Monolithic Shoulder..... | 87 |
| Table 57. Thickness Difference between 2009 and Proposed Framework, 30 Years, Asphalt Shoulder | 88 |
| Table 58. Thickness Difference between 2009 and Proposed Framework, 30 Years, Tied PCC Separate Shoulder..... | 89 |
| Table 59. Thickness Difference between 2009 and Proposed Framework, 30 Years, Monolithic Shoulder | 90 |
| Table 60. AADTT and ESALs Correlation for 20-Year Traffic Using TTFC1 Distribution..... | 91 |
| Table 61. AADTT and ESALs Correlation for 30-Year Traffic Using TTFC1 Distribution..... | 92 |
| Table 62. Comparison of CRCP Slab Thickness between Proposed CRCP Design Framework and AASHTOWare Pavement ME Design, 20-year Asphalt Shoulder..... | 93 |
| Table 63. Comparison of CRCP Slab Thickness between Proposed CRCP Design Framework and AASHTOWare Pavement ME Design, 30-year Asphalt Shoulder..... | 93 |
| Table 64. Comparison of CRCP Slab Thickness between Proposed CRCP Design Framework and AASHTOWare Pavement ME Design, 20-year Tied Separate Shoulder | 94 |
| Table 65. Comparison of CRCP Slab Thickness between Proposed CRCP Design Framework and AASHTOWare Pavement ME Design, 30-year Tied Separate Shoulder | 94 |
| Table 66. Comparison of CRCP Slab Thickness between Proposed CRCP Design Framework and AASHTOWare Pavement ME Design, 20-year Monolithic Shoulder | 95 |
| Table 67. Comparison of CRCP Slab Thickness between Proposed CRCP Design Framework and AASHTOWare Pavement ME Design, 30-year Monolithic Shoulder | 95 |

CHAPTER 1: INTRODUCTION

Illinois has been a leader in the design and construction of continuously reinforced concrete pavement (CRCP) for more than 50 years. The current design procedure for CRCP followed by the Illinois Department of Transportation (IDOT) is empirical and based on a modified AASHTO nomograph for jointed reinforced concrete pavement (JRCP). Although IDOT has been successfully designing and constructing CRCP on high-traffic-volume roadways, these designs extend well beyond the maximum traffic factors intended in the existing design charts to determine the required pavement thickness. The CRCP thickness design procedure needs updating given the advances in mechanistic-empirical (ME) design for CRCP, including a larger CRCP field performance database.

The state of Illinois began regularly constructing CRCP in the 1960s. Current traffic volumes in Illinois are significantly larger than the values expected when the existing CRCP design method for IDOT was developed, exceeding the current maximum traffic factor of 100 in the rigid pavement design charts in Chapter 54 of IDOT's *Bureau of Design and Environment Manual (BDE Manual)* (IDOT, 2023). Updating and extending the IDOT ME design procedure for CRCP will lead to more accurate and economical designs of new CRCP and CRCP overlays for critical roadways in Illinois.

In 2009, Beyer and Roesler developed a CRCP design framework for a new CRCP design procedure based on findings from the NCHRP 1-37 study (ARA, 2003) and a refined set of Illinois CRCP performance data. This new CRCP design framework has yet to be implemented into the current design practices in Chapter 54 of IDOT's *BDE Manual* (2023). Additionally, IDOT does not have a CRCP overlay method in Chapter 54, which currently recommends designing a new CRCP and subtracting 1 inch for the final thickness of the CRCP overlay. Given IDOT's application of multiple unbonded CRCP overlays, a rational ME CRCP overlay procedure is necessary (Heckel & Wienrank, 2018) and should be included in the BDE manual.

RESEARCH OBJECTIVE AND SCOPE

The objective of this research project is to update IDOT's thickness design procedure for new CRCP and to add a procedure for CRCP overlays of existing concrete pavements. Both the new CRCP and CRCP overlay design methods should be based on ME design principles. To achieve this objective, a performance review of existing CRCP, CRCP overlays, and extended-life (≥ 30 -year design life) CRCP constructed in Illinois and several key states was undertaken. The performance data were necessary for final design calibration of the punchout performance models for new CRCP and CRCP overlays. An ME CRCP design framework already exists from previous IDOT-sponsored research (Beyer & Roesler, 2009) but needs to be updated and calibrated. Additionally, the AASHTOWare Pavement ME method for new CRCP and CRCP overlays was also evaluated for design comparisons and potential implementation, respectively. The final design models for new CRCP and CRCP overlays will be implemented into Chapter 54 of the *BDE Manual* (IDOT, 2023).

CHAPTER 2: BACKGROUND REVIEW OF RECENT CRCP FINDINGS

To assist with updating the existing mechanistic-empirical CRCP framework and CRCP overlay design method, a literature review was performed on recent CRCP findings (e.g., the past 10 years of research findings that would not have been included in the 2009 Beyer and Roesler report). The literature review provided background information on the design criteria and features for CRCP, failure modes and criteria of CRCP, and additional background on CRCP designs from the state of Illinois, other locations within the United States, and internationally.

OVERVIEW OF CRCP DESIGN FEATURES AND CRITERIA

The primary design features of CRCP are the slab thickness, steel content and bar diameter, base layer type and thickness, lane width (e.g., widened lane), and shoulder type (asphalt or tied concrete). Other important concrete material input parameters that affect the CRCP design are the flexural strength, drying shrinkage, and the coefficient of thermal expansion. The primary design and material features are under the control of the pavement design engineer. A more detailed discussion of CRCP design features can be found in the *CRCP Manual: Guidelines for Design, Construction, Maintenance, and Rehabilitation* by Roesler et al. (2016).

The content of continuous steel reinforcement controls the magnitude of crack spacing and crack width for the regularly occurring transverse cracks in CRCP. The reinforcement steel ratio is typically between 0.55 to 0.85, with recent Illinois values ranging from 0.70 to 0.80. Transverse cracks result from internal tensile stresses developing over time under combined CRCP contraction from temperature drops and drying shrinkage as well as steel reinforcement restraint. The quantity of reinforcing steel influences the distances between these cracks and the width of the cracks. The desired spacing for transverse cracks in CRCP is between 2 to 8 ft (Plei & Tayabji, 2012) with typically recommended average spacing of 3 to 4 ft. A recent CRCP study performed in Belgium reported that multiple transverse cracks closer than 2 ft can lead to punchouts (Ren et al., 2014a). To maintain a high load transfer efficiency (LTE) across adjacent CRCP panels and control water or incompressible material from penetrating the pavement structure, crack widths less than 0.02 in. are desirable. Creating a uniform cracking pattern, e.g., active crack control (Kohler & Roesler, 2004; Ren et al., 2014b; Dahal & Roesler, 2021), with small crack width will also increase the performance reliability at a given slab thickness and steel content.

Punchouts are the main structural failure of CRCP and the key failure parameter predicted by mechanistic-empirical CRCP models. A punchout is a block or wedge that is defined by two consecutive transverse cracks, a longitudinal crack, and the pavement edge or longitudinal joint. Undesirable transverse cracking patterns (e.g., a cluster crack or excessively short crack spacing) or high transverse crack width increase the probability of punchout formation under repeated loading. The longitudinal crack formation typically occurs 2 to 5 ft from the edge of the pavement. Punchouts are typically accompanied by loss of support from the support layers (base, subbase, or subgrade) and reduced LTE from transverse crack widening and repeated loading. In 2013, a long-life CRCP performance study determined that as the steel percentage increased from 0.50% to 0.70%, the number of failures per kilometer reduced from 75 punchouts per kilometers to less than 20

punchouts per kilometer when the reinforcement ratio was greater than 0.70 (Darter & Rao, 2015). In general, the number of punchouts per mile at the end of the CRCP design life is typically recommended to be ≤ 10 punchouts per mile.

The typical range of CRCP slab thicknesses are 7 to 13 in. (178 to 330 mm). The thickness design of CRCP is based on fatigue loading from expected truck traffic and load levels. The induced tensile stress must be maintained below a certain percentage of the concrete flexural strength based on the truck traffic volume, local materials, and environmental conditions. The design features, such as slab thickness, base type, shoulder type (asphalt, tied concrete, or widened lane), and longitudinal steel content, are adjusted to meet the expected traffic and concrete fatigue.

CRACKING PATTERNS AND DISTRESSES ON CRCP

Several cracking patterns and distresses are present in CRCP and must be distinguished when collecting performance data for CRCP design model calibration. Multiple researchers and performance studies have reported undesirable cracking patterns on CRCP, which can lead to a variety of premature distresses (Tayabji et al., 1998a; Tayabji et al., 1998b; Kohler & Roesler, 2004; Dahal & Roesler, 2021; Stempihar et al., 2020; Won et al., 2008). Figure 1 illustrates the common cracking pattern (normal) and undesirable cracking patterns and distresses found on CRCP.

Undesirable cracking patterns can lead to premature punchout development, which typically are not part of a design method’s original intent for punchout prediction.

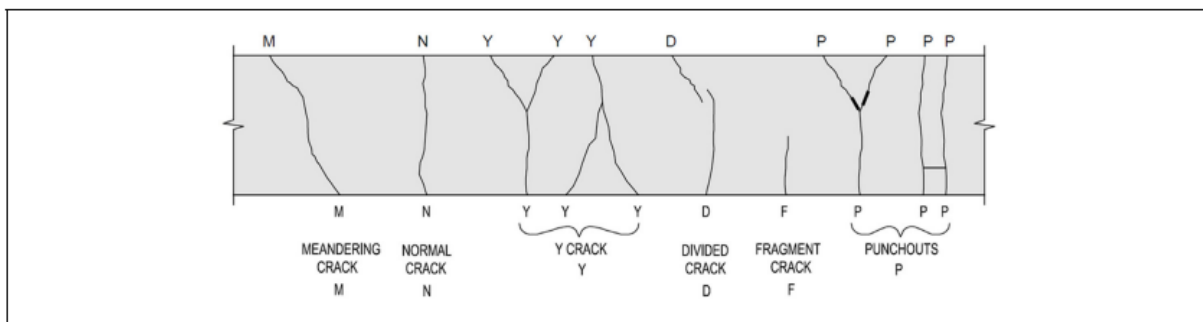


Figure 1. Schematic. Types of normal and undesirable cracks and distresses on CRCP.

Source: Stempihar et al. (2020)

Punchouts

Punchout distress results from repeated loading between two closely spaced transverse cracks. The punchout can be near the outside or inside edge. Figure 2 presents the formation of a punchout near the outside edge of the slab, which is the most common location (Beyer & Roesler, 2009). For this example, the longitudinal crack initiates at the top of the slab when the tensile capacity of the concrete was exceeded because of repeated loading, support layer erosion, and loss of LTE across the transverse crack. A punchout can also initiate near the inside of the lane at the bottom of the slab.

Transverse Crack Spalling

Spalling of transverse cracks can occur for multiple reasons. Multiple studies in Texas have linked severe near-surface spalling on CRCP to bond failure between the coarse aggregate and the cement paste as well as the magnitude of the concrete's coefficients of thermal expansion (Choi et al., 2020).

Y-Cracking

Y-shaped cracks form when a single transverse crack bifurcates into two cracks or when two transverse cracks merge at a point, as demonstrated in Figure 1. A Y-crack with additional branches is referred to as a complex Y-crack (Dahal & Roesler, 2021).

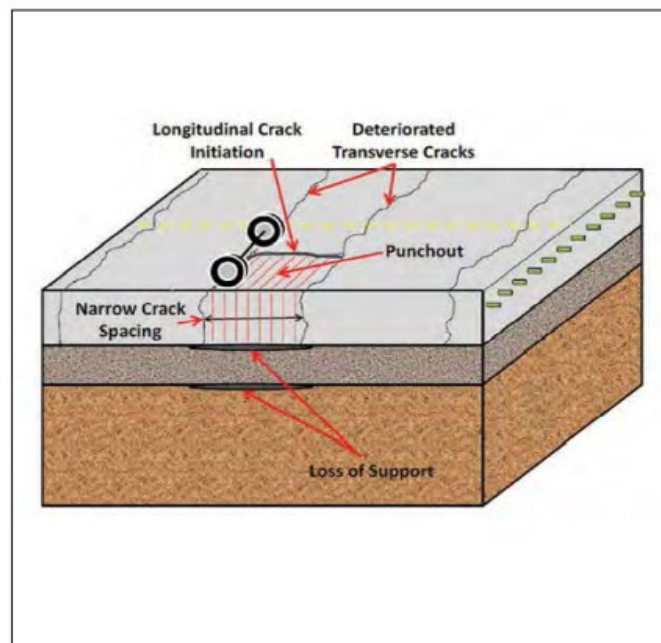


Figure 2. Schematic. CRCP punchout mechanism.

Source: *Beyer & Roesler (2009)*

Cluster Cracking

Cluster cracking is defined as groups of closely spaced transverse cracks having an average spacing (of five consecutive cracks) less than 1 ft (Stempihar et al., 2020). At cluster crack locations, the longitudinal distance between the cracks is much shorter than the lane width, which can lead to high transverse flexural stresses under loading and the potential for premature punchout distress (Dahal & Roesler, 2021; Rens et al., 2014b).

Horizontal Cracking

Horizontal cracking has been recently reported on CRCP (Rens et al., 2014b) with cracks running parallel to the surface at the depth of the longitudinal reinforcing steel. The exact cause of horizontal cracking is still not agreed upon, but researchers have suggested several causes, including poor bonding between the concrete and longitudinal reinforcing steel, differences in shrinkage and the

concrete coefficient of thermal expansion, and the initial transverse crack propagation from the surface to the steel turning horizontal. Studies have also suggested that it is related to CRCP sections containing asphalt interlayers between the CRCP surface and cement-treated base layer. The high degree of bonding to the asphalt interlayer appears to cause some transverse cracks to propagate full depth and to turn horizontally, while other transverse cracks on the surface are only partial depth. (Rens et al., 2014c; Kim & Won, 2004). One study noted at least one transverse crack from a cluster crack propagated to the steel, and this is where the horizontal cracking initiated (Rens et al., 2014c).

Active Crack Control Developments

CRCP produces transverse cracks because of steel restraint and base friction as the concrete material contracts from temperature drop and moisture loss. Transverse crack development can be erratic and nonuniform and lead to undesirable cracking patterns. The implementation of active crack control (ACC) techniques, originally proposed by McCullough and Dossey (1999) and Zollinger et al. (1999), can improve CRCP performance by minimizing the undesirable cracking patterns that can lead to premature failures in CRCP (Dahal & Roesler, 2021). The recommended minimum depth for the sawcut used for active crack control in CRCP is 25 mm but the potential for corrosion of the reinforced bars in the CRCP should be considered in the design of the sawcut for ACC (Zollinger et al., 1999). The depth of the sawcut is a function of the slab depth, time of sawing, and depth of the steel. The depth of the sawcut for ACC studies has ranged between 30 and 60 mm (Rens et al., 2014c). Recent test sections on the Illinois Tollway with ACC used saw cuts 2 in. deep, 2 ft long, and spaced 4 ft apart (Dahal & Roesler, 2021). Figure 3 shows a sample saw cut for ACC on CRCP used on Illinois Route 390. ACC saw cuts applied in Belgium were 15.75 in. long, 2.4 in. deep, and every 3.9 ft. The saw cuts should occur as soon as possible after surface finishing but without spalling the saw cut joint—approximately 4 to 12 hours after paving, depending on the concrete mix design and local climate conditions (Rens et al., 2014b; Rens et al., 2014c).



Figure 3. Photo. Active crack control saw cut notch.

Source: Dahal & Roesler (2021)

CRCP constructed with ACC methods have significantly reduced undesirable cracking patterns. For the Illinois Tollway, Dahal and Roesler were able to achieve 85% of transverse cracks propagating from an ACC saw cut notch and were able to significantly reduce or eliminate undesirable crack patterns. In Belgium, nearly 100% of transverse cracks propagated from saw cut notches once the 2.4 in. (6 cm) deep saw cut was implemented. Controlling the crack spacing and uniformity, by introducing saw cuts rather than relying only on longitudinal steel restraint to form transverse cracks, reduces cluster cracks, Y-cracks, and complex Y-cracks, which improves CRCP performance (Dahal & Roesler, 2021; Rens et al., 2014b; Rens et al., 2014c; Roesler et al., 2020; Dahal et al., 2020; Zhang & Roesler, 2020; Kohler & Roesler, 2004).

RECENT CRCP PERFORMANCE STUDIES

The following sections summarize recent performance findings from different states, countries, and agencies that design and construct CRCP.

Texas Performance Results

In general, Texas DOT design procedures for CRCP have performed well over the years except for the occurrence of severe spalling (Zollinger et al., 1999; Tayabji et al., 1998a; Tayabji et al., 1998b) in certain CRCP sections and at times horizontal cracking (Kim & Won, 2004; Won & Choi, 2017). Choi et al. (2020) studied 24 CRCP pavement sections with and without spalling. Nine of the 24 sections had no spalling, while 15 sections were identified to have spalling. No punchouts were observed on the sections studied. Cores were taken from areas of severe spalling distress and no spalling distress to assess the in-place material properties: elastic modulus of the material, Poisson's ratio, and coefficient of thermal expansion (CTE). The test results on 24 sections are summarized in Table 1. The researchers found little to no correlation between the modulus of elasticity of the concrete specimen and spalling. Likewise, there was little correlation between the modulus of elasticity or concrete CTE and horizontal cracking. The strongest correlation observed from the field data was between the concrete CTE and spalling distresses. In general, the smaller the concrete's CTE, the less likely spalling occurred. As demonstrated in Table 1, concrete cores with a CTE range of 5.2 to 5.5 microstrains/°F had no spalling. In 2014, TxDOT specifications were updated to set a maximum concrete CTE threshold for CRCP at 5.5 microstrains/°F. As of 2022, no new spalling issues have been reported (Choi et al., 2020). Additionally, Won and Choi (2017) reported transverse crack spacing was not significantly linked to long-term performance and that most cracks maintained good load transfer efficiency (LTE). Additionally, stabilized bases and tied concrete shoulders showed minimal pavement distresses whereas CRCP with asphalt shoulders and heavy truck traffic exhibited punchouts. The study noted that many of the distresses observed were because of poor construction materials or techniques (Won & Choi, 2017).

Table 1. Assessing Concrete Core Material Properties from Texas CRCP Sections

| District | Highway | Visual survey result | CTE (microstrain/°F) | Modulus of elasticity (psi) |
|------------|-----------|------------------------------|----------------------|-----------------------------|
| Houston | US 90 | Spalling | 6.27 | 6,990,000 |
| Atlanta | US 59 | Spalling and delamination | 6.26 | 6,625,000 |
| Houston | FM 523 #2 | Spalling | 6.02 | 6,646,000 |
| Houston | SH 99 | Spalling | 5.91 | 5,821,000 |
| Houston | FM 523 #1 | Spalling | 5.87 | 6,818,000 |
| Houston | FM 1301 | Spalling | 5.86 | 6,120,000 |
| Atlanta | US 79BR | Spalling | 5.78 | 5,621,000 |
| Atlanta | SL 151 | Spalling and delamination | 5.70 | 6,076,000 |
| Beaumont | FM 366 | Spalling | 5.68 | 6,347,000 |
| Houston | US 59 | Spalling | 5.67 | 6,165,000 |
| Beaumont | SL 573 | Spalling | 5.66 | 7,235,000 |
| Houston | BW 8 | Spalling | 5.58 | 5,657,000 |
| Houston | US 290 | Spalling | 5.57 | 5,749,000 |
| Paris | IH 30 | No spalling and delamination | 5.38 | 5,070,000 |
| Houston | SH 6 | Spalling | 5.31 | 4,925,000 |
| Yoakum | SH 71 | Spalling | 5.21 | 5,326,000 |
| Amarillo | IH 40 | No spalling and delamination | 4.83 | 5,793,000 |
| Dallas | SH 121 | No spalling | 4.22 | 6,816,000 |
| Dallas | IH 45 | No spalling and delamination | 4.13 | 6,581,000 |
| Fort Worth | IH 20 | No spalling and delamination | 3.94 | 5,233,000 |
| Paris | US 75 | No spalling and delamination | 3.94 | 5,787,000 |
| Laredo | IH 35 | No spalling and delamination | 3.83 | 6,350,000 |
| Dallas | IH 35 | No spalling | 3.33 | 4,972,000 |
| Dallas | SH 161 | No spalling | 2.75 | 5,304,000 |

Note: CTE = coefficient of thermal expansion; 1 psi = 0.00689 MPa; °C = (°F - 32)/1.8.

Source Choi et al. (2020)

California Performance Study

A recent study for the California Department of Transportation (Caltrans) assessed 14 CRCP projects constructed from 2009 to 2020, as presented in Figure 4. The objective of this study was to improve Caltrans’ design and construction practices for CRCP given its adoption approximately 10 years earlier. A broad range of CRCP performance data were collected on sections throughout California, which included undesirable cracking, cluster cracking, Y-cracking, spalling, and punchouts.

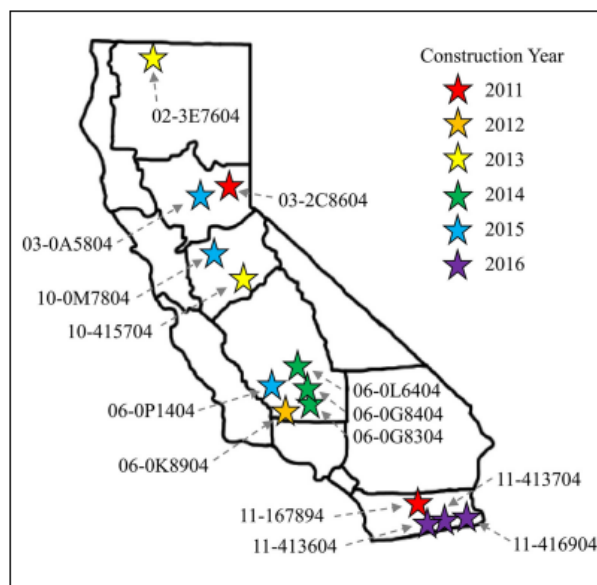


Figure 4. Map. Location and construction year of CRCP projects assessed.

Source: Stempihar et al. (2020)

One performance indicator that was reinforced from the Won and Choi (2017) study was that transverse crack spacing did not appear to significantly affect long-term CRCP performance, and many of the distresses observed at transverse cracks were because of poor construction practices. Stempihar et al. (2020) also stated that major spalling in pavements is correlated to a high concrete CTE, and punchout distresses were found mostly on projects with asphalt shoulders, heavy truck traffic, and non-stabilized bases. The study also mentioned the application of active crack control as a potential means to control undesirable cracking. Furthermore, Stempihar et al. (2020) noted that no trend was evident between average crack spacing and punchouts, and there were no correlations between annual average daily truck traffic (AADTT), climate, and punchouts. Stempihar et al.'s (2020) study compared the current Caltrans CRCP design standards with FHWA recommendations. Caltrans' design standards and the FHWA guidance, shown in Table 2 and Table 3, were similar.

Table 4 summarizes 14 CRCP project details studied in California. The longitudinal steel depth is 6 in. from the top of pavement for many of the projects, and no project had a shallower depth than 4 in. This depth of steel is significantly greater than IDOT specifications of 3.5 to 4.5 in. of cover to the top of the bars. Performance data were also collected from a series of 500 ft surveys on the outer lane of the selected roadway sections. The crack classification (patterns and distresses) was based on the Long-Term Pavement Performance (LTPP) manual (Miller & Bellinger 2014). The LTPP distress manual considers Y-cracks with spalling as a punchout. However, Y-cracking and spalling are typically linked to construction and material practices and are not related to repeated load behavior that constitutes a punchout. Table 5 is a summary of the cracking pattern frequency and punchouts in the California CRCP sections. Several sections have many punchouts when compared to other sections despite not having load-related punchouts. Caltrans' design target for punchouts per mile is 10, with 11 projects meeting this criterion and five having no punchouts. Three sections had significant punchouts; however, these punchouts were attributed to Y-cracking with spalling per LTPP guidelines. Data collected from this study suggested a correlation between Y-cracking and punchouts. The cause of the Y-cracks and spalling was not determined. One trend noted by Stempihar et al. (2020) was as the depth of longitudinal steel decreased, observed cluster cracking increased. Caltrans' desired transverse crack spacing is 3 to 7 ft, as noted in Table 2. Only five of the 14 projects resulted in a mean crack spacing between 3 to 7 ft. Seven sections had a mean crack spacing of less than 3 ft, and the remaining two projects had average crack spacings of 10.5 and 18.6 ft, respectively. The last two projects were constructed near the time of the survey.

Table 2. Comparison of California and FHWA CRCP Design Factors

| Area | CRCP property | Caltrans' requirement | FHWA guidance | |
|--------------------------------|---|--------------------------------------|-------------------------------------|------------|
| Performance | Transverse crack spacing (ft) ^a | 3–7 | 3–6 | |
| | Maximum crack width (inch) ^a | 0.040 | 0.020 | |
| | Punchouts on primary highways (max. #/mile) ^b | 10 | 10 ^{c,d} | |
| | IRI on primary highways (max. in/mi) ^b | 160 | 175 ^c , 158 ^d | |
| Structural design | CRCP thickness (inch) | 9–13 | 7–13 | |
| | Base type ^e | AC | ATB, CTB, LCB | |
| | Base thickness (inch) | 3 | 3–8 | |
| | Subbase type | Unbound granular | Unbound granular, treated subgrade | |
| | Subbase thickness (inches) | 8 | 6–12 | |
| | Widened-CRCP width (ft) | 14 ^e | 13–14 | |
| | Shoulder material | AC, un-tied JPCP, or tied CRCP | Tied concrete | |
| Longitudinal reinforcing steel | Maximum longitudinal joint spacing (ft) | 14 | 14 | |
| | Percent steel (%) | 0.55–0.70 | 0.70–0.80 | |
| | Steel grade | 60 | na | |
| | Steel tensile stress (% of ultimate strength) | 75 or less | na | |
| | Bar size | #6 | #4 to #7 | |
| | Bar spacing (center-to-center, inches) | 5.5–8 | 4–9 | |
| | First bar location (inches) (from joint or pavement edge) | 3–4 | Same as bar depth | |
| | Bar depth range (inches) (varies with slab thickness) | 4–5.5 | 3.5 to mid-depth | |
| | Transverse reinforcing steel | Steel grade | 60 | 60 |
| | | Bar size | #6 | #4 to #6 |
| | | Bar spacing (center-to-center, inch) | 48 | 24, 36, 48 |

Note: na = not applicable; IRI = International Roughness Index; FHWA = Federal Highway Administration; AC = asphalt concrete; ATB = asphalt treated base; CTB = cement treated base; JPCP = jointed plain concrete pavement; LCB = lean concrete base.

^aUsed to determine the amount of steel.

^bCaltrans' failure thresholds.

^cBased on AASHTOWare Pavement ME Design.

^dAmerican Concrete Pavement Association (average daily traffic greater than 10,000).

^eCaltrans also provides a design option for a 12 ft lane.

Source: Stempihar et al. (2020)

Table 3. Comparison of Concrete and Construction Requirements for CRCP

| | Continually reinforced concrete pavement property | Caltrans' requirement | FHWA guidance |
|------------------------------|--|--------------------------------------|------------------------------------|
| Concrete Design Requirements | Portland cement concrete (PCC) flexural strength (lb/in ²) | 570 (28 days) 650 (42 days) | na |
| | Coefficient of thermal expansion (CTE) for PCC mixture | 6 $\mu\epsilon/\text{°F}$ (max) | Low CTE is recommended |
| | Drying shrinkage | 0.05% (28 days) | As low as possible. |
| | Heat of hydration | Not specified | Prevent excessive heat generation. |
| | Maximum coarse aggregate size (inch) | 1, 1.5 | 1 (min), 1.5 is typical |
| Construction Requirements | Ambient temperature (°F) | Not specified | 90 max. |
| | Concrete temperature (°F) | 50–90 | na |
| | Longitudinal bar placement tolerance (inch) | Not specified | ± 1 (horizontal and vertical) |
| | Length of longitudinal bar splice (min, inch) | 45 times bar diameter | 25–33 times bar diameter |
| | Steel placement method | Chairs, transverse bar assemblies | Chairs, transverse bar assemblies |
| | Delay in concrete placement before joint required (max) | 30 minutes | 30–45 minutes |
| | Curing method | Curing compound, waterproof membrane | na |

Note: na = not applicable.

Source: Stempihar et al. (2020)

Table 4. Summary of CRCP Projects with Design Features in California

| Project | CRCP thickness (in.) | AC Base thickness (in) | Lane width (ft) | Shoulder material | Long. steel ^a (%) | Long. steel depth ^b (in.) | Long. steel spacing (in.) |
|------------------------|----------------------|------------------------|-----------------|-------------------|------------------------------|--------------------------------------|---------------------------|
| 02-3E7604 | 12.0 | 3.0 | 12 | CRCP | 0.63 | 6.0 | 6.0 |
| 03-2C8604 | 14.0 | 2.5–9.5 | 12 | CRCP | 0.73 | 6.0 | 4.5 |
| 03-0A5804 | 11.0 | 12.0 (Agg. only) | 11 - 13 | Curb/gutter | 0.67 | 4.0 | 6.5 |
| 06-0K8904 | 12.0 | 3.0 | 14 | AC | 0.64 | 4.75 | 5.5 |
| 06-0L6404 | 13.0 | 3.0 | 14 | JPCP | 0.64 | 4.75 | 5.5 |
| 06-0G8304 ^c | 12.5 | 3.0 | 12 | CRCP ^d | 0.63 | 6.0 | 5.75 |
| 06-0G8404 ^c | 12.5 | 3.0 | 12 | CRCP ^d | 0.63 | 6.0 | 5.75 |
| 06-0P1404 | 13.0 | 3.0 | 14 | AC | 0.62 | 5.5 | 5.5 |
| 10-0M7804 | 13.0 | 3.0 | 14 | AC | 0.63 | 6.0 | 5.5 |
| 10-415704 | 12.0 | 3.0 | 14 | JPCP | 0.65 | 4.25 | 6.0 |
| 11-167894 | 10.0 | 6.0 | 12 | CRCP | 0.67 | 4.0 | 7.0 |
| 11-413604 | 11, 11.5 | 3.0 | 12 | CRCP | 0.64, 0.66 | 4.0 | 6.25, 6.5 |
| 11-413704 | 11.0 | 3.0 | 12 | CRCP | 0.66 | 4.0 | 6.5 |
| 11-416904 | 11.0 | 3.0 | 12 | CRCP | 0.66 | 4.0 | 6.5 |

Note: AC = asphalt concrete; CRCP = continuously reinforced concrete pavement; JPCP = jointed plain concrete pavement.

^aNo. 6 bar, grade 60 steel.

^bTransverse bars placed on plastic support chairs.

^cCRCP was placed in the passing lane.

^dInside shoulder.

Source: Stempihar et al. (2020)

Table 5. Summary of CRCP Cracking Patterns and Distresses in California

| Project | Age in 2017 (years) | Avg. equivalent number of cracks (per lane-mile) | | | |
|-----------|---------------------|--|------------|----------|------------------------|
| | | Fragments | Meandering | Y-cracks | Punchouts ^a |
| 02-3E7604 | 4 | 66.4 | 1.5 | 47.3 | 14.6 |
| 03-2C8604 | 6 | 214.0 | 12.7 | 83.9 | 2.1 |
| 03-0A5804 | 2 | 741.3 | 0.0 | 86.6 | 4.2 |
| 06-0K8904 | 5 | 1,980.0 | 10.6 | 91.5 | 7.0 |
| 06-0L6404 | 3 | 585.0 | 0.0 | 97.2 | 4.2 |
| 06-0G8304 | 3 | 91.5 | 0.0 | 119.7 | 0.0 |
| 06-0G8404 | 3 | 103.8 | 1.8 | 142.6 | 1.8 |
| 06-0P1404 | 2 | 1,052.8 | 0.0 | 25.4 | 0.0 |
| 10-0M7804 | 2 | 269.3 | 0.0 | 496.3 | 42.2 |
| 10-415704 | 4 | 128.8 | 8.4 | 475.2 | 27.5 |
| 11-167894 | 6 | 123.2 | 1.8 | 119.7 | 3.5 |
| 11-413604 | <1 | 3.5 | 0.0 | 0.0 | 0.0 |
| 11-413704 | <1 | 91.5 | 14.1 | 28.2 | 0.0 |
| 11-416904 | <1 | 8.4 | 8.4 | 16.9 | 0.0 |

^aNone of the distresses classified as a punchout (per the Long Term Pavement Performance [LTPP] distress manual) exhibited differential settlement typically associated with punchouts.

Source: Stempihar et al. (2020)

Oregon Performance Study

Oregon began constructing CRCP overlays in the 1970s, as presented in Table 6. Initial pavement structures consisted of a 14 to 28 in. aggregate base, a 5 to 8 in. hot-mix asphalt layer, and an 8 in. CRCP overlay (Fick et al., 2021). The initial CRCP overlay performed well with few punchouts, and

additional CRCP overlays were constructed over hot-mix asphalt pavement structures. Oregon traffic levels turned out to be higher than the original 20-year design life estimates. More recently, Oregon has constructed thicker (10 to 11 in.) CRCP overlays to primarily slow down chain wear from truck traffic on the pavement. Oregon has experienced little to no punchout failures on their CRCP. Rather, the chain and studded tire wear control the functional life of CRCP overlays (Moderie & Burch, 2019).

Table 6. Performance Data for Unbonded CRCP Overlays in Oregon

| State | Location | Overlay Type | Overlay Construction Year | Status | Cumulative Millions of ESALs* (Traffic Years) | Pavement Condition** (2018) | IRI Data (2018) |
|--------|---------------------|--------------|---------------------------|-------------------|---|-----------------------------|-----------------|
| Oregon | I-5, Jackson County | 11 in. CRCP | 1989 | In Service 2020 | 36.5 (1989 to 2020) | 82 | 98 |
| Oregon | I-5, Douglas County | 11 in. CRCP | 2017 | In Service 2020 | 7.9 (2017 to 2020) | 100 | 69 |
| Oregon | I-84, Baker County | 10 in. CRCP | 1985 | In Service 2020 | 40.4 (1985 to 2020) | 79 | 108 |
| Oregon | I-5, Marion County | 8 in. CRCP | 1976 | Overlaid 1998**** | 98 (1976 to 1998) | 64*** | 97*** |

* ESALS were estimated from 2018 OTMS traffic data using the growth rate of the 2018 traffic data.
 ** Pavement condition is a 100 to 0 point scale where 100-95 is very good, 94-76 is good, 75-46 fair, 45-25 is poor, and 25-0 is very poor.
 *** These values were measured before the asphalt overlay in 1998. The pavement condition score for this project is controlled by rutting and not structural failure.
 **** The 1998 overlay was needed to fill in ruts in the concrete caused by studded tire wear.

Source: Fick et al. (2021)

Illinois Performance Studies

IDOT has constructed seven unbonded overlays beginning in 1967, and four are still in service (Table 7). Three CRCP overlay sections have been rehabilitated because the traffic levels and performance (e.g., CRS) exceeded the design values. The three sections that were rehabilitated were I-70 in Bond County (1967–1987), I-55 in Springfield (1970–2001), and I-55 in Springfield (1976–1997) (Heckel & Wienrank, 2018) with the ratio of actual to design traffic at 175%, 222%, and 174%, respectively. Additionally, the existing CRCP overlay sections are expected to exceed the design repetitions (ESALs) by the end of their design lives. The existing CRCP overlays in service have good to excellent condition rating survey (CRS) values.

Increasing the design life of CRCP requires minimizing the undesirable transverse cracking patterns that develop over time. One objective of the Illinois Tollway research study was to minimize cluster cracks, Y-cracks, and divided cracks (undesirable cracking patterns) through either construction techniques or materials. For example, internal curing with fine lightweight aggregates can improve the surface properties and shrinkage behavior of the concrete, which can impact crack development.

Additionally, ACC can produce more uniform transverse cracking patterns (Dahal & Roesler, 2021). As presented in Table 8, three CRCP sections were constructed on Illinois Tollway Route 390. Section 1 contained internal curing with prewetted fine lightweight aggregate. Section 2 was the control section with the standard concrete used for CRCP. Section 3 contained internal curing coupled with ACC. The two test sections with internal curing had 37% fine lightweight aggregate by volume.

Table 7. Performance of CRCP Overlays in Illinois

| State | Location | Overlay Type | Overlay Construction Year | Status | Cumulative Millions of ESALs (Traffic Years) | IDOT CRS Value* | IRI Data |
|----------|------------------------|------------------------------|---------------------------|----------------------|--|-----------------|----------|
| Illinois | I-70, Bond County | 6-in., 7-in., and 8-in. CRCP | 1967 | Removed service 1987 | 23.4 (1967-1987) | 5.7** | |
| Illinois | I-55, Springfield | 8-in. CRCP | 1970 | Removed service 2001 | 38.1 (1970-2001) | 5.5** | |
| Illinois | I-55, Springfield | 9-in. CRCP | 1976 | Removed service 1997 | 27.5 (1976-1997) | 5.7** | |
| Illinois | I-74, Knox County | 9-in. CRCP | 1995 | In service 2020 | 29.6 (1995-2020) | 7.8 | 68 |
| Illinois | I-88, Whiteside County | 9-in. CRCP | 2000-2001 | In service 2020 | 17.8 (2001-2020) | 7.8 | 60 |
| Illinois | I-70, Clark County | 12-in. CRCP | 2002 | In service 2020 | 59.1 (2002-2020) | 7.9 | 69 |
| Illinois | I-57/64, Mt. Vernon | 10-in. CRCP | 2014 | In service 2020 | 25.5 (2014-2020) | 8.2 | 70 |

*IDOT CRS values range from 9.0 for newly constructed pavement surfaces to 1.0 for total failure. Values ranging from 9.0 to 7.6 are “excellent,” 7.5 to 6.1 are “good,” and 6.0 to 4.6 are “fair.” A value of 4.5 is “poor.” Preservation treatments are considered for interstates when the CRS value reaches 5.5.
 **At the end of service

Source: Adapted from Heckel & Wienrank (2018)

Table 8. Illinois Tollway Route 390 CRCP Sections

| Section | Length (ft) | Thickness (in.) | Internal curing | Active cracking | Construction date | Construction time start | Construction air temp. (F) |
|-----------|-------------|-----------------|-----------------|-----------------|-------------------|-------------------------|----------------------------|
| Section 1 | 1,970 | 10.5 | Yes | No | August, 2016 | Morning (8:00 a.m.) | 70–84 |
| Section 2 | 1,044 | 10.5 | No | No | July, 2016 | Night (8:00 p.m.) | 60–65 |
| Section 3 | 1,000 | 9 | Yes | Yes | April, 2017 | Morning (8:00 a.m.) | 46–48 |

Source: Dahal & Roesler (2021)

To assess the effectiveness of internal curing and ACC methods, the three test sections were surveyed multiple times between construction in 2016 to 2020 to document the cracking patterns. The four-year performance of the three CRCP sections was quantified by mean crack spacing, crack width, Y-cracks, divided cracks, and cluster cracks. As presented in Figure 5, transverse cracks developed rapidly through the first 300 days, approximately one year after placement. Most cracks formed during the first-year period, but transverse cracks continued to form at a much slower rate even into the second and third years. Sections 1 and 2 had larger crack widths over time relative to section 3 (Figure 6). However, each section was placed at a different temperature (Table 8), which significantly impacts the working crack widths. The use of ACC in Section 3 reduced the crack width and maintained a more uniform crack spacing. Figure 7 shows the percentage of saw cuts from ACC with a transverse crack propagating from the saw cut notch. At the end of the first year, approximately 71% of saw cut notches had a transverse crack propagating from it. By 1,200 days after construction, 85% of saw cut notches had a transverse crack propagating from the notch.

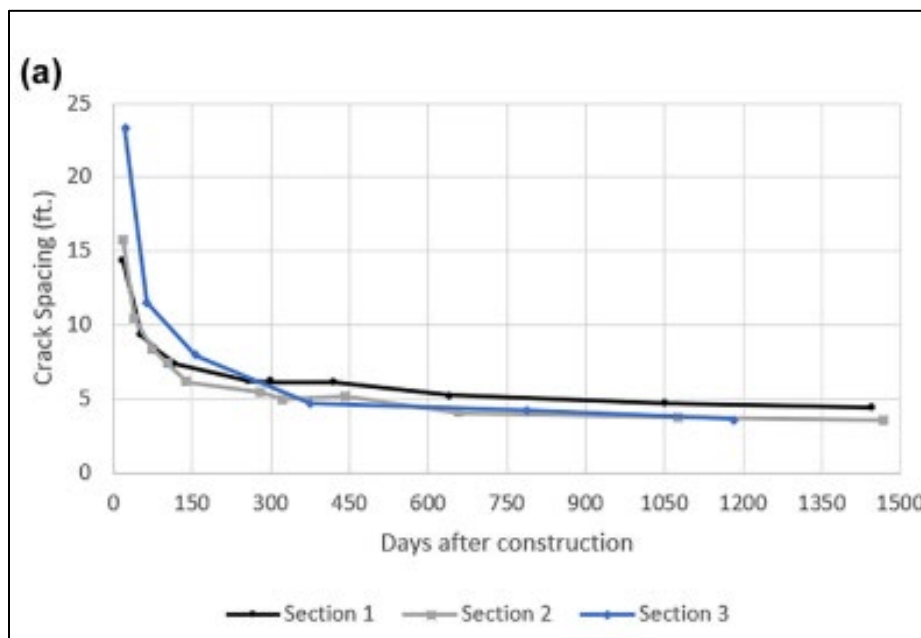


Figure 5. Graph. Transverse crack spacing on Illinois Tollway CRCP test sections.

Source: Dahal & Roesler (2021)

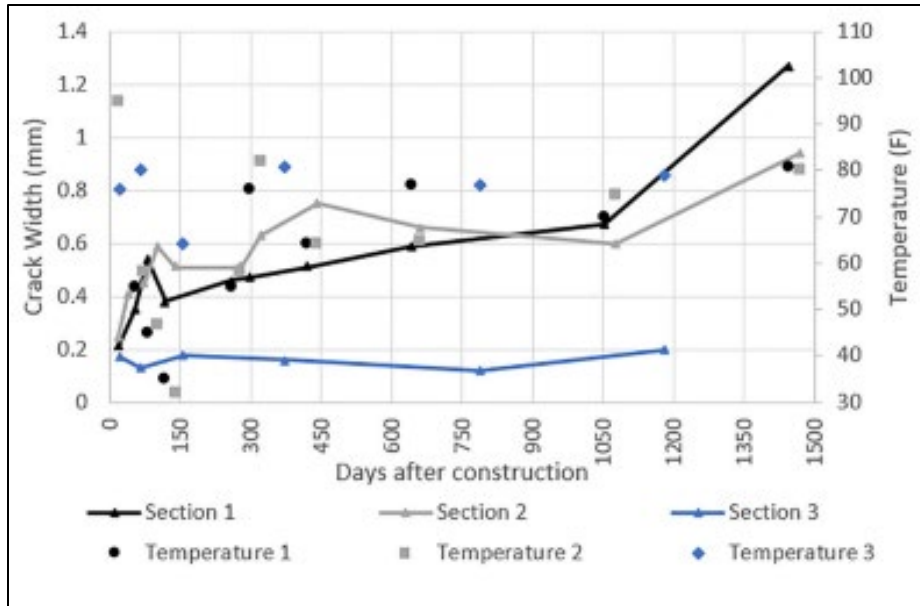


Figure 6. Graph. Transverse crack width on Illinois Tollway CRCP test sections.

Source: Dahal & Roesler (2021)

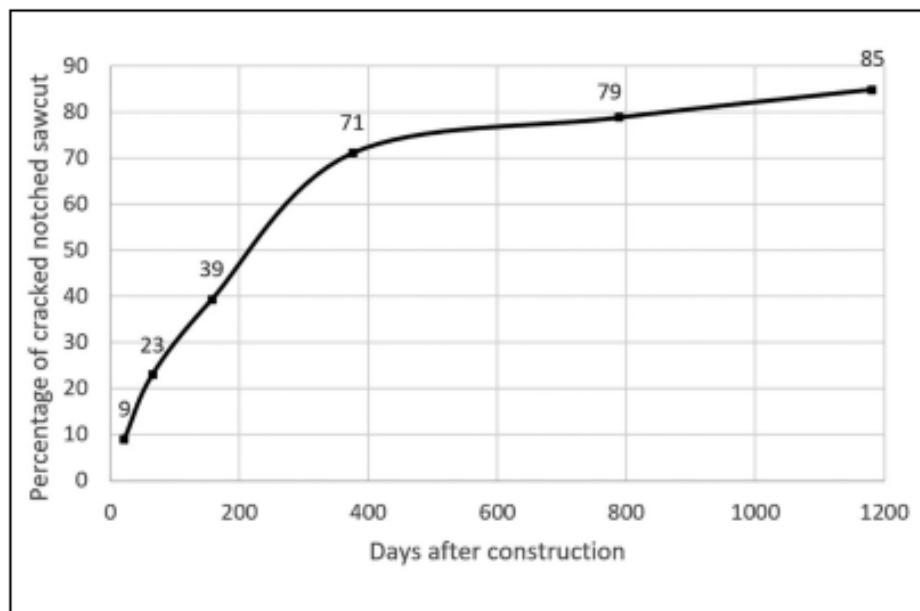


Figure 7. Graph. Percentage of saw cuts with cracks propagating from the saw cut notch in section 3.

Source: Dahal & Roesler (2021)

The crack survey data collected were eventually normalized per 1,000 ft. Figure 8 presents the number of occurrences of each type of undesirable cracking in each CRCP section. The sections with crack control (internal curing concrete [ICC] or active crack control [notch]) performed the best, meaning the least number of undesirable cracks occurred. The combination of both internal curing

and ACC presented the least occurrences of undesirable cracks over all three sections. The presence of complex and cluster cracks can increase the probability of punchouts in CRCP, as mentioned earlier. Section 3 also had zero cluster cracks and only one complex Y-crack. Temperature control during construction and curing conditions are also significant factors in avoiding undesirable crack patterns. Section 3 also contained macrofibers as part of the concrete mixture.

Locations that had the highest cluster cracks (section 2) had lower mean crack widths than sections 1 and 2. Additionally, section 3 exhibited less cluster cracking than sections 1 and 2. Areas near the terminal joints (end of the sections or near bridges) had the highest transverse crack spacing due to lower restraint and tensile stresses, which reduced the number of cracks that formed (Dahal & Roesler, 2021). For more effective cracking near terminal joints, deeper notches (active crack control) should be cut to influence transverse cracks to form closer to the desired interval of 4 ft.

The recent Illinois Tollway study demonstrated the combined use of ACC and internal curing was successful. Transverse cracks originated at 85% of the saw cut notches, and a mean crack spacing of 3.6 ft was recorded after three years. ICC reduced Y-cracks and cluster cracks, but ACC was more effective in eliminating cluster cracking in the test section. This significantly improves the performance of CRCP, as cluster cracks can increase the probability of punchout development.

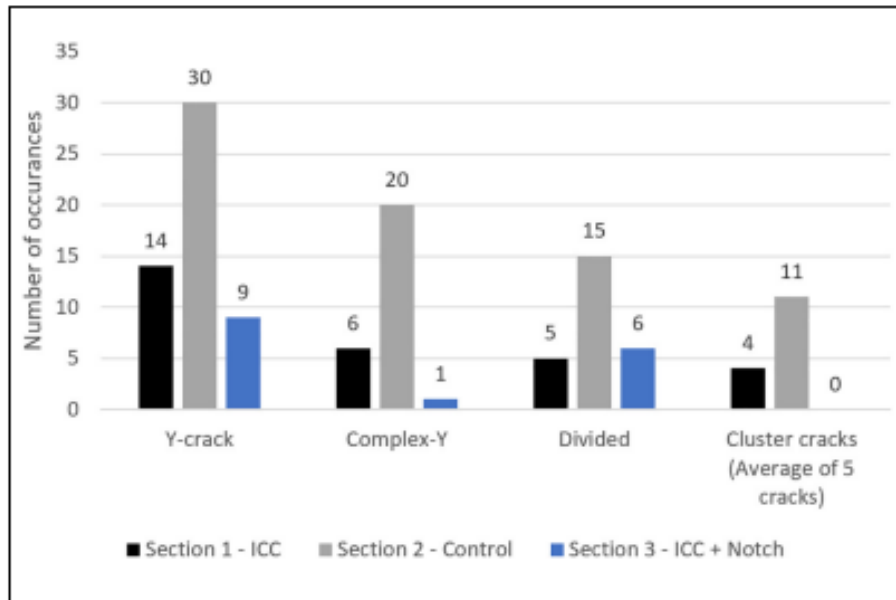


Figure 8. Graph. Occurrences of undesirable cracks normalized per 1,000 ft.

Source: Dahal & Roesler (2021)

Belgium Performance Study

Belgium has been constructing CRCP for approximately 60 years (Rens et al., 2014c) and continues to search for ways to improve CRCP performance. Cluster and Y-cracking are two undesirable crack patterns Belgium is attempting to mitigate (Rens et al., 2014c). Past findings showed that longitudinal reinforcement content had little impact on CRCP crack spacing and crack width, whereas the

temperature control during construction was more vital to crack development, as mentioned by Dahal and Roesler (2021).

Belgium also recently designed trials for ACC methods based on the findings of Kohler and Roesler (2004). Initially the saw cuts were 15.75 in. (40 cm) long, 1.2 in. (3 cm) deep, and with 3.9 ft (1.2 m) spacing. The initial results of this trial were unsatisfactory, with approximately 60% of cracks originating near a saw cut notch (see Table 9). A field decision was made to increase the depth of the saw cut to 2.4 in. (6 cm) with a maximum saw cut window of 24 hours. Saw cutting was recommended as soon as possible without inducing spalling. This change resulted in nearly 100% of early age cracks originating at a saw cut, as shown in Table 9. The section with the 6 cm saw cut had 98.9% of cracks originating at a notch four days after construction and 78.2% of cracks originating at a notch one year after construction.

The study by Rens et al. (2014b) in Belgium demonstrated that deeper saw cuts that do not exceed the reinforcement depth and notched early, improved crack initiation, and resulted in a more favorable pattern. (Rens et al., 2014b).

Table 9. Percentage of Cracks Initiated at Notches from Belgium CRCP Study

| Road Section | Length (m) | Age (days) | Number of Notches (N1) | Number of Cracks (N2) | Number of Cracks at Notches (N3) | Effectiveness of Notches, N3/N1 (%) | Percentage of Cracks in Category by Distance to Nearest Notch (m) | | | |
|--------------|------------|------------|------------------------|-----------------------|----------------------------------|-------------------------------------|---|-------|---------|---------|
| | | | | | | | 0 | 0-0.2 | 0.2-0.4 | 0.4-0.6 |
| 6 cm | 1,100 | 4 | 897 | 193 | 191 | 21.3 | 98.9 | 0 | 0 | 1.1 |
| | 1,100 | 65 | 897 | 664 | 555 | 61.9 | 83.5 | 2.4 | 7.7 | 6.4 |
| | 1,100 | 204 | 897 | 762 | 597 | 66.6 | 78.4 | 3.8 | 9.8 | 8.0 |
| | 1,100 | 378 | 897 | 775 | 606 | 67.6 | 78.2 | 3.8 | 9.9 | 8.1 |
| 3 cm | 500 | 123 | 422 | 417 | 245 | 58.1 | 58.7 | 9.4 | 15.9 | 16.0 |
| | 500 | 262 | 422 | 497 | 281 | 66.5 | 56.5 | 8.7 | 17.5 | 17.3 |
| | 500 | 436 | 422 | 502 | 285 | 67.5 | 56.8 | 8.6 | 17.3 | 17.3 |

Source: Ren et al. (2014a)

CHAPTER 3: CRCP AND CRCP OVERLAY PERFORMANCE DATA FROM ILLINOIS

To expand the CRCP performance data available for CRCP design calibration, the IDOT database of images collected from CRCP sections was reviewed. Approximately 93.7 miles of CRCP or CRCP overlay were surveyed with the Illinois Roadway Analysis Database System (IROADS) to obtain CRCP performance data. The CRCP database includes 28 newly built CRCP sections in Illinois and 7 unbonded CRCP overlay sections from Illinois. CRCP performance data extracted from the IROADS database (condition ratings and images) include condition rating survey (CRS), international roughness index (IRI), punchouts per mile, crack spacing, and the presence of longitudinal cracking. The two primary outputs needed from IROADS images are the crack spacing and number of punchouts. The performance information could then be compared with the proposed CRCP design framework. A summary of IROADS sections where data was collected is shown in Table 10 for CRCP overlays and Table 11 for new CRCP. IDOT provided design input data (design features, materials, and traffic) for the CRCP sections on contract ID numbers 62304, 80954, 60401, 60N87, 64E97, 64B78, and 70044. The remaining CRCP design and traffic data were gathered by reviewing electronic plan documents and using IROADS. The cumulative traffic was calculated based on the measured or estimated average daily traffic (ADT) converted into ESALs.

Cumulative ESALs for each section were calculated in accordance with Chapter 54 of the *BDE Manual* (IDOT, 2023) using a traffic factor (TF) equation, as shown in Figure 9. Volume, vehicle class, and percent truck traffic were derived from the IROADS database. The process involved back-calculating the initial service AADT from the most current year's AADT obtained from IROADS, assuming a 1% growth rate since the opening of the traffic. The cumulative ESALs were calculated until the punchout evaluation year to ensure a correlation between the number of punchouts and cumulative traffic. For more detailed information on the ESALs calculation, refer to Appendix A.

$$TF = DP * \frac{(0.15 * P * PV) + (143.81 * S * SU) + (696.42 * M * MU)}{1 * 10^6}$$

Figure 9. Equation. Traffic factor equation used to calculate ESALs.

Source: Chapter 54 of the BDE Manual, IDOT (2023)

Where *PV*, *SU*, and *MU* are design traffic expressed as the number of passenger, single-unit, and multiple-unit vehicles. *P*, *S*, and *M* are the percent of *PV*, *SU*, and *MU* in the design lane expressed as a decimal, and *DP* is the design period.

The average crack spacing for each section in Table 10 that is in service was surveyed from images available in IROADS. The mean crack spacing was calculated by counting the number of transverse cracks in a 0.10-mile section from each CRCP section. Table 12 summarizes the estimated mean crack spacing for each CRCP section, ranging from 3.1 to 33 ft. Because these sections were surveyed digitally, there is likely some slight measurement error coming from the individual frame. Additionally, inconsistencies in lighting could have reduced the visibility of the cracks to the camera or computer screen, or both. These issues will be discussed later. Appendix A contains the full section

details. Only three CRCP sections had visual signs of punchouts (i.e., contract ID 62105, 80954, and 70044), as shown in Table 12. Sections with punchouts had crack spacings above 6 ft and two of these sections (contract ID 62105 and 80954) also exhibited longitudinal cracking. The other CRCP sections exhibited little damage. The presence of only a few punchouts indicated that CRCP sections are performing well under actual traffic conditions and/or that patching had occurred. The overall CRS value for all CRCP sections is 8.0 with an average IRI of 82 in/mile.

Table 10. CRCP Overlay Data from IDOT

| Interstate | Location | CRCP Overlay Thickness | Overlay Construction Year | Status | Cumulative Millions of ESALs (Traffic Years) | IDOT CRS Value | IRI Value |
|------------|------------------|------------------------|---------------------------|---------------------------|--|----------------|-----------|
| I-70 | Bond County | 6,7,8 | 1967 | Removed from service 1987 | 23.4 | 5.7 | N/A |
| I-55 | Springfield | 8 | 1970 | Removed from service 2001 | 38.1 | 5.5 | N/A |
| I-55 | Springfield | 9 | 1976 | Removed from service 1998 | 27.5 | 5.7 | N/A |
| I-74 | Knox County | 9 | 1995 | In service 2021 | 29.6 | 7.8 | 68 |
| I-88 | Whiteside County | 9 | 2001 | In service 2021 | 17.8 | 7.8 | 60 |
| I-70 | Clark County | 12 | 2002 | In service 2021 | 59.1 | 7.9 | 69 |
| I-57/I-64 | Jefferson County | 10 | 2014 | In service 2021 | 25.5 | 8.2 | 70 |

Source: Adapted from Heckel & Wienrank (2018)

Table 11. CRCP Section Details in Illinois

| | Contract_ID | County | Location | Miles | Servicing Period (2021 time of survey) | Traffic Opening Year | Design Life, yrs | Shoulder Type | Base Type | Base Thickness, in. | PCC Thickness, in. | Percent Steel, % | Steel Diameter, in. | Depth to Steel, in. |
|----|-------------|-------------|-----------|-------|--|----------------------|------------------|---------------|-----------|---------------------|--------------------|------------------|---------------------|---------------------|
| 1 | 82989 | Cook | I-55 | 4.16 | 21 | 2000 | 20 | Tied PCC | BAM | 4 | 14 | 0.7 | 0.875 | 4.5 |
| 2 | 62304 | Cook | I-57 | 1.25 | 13 | 2008 | 30 | Tied PCC | HMA | 6 | 14 | 0.8 | 0.875 | 4.5 |
| 3 | 62105 | Cook | I-80 | 3.19 | 15 | 2006 | 30 | Tied PCC | BAM | 4 | 14 | 0.8 | 0.875 | 4.5 |
| 4 | 80954 | Cook | I-94 | 7.17 | 28 | 1993 | 20 | Tied PCC | BAM | 4 | 12 | 0.7 | 0.75 | 3.5 |
| 5 | 62300 | Cook | I-94 | 8.07 | 14 | 2007 | 30 | Tied PCC | HMA | 6 | 14 | 0.8 | 0.875 | 4.5 |
| 6 | 60401 | Cook | I-290 | 3.12 | 18 | 2003 | 40 | Tied PCC | HMA | 6 | 14.17 | 0.8 | 0.875 | 4.5 |
| 7 | 60N87 | Will | I-80 | 1.36 | 3 | 2018 | 20 | Tied PCC | HMA | 4 | 13 | 0.7 | 0.875 | 3.5 |
| 8 | 64E97 | Lee | I-39 | 0.36 | 9 | 2012 | 20 | Tied PCC | HMA | 4 | 12.25 | 0.7 | 0.875 | 3.5 |
| 9 | 64B78 | Henry | I-80 | 0.46 | 5 | 2016 | 20 | Tied PCC | BAM | 4 | 12.25 | 0.7 | 0.875 | 3.5 |
| 10 | 64933 | Rock Island | I-80 | 1.35 | 12 | 2009 | 20 | Tied PCC | HMA | 4 | 12 | 0.7 | 0.875 | 3.5 |
| 11 | 64B78 | Rock Island | I-80 | 0.51 | 6 | 2015 | 20 | Tied PCC | HMA | 4 | 12.25 | 0.7 | 0.875 | 3.5 |
| 12 | 64219 | Whiteside | I-88 | 8.59 | 20 | 2001 | 20 | Tied PCC | HMA | 4 | 9 | 0.7 | 0.875 | 3.5 |
| 13 | 64C29 | Winnebago | I-90/I-39 | 2.71 | 9 | 2012 | 20 | Tied PCC | HMA | 4 | 12.75 | 0.7 | 0.875 | 3.5 |
| 14 | 66F23 | Livingston | I-55 | 0.2 | 4 | 2017 | 20 | HMA | Granular | 12 | 11 | 0.7 | 0.875 | 3.5 |
| 15 | 66H50 | Livingston | I-55 | 0.29 | 2 | 2019 | 20 | Tied PCC | HMA | 4 | 10 | 0.7 | 0.875 | 3.5 |
| 16 | 66686 | Bureau | I-80 | 0.73 | 9 | 2012 | 20 | Tied PCC | HMA | 4 | 10 | 0.7 | 0.875 | 3.5 |
| 17 | 66044 | Grundy | I-80 | 10.89 | 19 | 2002 | 20 | Tied PCC | HMA | 4 | 14 | 0.7 | 0.875 | 3.5 |
| 18 | 68200 | Peoria | I-74 | 5.25 | 17 | 2004 | 30 | Tied PCC | HMA | 6 | 11.5 | 0.8 | 0.875 | 4.5 |
| 19 | 68201 | Tazewell | I-74 | 2.23 | 16 | 2005 | 30 | Tied PCC | HMA | 6 | 11.5 | 0.8 | 0.875 | 4.5 |
| 20 | 68620 | Tazewell | I-74 | 2.74 | 9 | 2012 | 20 | Tied PCC | HMA | 4 | 11 | 0.7 | 0.875 | 3.5 |
| 21 | 70757 | McLean | I-55 | 9.53 | 18 | 2003 | 20 | Tied PCC | HMA | 4 | 12.5 | 0.7 | 0.875 | 3.5 |
| 22 | 70044 | Clark | I-70 | 9.98 | 19 | 2002 | 30 | Tied PCC | HMA | 6 | 13 | 0.8 | 0.875 | 4.5 |
| 23 | 74295 | Effingham | I-57A | 0.53 | 8 | 2013 | 20 | Tied PCC | HMA | 4 | 13 | 0.7 | 0.875 | 3.5 |
| 24 | 74296 | Effingham | I-70 | 8.35 | 8 | 2013 | 20 | Tied PCC | HMA | 4 | 13 | 0.7 | 0.875 | 3.5 |
| 25 | 76C52 | St. Clair | I-64 | 0.11 | 9 | 2012 | 30 | Tied PCC | HMA | 4 | 14 | 0.8 | 0.875 | 4.5 |
| 26 | 76C43 | St. Clair | I-70A | 1.21 | 9 | 2012 | 20 | Tied PCC | HMA | 4 | 11.25 | 0.7 | 0.875 | 3.5 |
| 27 | 76A91 | Madison | I-270 | 0.35 | 10 | 2011 | 30 | Tied PCC | HMA | 4 | 12 | 0.8 | 0.875 | 4.5 |
| 28 | 78172 | Jefferson | I-57 | 2.71 | 7 | 2014 | 20 | Tied PCC | HMA | 4 | 12 | 0.7 | 0.875 | 3.5 |

Table 12. CRCP Section Performance Data in Illinois

| | Contract_ID | County | Location | Miles | Servicing Period (2021 time of survey) | Traffic Opening Year | ADT | Total of Million ESALs at time of survey | IRI (in/mi) | IDOT CRS | Avg Crack Spacing (ft) | Observed PO (2-way) | Total Punchouts/mile | Longitudinal cracking |
|----|-------------|-------------|-----------|-------|--|----------------------|----------------|--|-------------|----------|------------------------|---------------------|----------------------|-----------------------|
| 1 | 82989 | Cook | I-55 | 4.16 | 21 | 2000 | 157,700 (2022) | 44.1 | 123 | 7.1 | 5.3 | 0 | 0 | Yes |
| 2 | 62304 | Cook | I-57 | 1.25 | 13 | 2008 | 153,700 (2022) | 17.0 | 92 | 8.1 | 12.0 | 0 | 0 | Yes |
| 3 | 62105 | Cook | I-80 | 3.19 | 15 | 2006 | 193,600 (2022) | 178.9 | 84 | 7.8 | 4.3 | 1 | 0.16 | Yes |
| 4 | 80954 | Cook | I-94 | 7.17 | 28 | 1993 | 246,100 (2022) | 53.6 | 136 | 7 | 10.6 | 1 | 0.03 | Yes |
| 5 | 62300 | Cook | I-94 | 8.07 | 14 | 2007 | 315,700 (2022) | 134.3 | 92 | 8.1 | 5.5 | 0 | 0 | No |
| 6 | 60401 | Cook | I-290 | 3.12 | 18 | 2003 | 158,100 (2022) | 51.2 | 148 | 7 | 4.4 | 0 | 0 | No |
| 7 | 60N87 | Will | I-80 | 1.36 | 3 | 2018 | - | - | 137-157 | 5.9 | N/A | - | - | - |
| 8 | 64E97 | Lee | I-39 | 0.36 | 9 | 2012 | 19,400 (2021) | 18.2 | 41 | 7.6 | 6.4 | 0 | 0 | Yes |
| 9 | 64B78 | Henry | I-80 | 0.46 | 5 | 2016 | 20,400 (2021) | 10.5 | 83 | 8.4 | 5.1 | 0 | 0 | No |
| 10 | 64933 | Rock Island | I-80 | 1.35 | 12 | 2009 | 23,000 (2021) | 24.9 | 67 | 8.4 | N/A | 0 | 0 | No |
| 11 | 64B78 | Rock Island | I-80 | 0.51 | 6 | 2015 | 23,000 (2021) | 13.2 | 78 | 7.8 | 19.6 | 0 | 0 | No |
| 12 | 64219 | Whiteside | I-88 | 8.59 | 20 | 2001 | 11,600 (2022) | 18.1 | 60 | 7.8 | 3.3 | 0 | 0 | Yes |
| 13 | 64C29 | Winnebago | I-90/I-39 | 2.71 | 9 | 2012 | 56,300 (2022) | 41.5 | 55 | 8.5 | 5.4 | 0 | 0 | No |
| 14 | 66F23 | Livingston | I-55 | 0.2 | 4 | 2017 | 16,500 (2019) | 6.9 | 46 | 8.6 | 33.0 | 0 | 0 | No |
| 15 | 66H50 | Livingston | I-55 | 0.29 | 2 | 2019 | 20,600 (2021) | 4.1 | 63 | 8.6 | 29.3 | 0 | 0 | No |
| 16 | 66686 | Bureau | I-80 | 0.73 | 9 | 2012 | 21,000 (2021) | 10.4 | 61 | 7.3 | 5.5 | 0 | 0 | No |
| 17 | 66044 | Grundy | I-80 | 10.89 | 19 | 2002 | 50,300 (2021) | 53.3 | 61 | 7.7 | 8.3 | 0 | 0 | Yes |
| 18 | 68200 | Peoria | I-74 | 5.25 | 17 | 2004 | 50,000 (2021) | 10.2 | 64-66 | 8.3 | 5.4 | 0 | 0 | No |
| 19 | 68201 | Tazewell | I-74 | 2.23 | 16 | 2005 | 52,800 (2021) | 11.1 | 97 | 8.3 | 4.4 | 0 | 0 | Yes |
| 20 | 68620 | Tazewell | I-74 | 2.74 | 9 | 2012 | 49,400 (2021) | 15.3 | 69 | 8.5 | 17.6 | 0 | 0 | No |
| 21 | 70757 | McLean | I-55 | 9.53 | 18 | 2003 | 42,500 (2021) | 63.2 | 59-82 | 8.5-9.0 | 3.4 | 0 | 0 | Yes |
| 22 | 70044 | Clark | I-70 | 9.98 | 19 | 2002 | 29,300 (2021) | 66.9 | 68 | 7.9 | 3.1 | 6 | 0.3 | No |
| 23 | 74295 | Effingham | I-57A | 0.53 | 8 | 2013 | 20,700 (2021) | 22.1 | 50 | 7.9 | N/A | - | - | No |
| 24 | 74296 | Effingham | I-70 | 8.35 | 8 | 2013 | 45,100 (2022) | 44.8 | 61 | 8.6 | 4.1 | 0 | 0 | No |
| 25 | 76C52 | St. Clair | I-64 | 0.11 | 9 | 2012 | 82,900 (2021) | 21.2 | 118-119 | 8.3 | | 0 | 0 | No |
| 26 | 76C43 | St. Clair | I-70A | 1.21 | 9 | 2012 | 44,300 (2019) | 12.0 | 145 | 8.0 | 6.4 | 0 | 0 | No |
| 27 | 76A91 | Madison | I-270 | 0.35 | 10 | 2011 | 49,200 (2021) | 22.0 | 82 | 8.4 | N/A | - | - | No |
| 28 | 78172 | Jefferson | I-57 | 2.71 | 7 | 2014 | 45,800 (2022) | 37.3 | 75 | 8.2 | 11.7 | 0 | 0 | No |

IMAGE AND VIDEO ASSESSMENT DIFFICULTIES

While IROADS was helpful in providing visual access to CRCP sections throughout Illinois, there were some issues encountered with the images. First, roadside references had to be used to determine crack spacing or overall distances because the camera angle was pointed down, which gave a low field of view. For example, other cars, lane markings, and light pole spacings were used to estimate the distance between cracks in a single frame given the distance between frames was non-uniform. Additionally, a crack with a width less than 0.5 mm was difficult to see in the images. Figure 10 and Figure 11 present a sample image illustrating these issues. Figure 10 is a “stock” image from IROADS. Figure 11 highlights the cracks, which are difficult to see in the first image. The use of the lane markings, the light pole, and the rumble strips provided a rough estimate of crack spacing. This also illustrates that it is not possible to determine crack width from these images. IDOT provided video imagery with software-highlighted cracks. However, only large cracks were detected such as bridge joints or pavement repairs. Overall punchout data was the easiest and most relevant to identify and collect with the video images.



Figure 10. Image. IROADS image of transverse cracks in right driving lane with light pole, pavement stripes, shoulder grooves, and pavement width as reference distances.

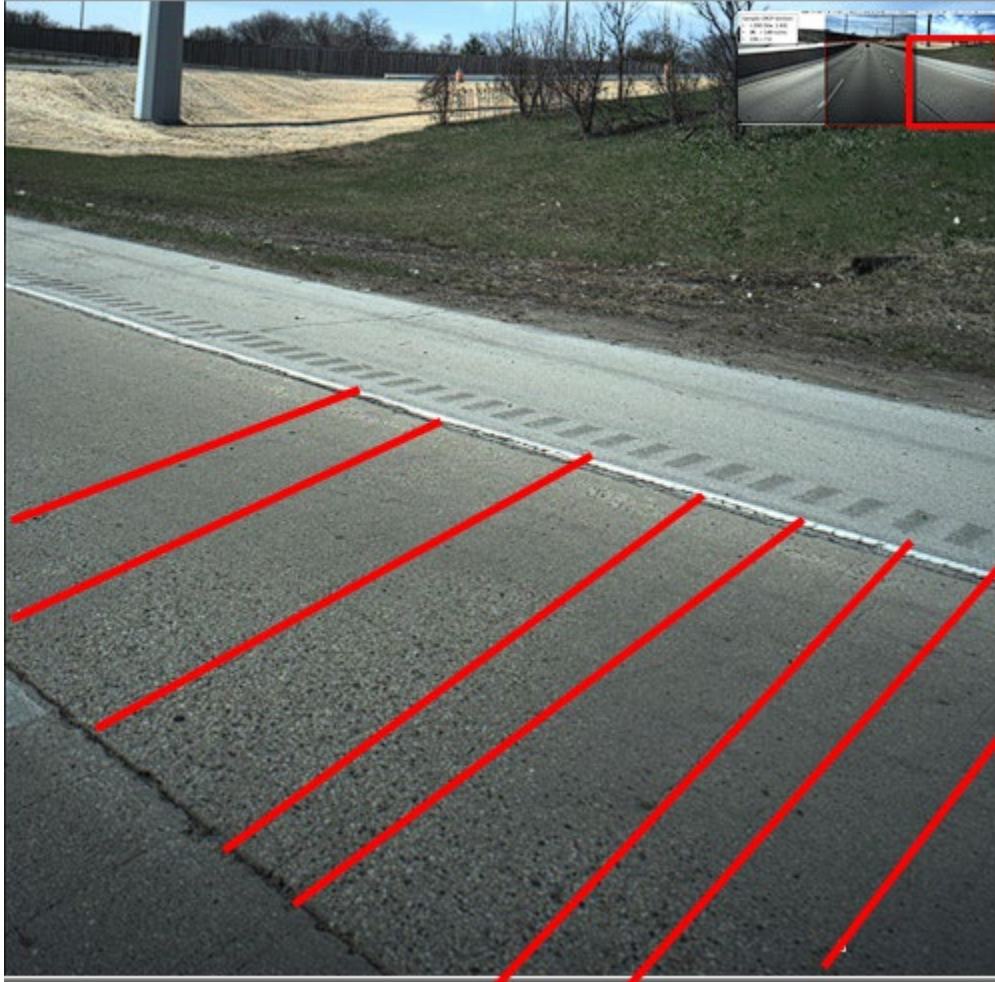


Figure 11. Image. IROADS image of highlighted transverse cracks in right driving lane with light pole, pavement stripes, and shoulder grooves.

CHAPTER 4: NEW CRCP DESIGN—PUNCHOUT PERFORMANCE MODEL UPDATE

REVIEW OF EXISTING CRCP DESIGN SOFTWARE

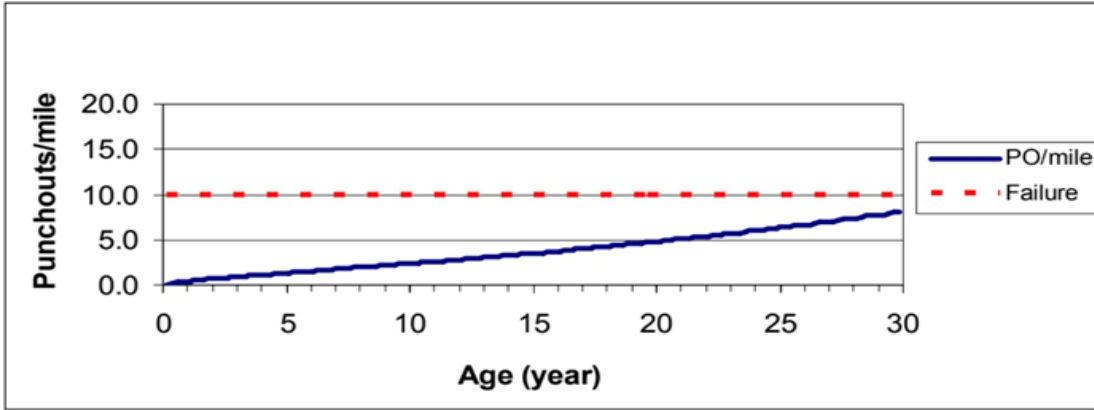
A calibration check was conducted on the existing CRCP design framework originally developed by Beyer and Roesler (2009). This design framework was implemented into an Excel spreadsheet. The objective of the software review was to ensure the spreadsheet still produces accurate outputs, as it was originally designed back in 2009, and to make sure no coding had been inadvertently disabled or broken because of subsequent updates to Excel. The design review checks were compared with the original design outputs published in Beyer and Roesler (2009). A sample set of inputs is shown in Table 13 with the original outputs shown in Figure 12 and Figure 13. The outputs generated from the updated Excel CRCP design framework are shown in Figure 14 and Figure 15.

Upon comparing Figure 14 and Figure 15 with the original plots in Figure 12 and Figure 13, using the same design inputs, the updated Excel version of the design framework yielded similar outputs. The power function punchout model originally predicted eight punchouts per mile (as seen in Figure 12 from 2009), and the updated Excel power function punchout model similarly predicted eight punchouts (as shown in Figure 14). However, while the 2009 S-curve punchout model forecasted seven punchouts per mile (Figure 13), the revised calibration indicated a slight increase, predicting nine punchouts per mile (Figure 15). Given the updated design framework was confirmed to function properly for a small set of inputs, a sensitivity analysis of the CRCP inputs was subsequently performed to further assess the program.

Table 13. Sample Inputs for Design Input

| Design Input | | Design Input | |
|-----------------------------|--------------------------------|----------------------------|---------------------------|
| <i>Design life</i> | variable | γ_{PCC} | 1.22 ft ² /day |
| <i>Aggregate type</i> | limestone | <i>CC</i> | 600 lb/yd ³ |
| <i>Shoulder type</i> | variable | <i>Base type</i> | ATB |
| <i>Design ESALs</i> | variable | <i>f</i> | 7.5 |
| <i>Annual growth factor</i> | 0% | <i>LTE_{base}</i> | 30% |
| E_{PCC28} | 4.40 x 10 ⁶ psi | <i>Construction season</i> | summer |
| μ_{PCC} | 0.15 | $rh_{PCC,\zeta}$ | 85% |
| α_{PCC} | 5.50 x 10 ⁻⁶ 1/°F | <i>R</i> | 1.0 |
| f'_{c28} | 4,500 psi | <i>k-value</i> | 100 psi/in. |
| MOR_{90} | 750 psi | <i>Fatigue equation</i> | zero-maintenance |
| \hat{R} | 0.8 | <i>Reliability</i> | variable |
| ϵ_{∞} | 780 x 10 ⁻⁶ in./in. | <i>Failure criterion</i> | 10 PO/mile |

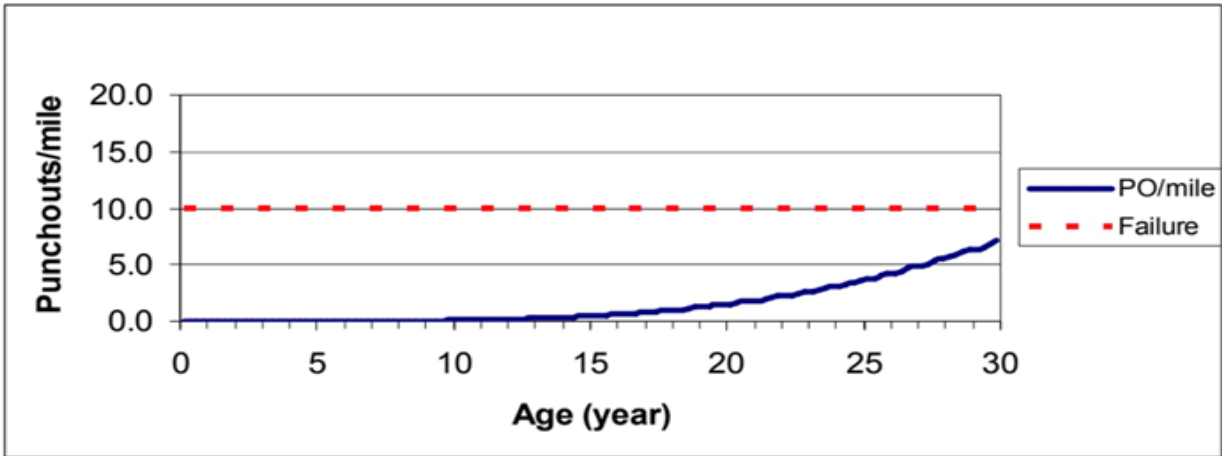
Source: Beyer & Roesler (2009)



Relationship between number of punchouts per mile and age for 30-year design life, $h_{pcc}=11$ in., $k_d=100$ psi/in., tied concrete (separated) shoulders, 70 million ESALs, and 95% reliability (power function punchout model)

Figure 12. Graph. Power function punchout model prediction.

Source: Beyer & Roesler (2009)



Relationship between number of punchouts per mile and age for 30-year design life, $h_{pcc}=11$ in., $k_d=100$ psi/in., tied concrete (separated) shoulders, 70 million ESALs, and 95% reliability (S-Curve Punchout)

Figure 13. Graph. S-Curve punchout model prediction.

Source: Beyer & Roesler (2009)

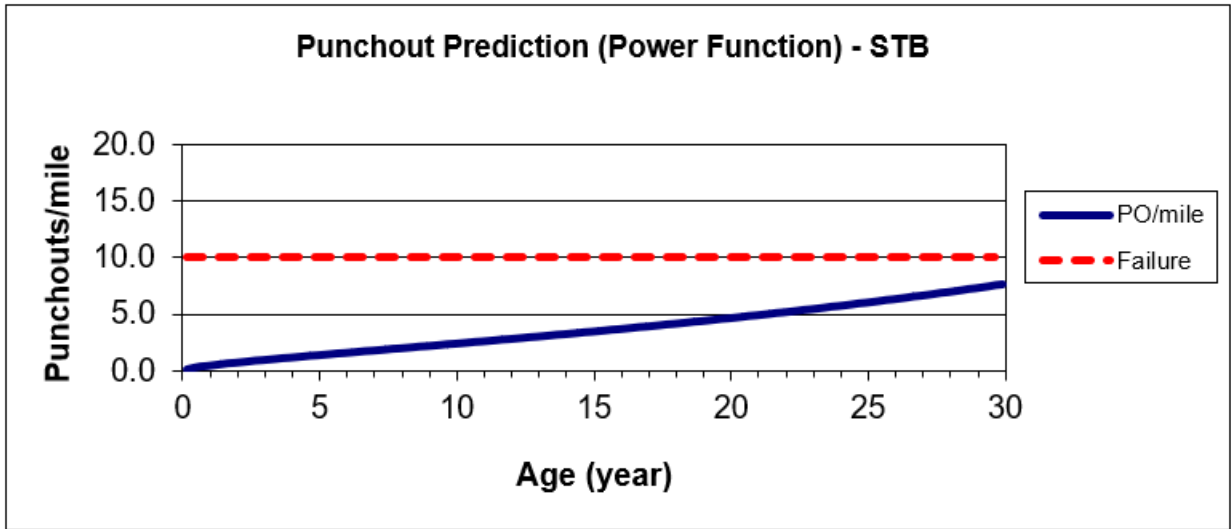


Figure 14. Graph. Power function punchout model prediction, updated Excel.

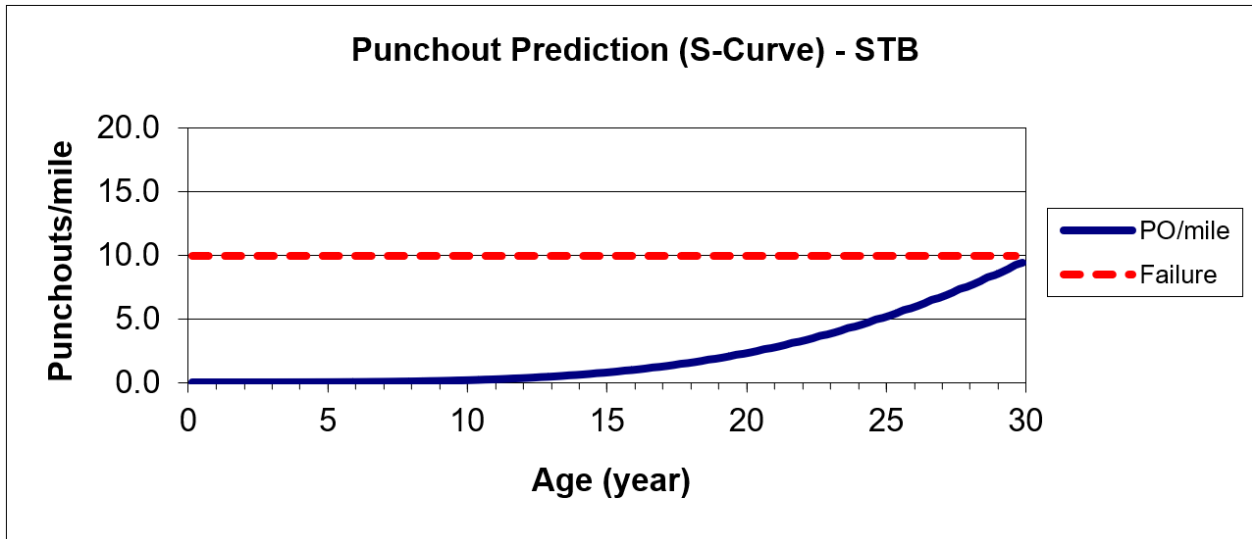


Figure 15. Graph. S-Curve punchout model prediction, updated Excel.

CRCP Design Framework Sensitivity Analysis

A sensitivity analysis of the CRCP design framework was then performed to check for rationality of predicted design thicknesses for various important design features with the updated Excel version. The inputs are the same as Table 13 with specific design features and inputs varied. Appendix B contains the full datasets used for the sensitivity analysis and outputs. The sensitivity of the modulus of subgrade reaction (dynamic), traffic level (ESALs), and shoulder type on CRCP design thicknesses were output from the updated Excel program and compared with each other and IDOT’s current JPCP method from Chapter 54 of the *BDE Manual* (IDOT, 2023). The design thickness for 20- and 30-year design lives at 95% reliability was evaluated at steel contents of 0.7% and 0.8%, respectively.

Figure 16 illustrates the sensitivity of CRCP steel contents and subgrade conditions to the design thickness of CRCP containing tied shoulders. CRCP with 0.8% steel content, compared to 0.7%, requires a lower slab thickness by approximately 0.25 to 0.5 inches for design traffic ranging from 10 to 200 million ESALs. The design traffic level was the most significant factor affecting CRCP slab thickness, resulting in an increase of 2.5 inches from 10 million to 200 million ESALs. Additionally, the substantial variation in the modulus of subgrade reactions from poor support (50 psi/in.) to good support (200 psi/in.) leads to an increase in CRCP slab thickness by approximately 1 inch. Figure 17 illustrates the CRCP slab thickness sensitivity to the modulus of subgrade reaction (K-value) and shoulder type at 0.7% steel content. According to Beyer and Roesler (2009), CRCP slab thickness for asphalt shoulders generally had a higher thickness than the CRCP slab with tied shoulder because it does not provide load transfer across the longitudinal edge as tied PCC shoulders do, leading to the expectation of a thinner CRCP slab. However, designs with asphalt shoulders in the updated framework were found to be nearly 0.5 inches thinner than those with tied PCC shoulders at high traffic levels, as seen in Figure 17. This behavior is partly because bottom cracking occurs on the inside of the lane for tied shoulders, whereas top stresses control for asphalt shoulders that occur near the outer slab edge. Additionally, the top tensile stress location has lower curling stress magnitudes relative to the bottom tensile stress location, which can be another reason for differences in top and bottom tensile stress locations. Furthermore, at a strong support condition ($k = 200$ psi/in.), the result shows that the required CRCP thickness for asphalt shoulders is consistently lower than that for tied concrete shoulders across all traffic conditions. This behavior is likely due to the higher curling tensile stress at the bottom of the slab on strong subgrade compared to poor subgrade.

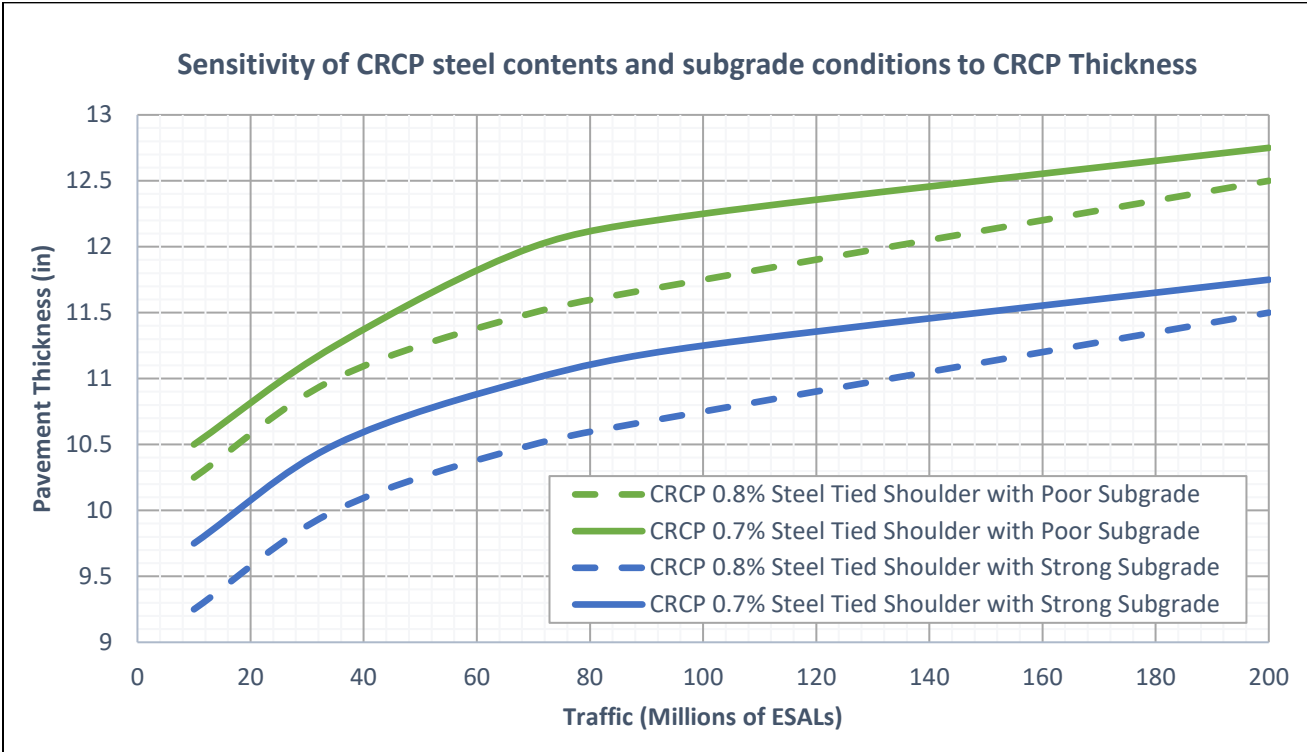


Figure 16. Graph. CRCP thickness sensitivity to CRCP steel contents and subgrade conditions.

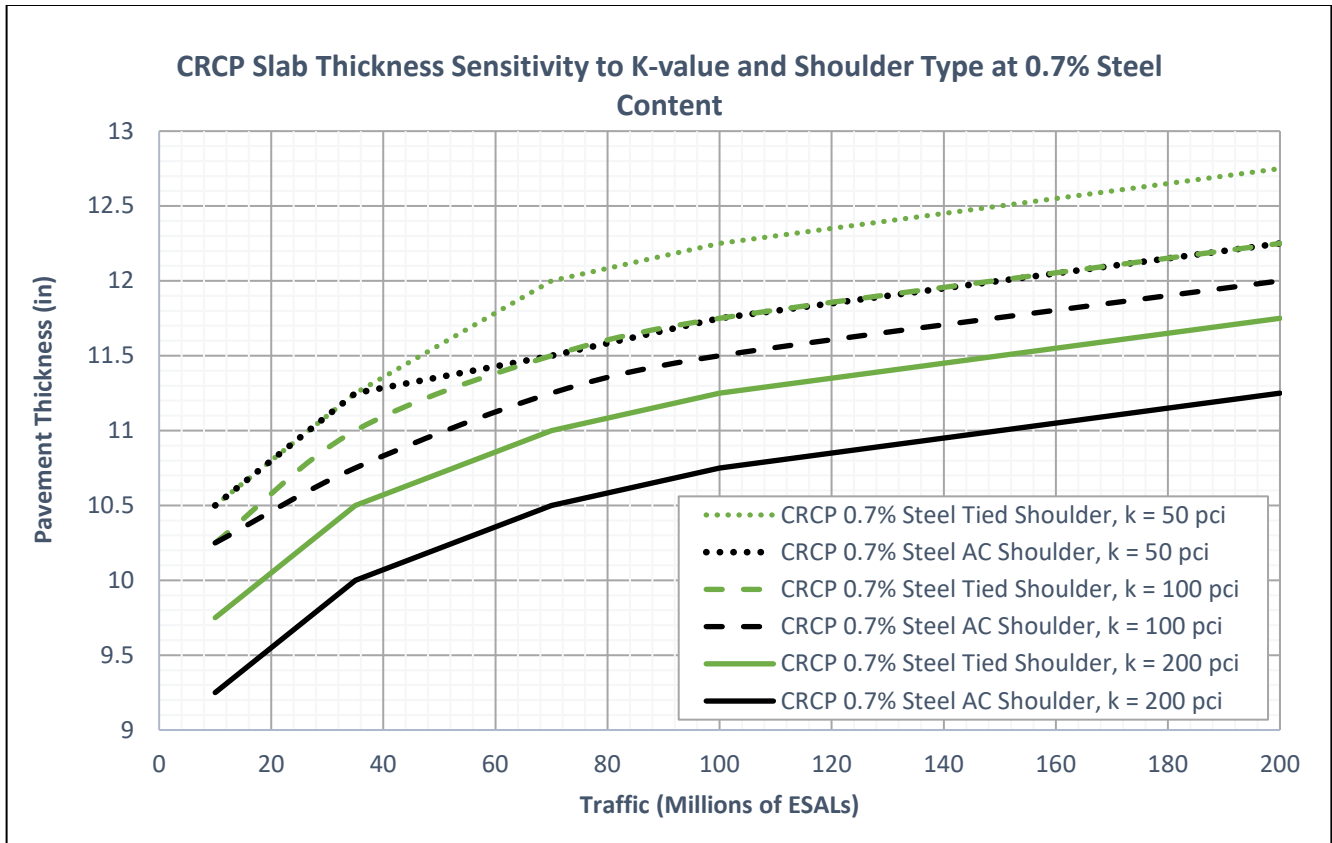


Figure 17. Graph. CRCP slab thickness sensitivity to K-value and shoulder type.

CONCRETE FATIGUE EQUATIONS

Historically, pavement engineers have designed thinner CRCP than JPCP for similar inputs, and, therefore, the expectations were to see CRCP slab thicknesses less than JPCP results. The steel in CRCP is not designed to carry the traffic loads but is designed to initiate and maintain a certain crack spacing and crack width to achieve the desired performance.

A review of concrete fatigue equations assessed the algorithm for CRCP, comparing the MEPDG, zero-maintenance (UIUC CRCP Excel), and ACPA equations, the latter utilized in Chapter 54 of the *BDE Manual* (IDOT, 2023). Figures 18, 19, and 20 depict the zero-maintenance (Darter, 1977; Zollinger & Barenberg, 1989), MEPDG (AASHTO, 2024), and ACPA equations (Titus-Glover et al., 2004), respectively. The MEPDG equation modifies the allowable repetitions by reducing them by one logarithmic cycle compared to the JPCP MEPDG procedure. The zero-maintenance equation used in the 2009 CRCP framework is based on fatigue testing of laboratory beams from multiple researchers. A comparison of JPCP versus CRCP slab thicknesses was plotted in Figure 21 through Figure 23 with more comparison charts shown in Appendix C. As expected, when plotting slab thickness of pavements with similar design inputs, the zero-maintenance fatigue equation of the CRCP software generated slightly different curves than the JPCP design charts in Chapter 54.

$$\log N_{ij} = 17.61 - 17.61(SR_{ij})$$

Figure 18. Equation. Zero-maintenance fatigue equations.

Source: Darter (1977)

$$\log N_{ij} = 2.0 * \left(\frac{1}{SR_{ij}}\right)^{1.22} - 1$$

Figure 19. Equation. MEPDG (AASHTO Pavement ME) fatigue equations.

Source: AASHTO (2024)

$$\log N_f = \left[\frac{-SR^{-10.24} \log(1 - P)}{0.0112} \right]^{0.217}$$

$$P = 1 - R \frac{SC}{50}$$

$$SR = \frac{\sigma_{eq}}{MR}$$

Figure 20. Equation. ACPA fatigue equations.

Source: Titus-Glover et al. (2004)

- Where,
- N = allowable applications to failure
 - SR = stress ratio, %
 - P = probability of failure, %
 - R = reliability (inputted by user), %
 - SC = percent slabs cracked at the end of pavement's life (assumed as 15%), %
 - σ_{eq} = equivalent stress at the slab edge, psi
 - MR = flexural strength of the concrete, psi

The comparisons on the design thickness of JPCP and CRCP were completed for a 20-year design life unless otherwise stated and at 95% reliability, as illustrated from Figure 21 to Figure 23. The JPCP and CRCP designs were analyzed under the same subgrade conditions, where a “Poor” SSR corresponds to a K-value of 50 psi/in., and a “Granular” subgrade corresponds to a K-value of 200 psi/in. The corresponding pavement thicknesses were rounded to the nearest 0.25 in. Comparison of CRCP and IDOT JPCP slab thicknesses for tied concrete shoulder is illustrated in Figure 21. Under poor subgrade support conditions, the JPCP thickness was slightly lower than the CRCP thickness for both 0.7% and 0.8% steel contents, with differences of approximately 0.5 inches and 0.25 inches, respectively.

For concrete pavements with asphalt shoulders under low traffic volumes with granular support, as depicted in Figure 22, the JPCP and CRCP (0.7% steel) thicknesses are comparable. However, with increasing traffic volumes, JPCP requires greater thickness than CRCP, by up to approximately 0.5 inches. Nonetheless, under poor subgrade conditions and traffic volumes below 50 million ESALs, JPCP with AC shoulders requires a thinner slab compared to CRCP.

Figure 23 presents the sensitivity of JPCP thickness to shoulder type and subgrade condition, whether tied or untied shoulders, and strong or poor subgrades. The differences in JPCP thickness across these variables ranged from 0.25 inches to 1 inch. The results indicate that a granular subgrade with a tied shoulder requires a lower slab thickness compared to a granular subgrade with an untied shoulder, followed by a poor subgrade with a tied shoulder, and the greatest thickness was required for a poor subgrade with an untied shoulder. Subgrade conditions have a more pronounced impact on JPCP thickness than the shoulder type.

Overall, the 2022 updated CRCP design framework in Excel yields slab thicknesses that are in similar ranges to the IDOT JPCP design charts in Chapter 54 but are also plotted from 100–200 million ESALs. At around 70 million ESALs, the IDOT JPCP design charts reach a horizontal asymptote without significant slab thickness increases from 70 to 100 million ESALs, as seen in Figures 21 through 23. In contrast, the CRCP design framework implemented in Excel demonstrates a steady increase in slab thickness up to at least 200 million ESALs. The thinner slab thicknesses for JPCP relative to CRCP are because of implementation of different concrete fatigue equations (ACPA fatigue versus zero-maintenance fatigue) and failure criteria (20% slab cracking versus 10 punchout per mile).

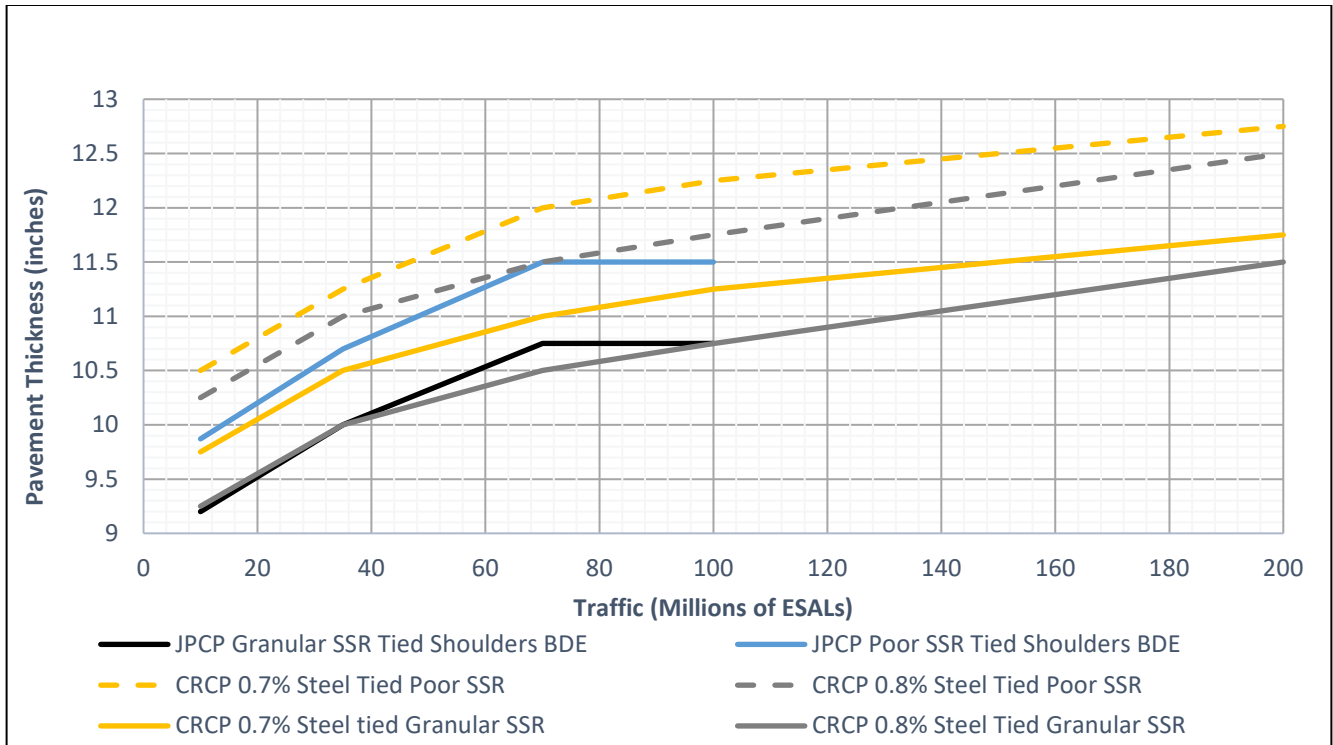


Figure 21. Graph. Comparison of CRCP and IDOT JPCP slab thicknesses for tied concrete shoulder.

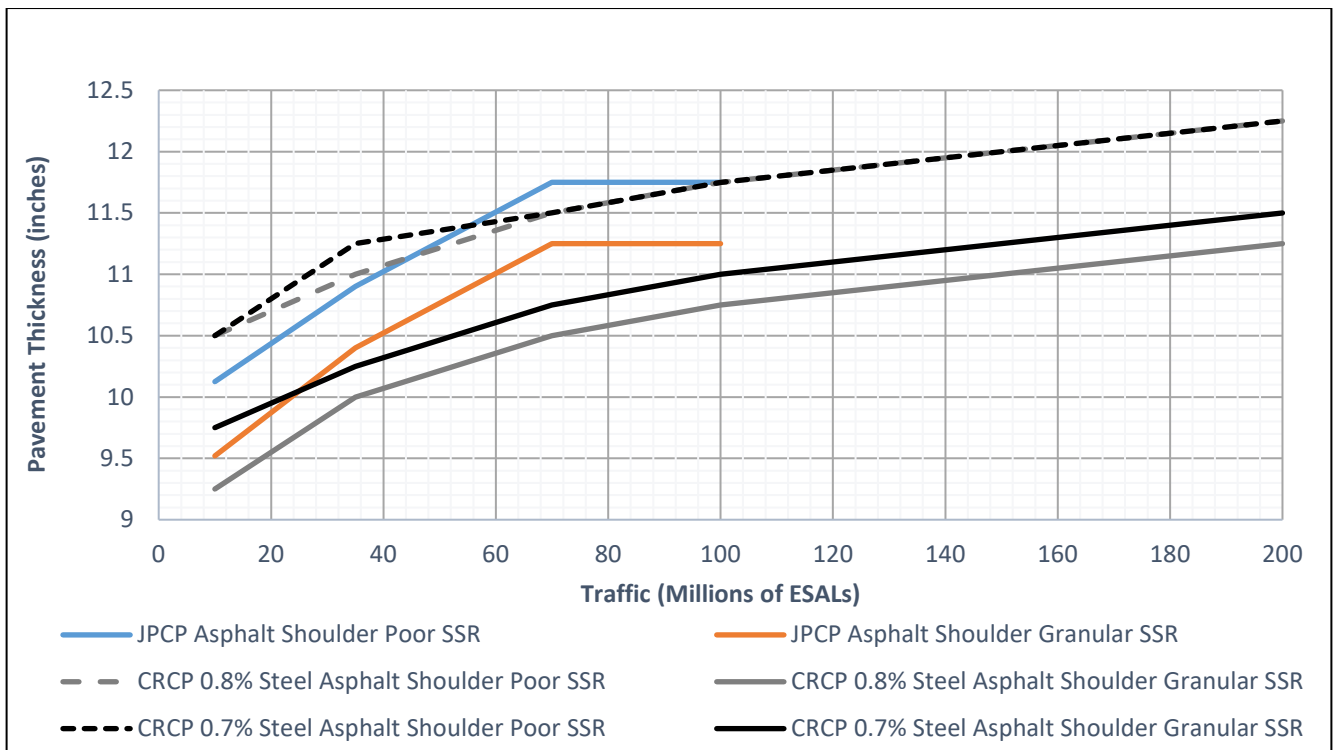


Figure 22. Graph. CRCP vs IDOT JPCP thicknesses with asphalt shoulders and poor and granular subgrade.

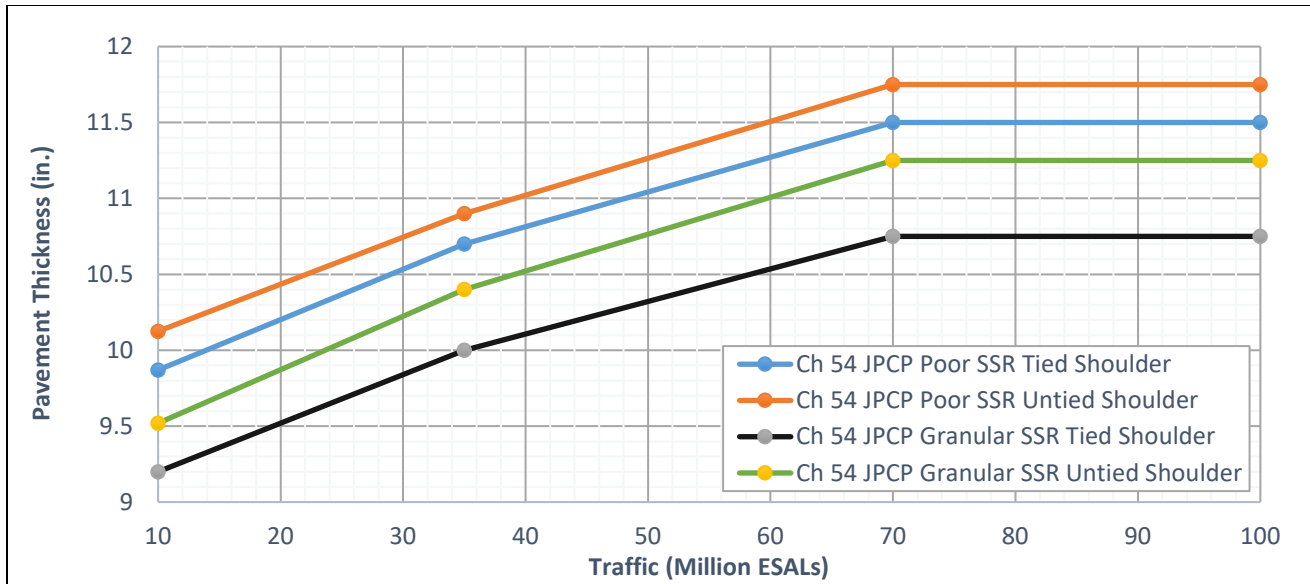


Figure 23. Graph. JPCP tied and untied shoulders on poor and granular subgrade support conditions (poor: K-value = 50 psi/in.; granular: K-value = 200 psi/in.).

Recalibration of Punchout-to-Damage Model

One major objective of this research was to recalibrate the punchout-to-damage equation to account for new CRCP performance data that was not available 15 years ago. The recalibration of the punchout-damage model was based on field CRCP performance data and corresponding design inputs (e.g., traffic, pavement structural layers and thicknesses, steel reinforcement bar size, reinforcement ratio, and depth of steel) collected from this research project. With the performance data, design inputs, and pavement geometry, the CRCP design software calculated the fatigue damage in the CRCP slab at two locations (the top near the outer wheel path and the bottom in the inner wheel path). The number of punchouts was calculated for each section (Figure 24) based on the predicted fatigue damage in the CRCP slab based on the zero-maintenance fatigue equation in Figure 18.

$$PO_i = \frac{1}{a + b * c^{-\log D_{TOT,i}}}$$

Figure 24. Equation. S-Curve punchout prediction model.

Where:

PO_i = the total predicted number of punchouts per mile at the end of seasonal increment i

$D_{TOT,i}$ = the accumulated fatigue damage at either the top or bottom tensile stress location at the end of seasonal increment i ;

a, b, c = field calibration constants for punchout-to-damage function.

In the CRCP design framework, the CRCP slab (tensile) stresses for a fixed set of inputs are either located at the top or bottom of the slab because of loading and curling, as seen in Figure 25. The slab stress ratios are then passed to the zero-maintenance fatigue equation to predict allowable load repetitions. An equivalent damage ratio concept is used to provide the same damage equivalency of the total traffic distribution across the pavement width by only placing a percentage of traffic at one lateral location. The CRCP fatigue damage is calculated in seasonal increments based on the specific temperature differential, expected load repetitions, and allowable load repetitions for both the top and bottom of the slab locations, as shown in Figure 26. The total fatigue damage for each seasonal increment is calculated and then summed throughout the life of the CRCP at the top and bottom of the slab. The punchout prediction is based on the location in the slab (top or bottom) that has the higher total accumulated damage.

The punchout-damage model assumed an S-curve (logistic function) behavior, as seen in Figure 24. The field calibration coefficients needed to be determined to fit the expanded CRCP performance dataset. To determine the new coefficients, the sum of squares error (SSE) between the calculated (predicted) punchouts and the observed punchouts was minimized to produce the best fit given a set of a, b, and c coefficients. The “a” coefficient remained fixed to achieve a maximum punchout level of 50 per mile once a threshold damage level is reached. The next step was to determine iteratively by solver function in Excel the coefficients “b” and “c” by minimizing the overall model SSE. When the calculated accumulated damage is small (e.g., 1×10^{-9}), the pavement is expected to have few to no punchouts. Coefficient “b” adjusts the slope of the middle portion of the curve left or right, and coefficient “c” adjusts the bottom boundary of the curve. The CRCP software in Excel for calibration has been updated to allow for addition of performance data and to make it more user friendly.

2.7.4.1.1 Stress ratio

Both concrete fatigue equations are functions of the slab stress ratio. The stress ratio for each temperature frequency bin j of seasonal increment i (SR_{ij}) is calculated as:

$$SR_{STT,ij} = \begin{cases} IF & \sigma_{TOT,ij} / (\hat{R} \cdot MOR_i) > 0.02 \\ ELSE & 0.02 \end{cases}, \quad \sigma_{TOT,ij} / (\hat{R} \cdot MOR_i)$$

$$SR_{STB,ij} = \begin{cases} IF & \sigma_{TOT,ij} / MOR_i > 0.02 \\ ELSE & 0.02 \end{cases}, \quad \sigma_{TOT,ij} / MOR_i$$

Figure 25. Equation. Slab stress ratio equation for top and bottom tensile stresses.

Source: Beyer & Roesler (2009)

Where:

$\sigma_{tot,ij}$ = the total stress for temperature frequency bin j of seasonal increment i , (psi)

R = the top of slab tensile strength reduction factor

MOR_i = the concrete modulus of rupture for seasonal increment i , (psi)

$SR_{STT,ij}$ = the stress ratio where nondimensional tensile stress is located at the top of the slab.

$SR_{STB,ij}$ = the stress ratio where nondimensional tensile stress is located at the bottom of the slab.

$$D_{STT,ij} = F_j \cdot \frac{n_{STT,i}}{N_{STT,ij}}$$
$$D_{STB,ij} = F_j \cdot \frac{n_{STB,i}}{N_{STB,ij}}$$

Figure 26. Equation. Cumulative fatigue damage calculation.

Source: Beyer & Roesler (2009)

Where:

F_j = the frequency of occurrence for temperature frequency bin j

n_i = the number of expected load repetitions for seasonal increment i

N_j = the number of allowable load repetitions for each temperature frequency bin j of seasonal increment i

$D_{STT,ij}$ = the fatigue damage for each seasonal increment for critical top position in the CRCP slab

$D_{STB,ij}$ = the fatigue damage for each seasonal increment for critical bottom position in the CRCP slab

Updated CRCP Punchout Prediction Model

The 2009 punchout-to-accumulated-damage calibration curve for CRCP had the following coefficients and statistics: $a = 0.02$, $b = 1 \times 10^{-32}$, $c = 32,386$, $SSE = 371$, and $R^2 = 95\%$. The relationship between observed and predicted punchouts per mile in the 2009 punchout-damage model is depicted in Figures 27 and 28. After new CRCP performance sections were input and the damage calculated in this research, the calibration coefficients “ b ” and “ c ” were slightly changed to the following: $a = 0.02$, $b = 1 \times 10^{-32}$, $c = 30,000$, $SSE = 362$, and $R^2 = 95\%$. Figures 29 and 30 illustrate these relationships for the current punchout-damage model. The inclusion of 28 additional CRCP sections in the database for the 2009 model led to a marginal decrease in the sum square of error (SSE) value from 371 to 362.

ARA’s initial calibration of a CRCP punchout-damage model in 2003 (see Figure 31) based on LTPP and Illinois sections is shown in Figure 32. The MEPDG CRCP punchout prediction achieved an R^2 value of 67% as depicted in Figure 33. The updated punchout-damage model for Illinois in the CRCP Excel design software was found to be reasonable when compared with this previous model. With the improved S-curve punchout performance model and CRCP design framework, updated CRCP design

charts were plotted with the zero-maintenance fatigue equation for 20- and 30-year designs at 50% and 95% reliability including higher traffic factors than the 2009 study.

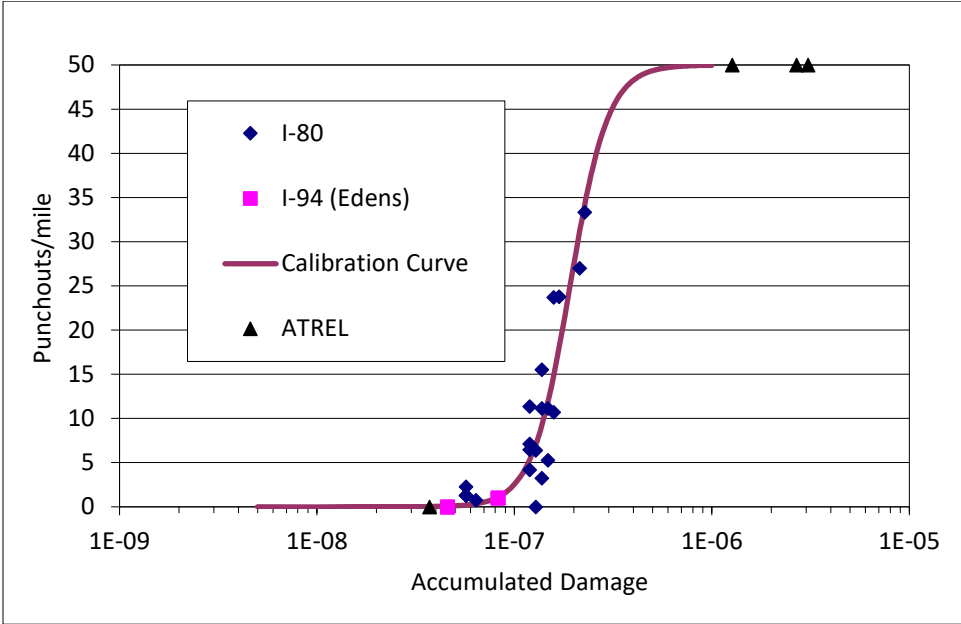


Figure 27. Graph. 2009 S-curve punchout-to-damage model.

Source: Beyer & Roesler (2009)

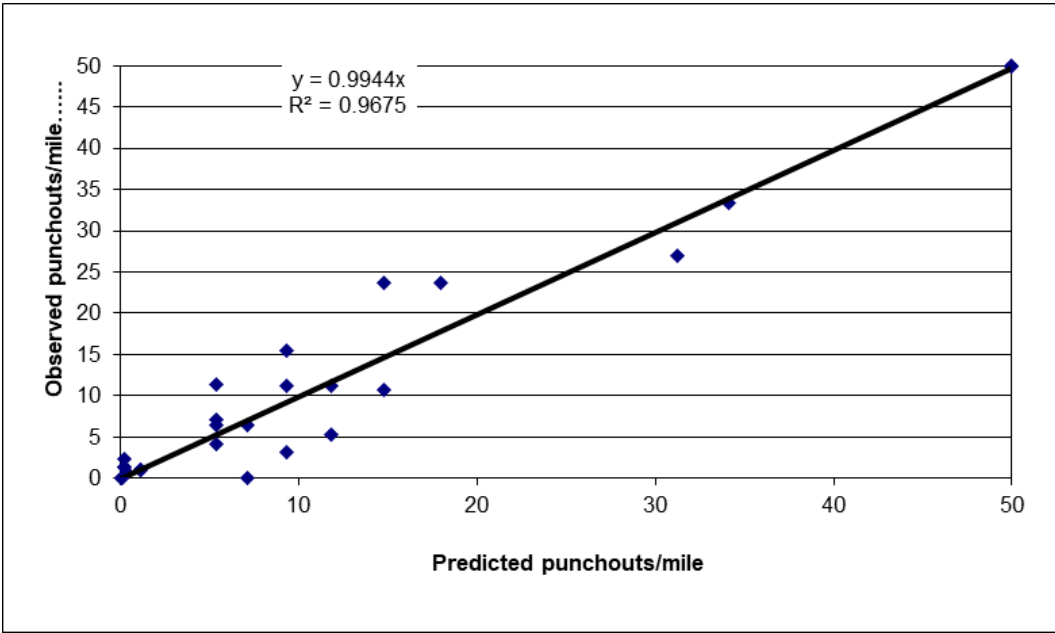


Figure 28. Graph. Accumulated damage versus observed punchout for the 2009 calibration.

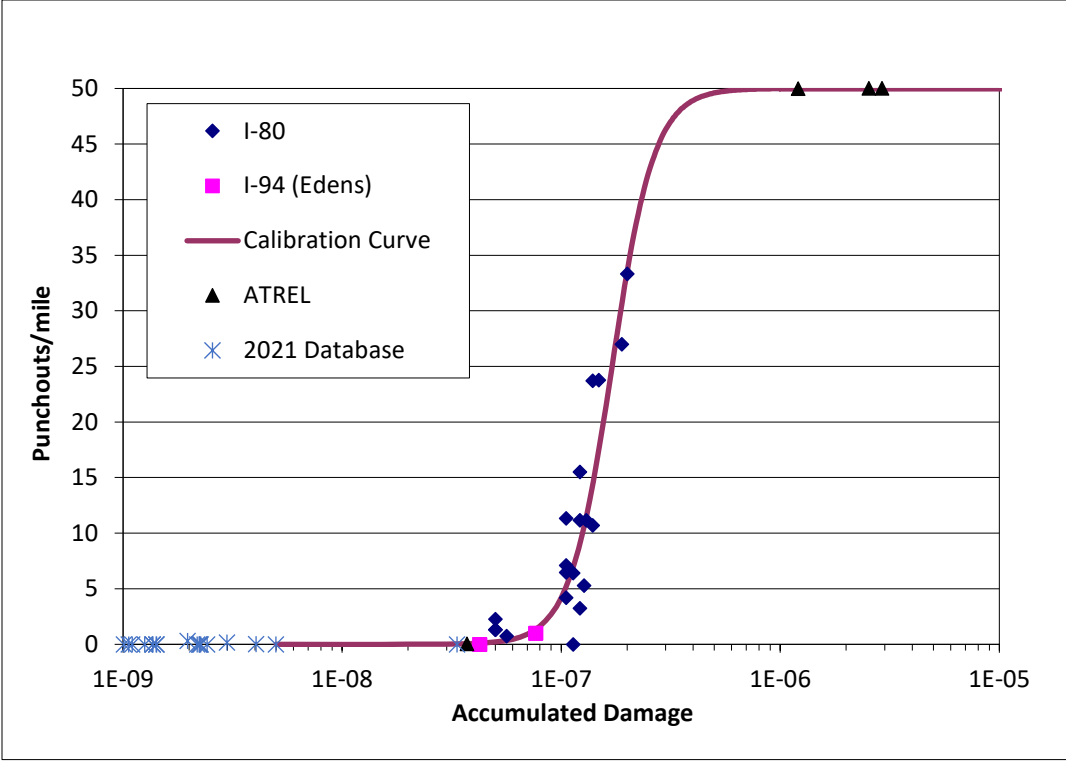


Figure 29. Graph. Current S-Curve punchout-to-damage model.

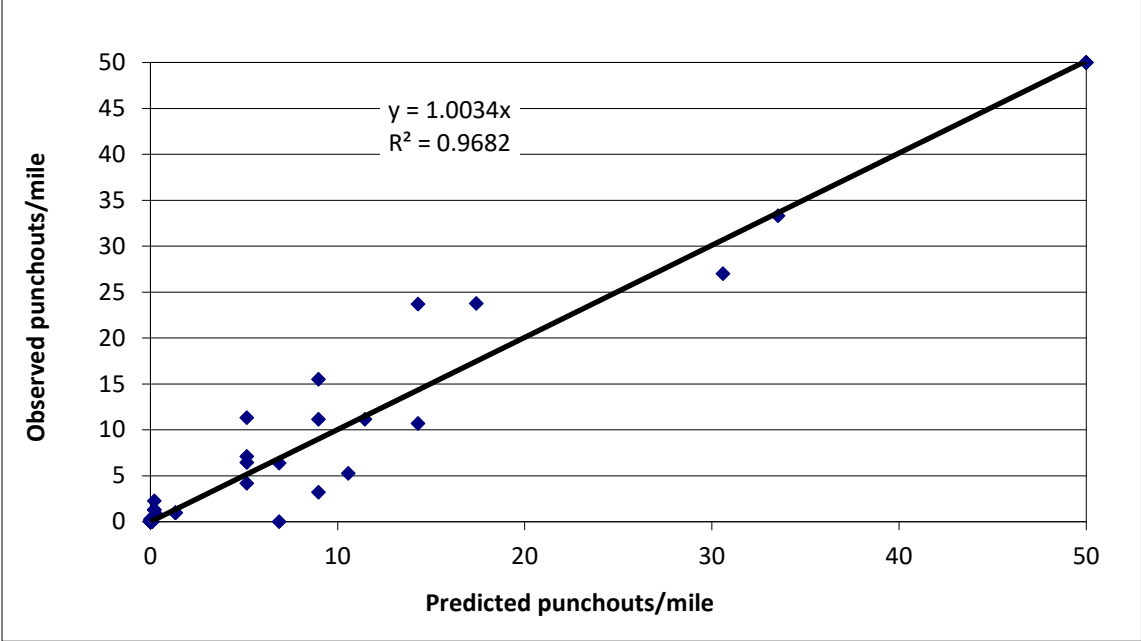


Figure 30. Graph. Accumulated damage versus observed punchout from current recalibration.

$$PO = \frac{C_3}{1 + C_4(DI_{PO})^{C_5}}$$

Figure 31. Equation. Punchout equation used in MEPDG.

Source: AASHTO (2024)

Where:

PO = Total predicted number of medium and high severity punchouts per mile

DI_{PO} = Accumulated fatigue damage (due to slab bending in the transverse direction) at the end of yth year

C₃, C₄, C₅ = Calibration constants (107.73, 2.475, and -0.785, respectively)

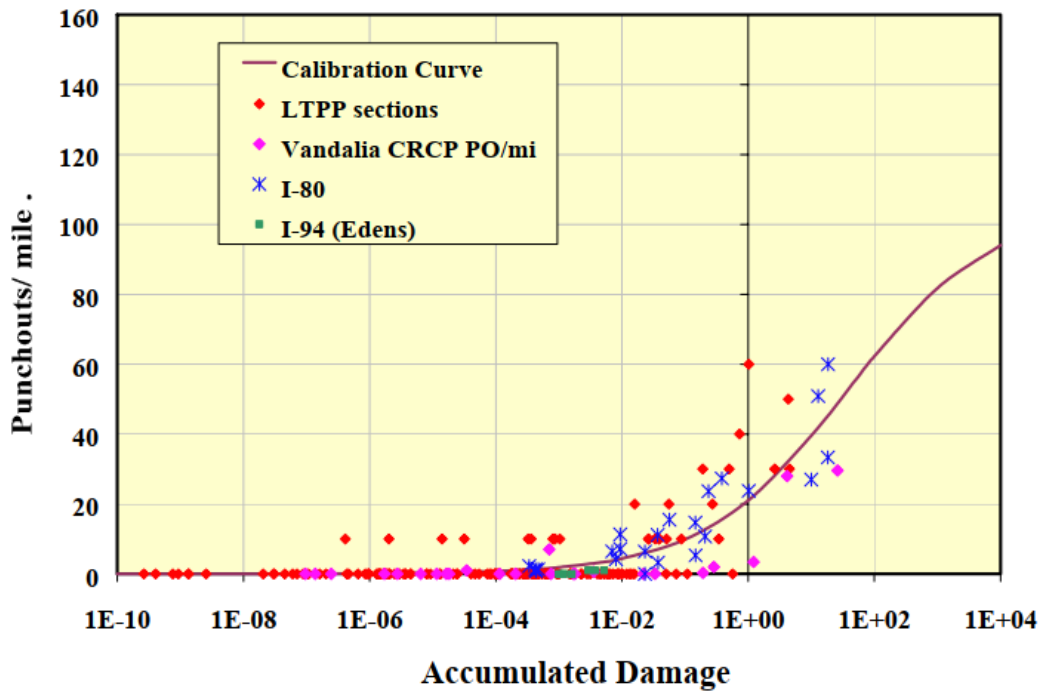


Figure 32. Graph. Relationship between accumulated damage and punchouts from *Guide for Mechanistic Empirical Design of New and Rehabilitated Pavement Structures*.

Source: ARA (2003)

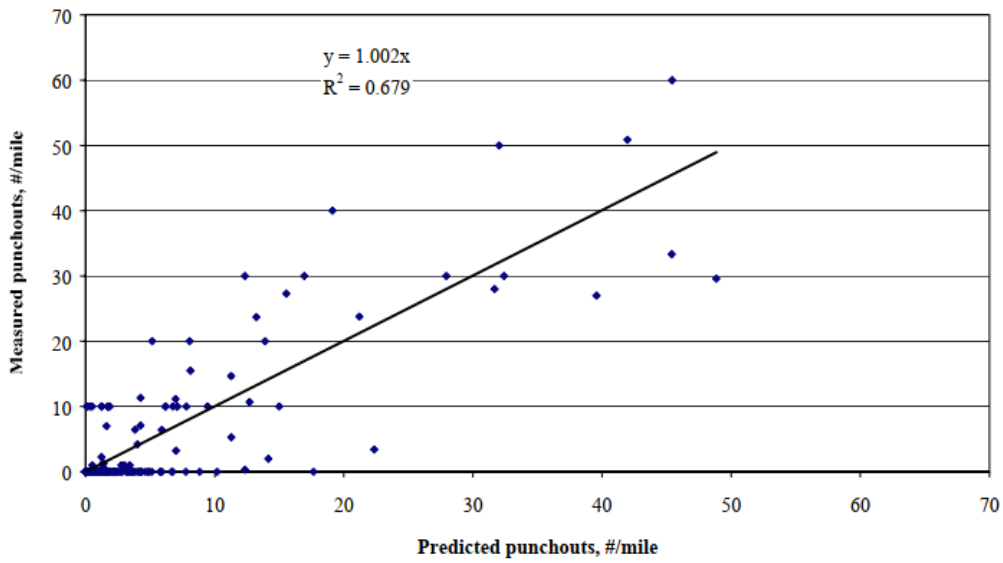


Figure 33. Graph. Predicted vs observed punchouts for nationwide CRCP calibration database ($R^2= 68\%$).
Source: ARA (2003)

CHAPTER 5: UPDATED CRCP DESIGN CHARTS FOR ILLINOIS

With the final punchout to fatigue damage calibration coefficients determined, new CRCP design charts were generated for several design lives, ESAL magnitudes, shoulder types, and K-value support conditions. The CRCP design software implemented in Excel iteratively changes the input slab thickness until less than 10 punchouts per mile were predicted for the design conditions and target life. The recalibration of the performance model was expected to slightly reduce the required slab thicknesses for a given set of design inputs between the 2009 and current CRCP design models.

Design charts were calculated with similar inputs to the 2009 proposed charts except the maximum traffic factor was increased to 300 (i.e., 300 million rigid ESALs) to accommodate expected traffic growth. While maintaining consistent steel diameter and depth requirements for the 20- and 30-year design lives, the steel content has been set at 0.7% for the 20-year design life and 0.8% for the 30-year design life. CRCP design charts were calculated at 50% and 95% reliability for a given set of input conditions. A summary of the inputs for the current CRCP design chart runs is shown in Table 14. The resulting CRCP slab thicknesses are presented in Table 15 and Table 16. Figures 34 to 36 illustrate the results of Table 15 for a 20-year design life at 95% reliability, while Figures 37 to 39 represent the results of Table 16 for a 30-year design at 95% reliability. The accuracy of the updated design charts was improved by reducing the thickness increment in each iteration from 0.5 inches to 0.25 inches, compared with the 2009 charts. For this reason, the design slab thicknesses in the updated CRCP design framework for Illinois for both 20- and 30-year scenarios at 50% and 95% reliability showed an average reduction when compared to the 2009 CRCP design framework (see figures in Appendix D). Specifically, the 20-year CRCP charts revealed a decrease of approximately a quarter inch for asphalt shoulders, and 0.15 and 0.07 inches for tied (monolithic) and tied (separated) PCC shoulders, respectively, relative to the 2009 framework. Additionally, the updated 30-year design charts demonstrated an average thickness reduction of 0.21 inches for asphalt shoulders, 0.09 inches for tied (monolithic), and 0.18 inches for tied (separated) PCC shoulders, compared to the 2009 CRCP design charts.

The sensitivity analysis on the slab thickness of the Updated CRCP Design for 20- and 30-year designs at 95% reliability level with K-values ranging from 50 to 200 psi/in, are detailed as illustrated from Figures 34 to 39. For the 20-year design, under weak subgrade conditions and traffic volumes less than 100 million ESALs, CRCP with monolithic PCC shoulders required less slab thickness than those with asphalt and separate PCC shoulders. However, as traffic volumes increased beyond 140 million ESALs, CRCP designs with asphalt shoulders demanded the least slab thickness, and the gap widened notably once traffic reached beyond 200 million ESALs. On the other hand, in strong subgrade conditions, the CRCP with PCC monolithic shoulder required less thickness than those with asphalt and separate PCC shoulders from the entire traffic range up to 300 million ESALs.

Comparative analysis of the design charts reveals that the trends in the 30-year design are more consistent than those in the 20-year design. As depicted in Figures 37 to 39, the variations in CRCP slab thickness across the different shoulder types are less pronounced in the 30-year design. Notably, in every assessed scenario, the CRCP design incorporating a PCC monolithic shoulder consistently required the least slab thickness. In contrast, the CRCP designs with asphalt shoulders and those with

separate PCC shoulders exhibited only minor differences in their thickness requirements. The 30-year design charts had thinner CRCP slab thickness than the 20-year design chart because for the same traffic level over the design life, a 30-year pavement experiences annually below two-thirds of the AADTT of a 20-year pavement.

Table 14. Inputs for 20- and 30-Year CRCP Design Charts for Updated CRCP Design Framework

| Input | Value | | | Unit |
|---|------------------|---------------|-----------|----------------------|
| | 20 | 30 | | |
| Design Life (20 or 30) | 20 | 30 | | years |
| Steel content | 0.007 | 0.008 | | fraction |
| Reinforcing steel bar diameter | 0.75 | 0.875 | | inches |
| Aggregate type | Limestone | | | |
| Shoulder type | Asphalt | Tied Separate | Tied Mono | |
| Stiffness of the shoulder/lane joint | 0.04 | 0.77 | 4 | |
| Shoulder load transfer efficiency | 5 | 40 | 73 | % |
| Total 18 k ESALs – Design Lane | Varies | | | ESALs |
| Annual growth factor | 0 | | | |
| PCC Elastic modulus, 28 days | 4,400,000 | | | psi |
| PCC Poisson’s ratio | 0.15 | | | |
| PCC Coefficient of thermal expansion | 0.0000055 | | | 1/°F |
| PCC Compressive strength, 28 days | 4500 | | | psi |
| PCC Modulus of rupture, 90 days | 750 | | | psi |
| PCC Modulus of rupture, 28 days | 675 | | | psi |
| PCC Top of Slab Strength Reduction Factor | 0.8 | | | |
| PCC Tensile strength, 28 days | 472.5 | | | psi |
| PCC Ultimate drying shrinkage | 0.00078 | | | in/in |
| PCC Thermal diffusivity | 1.22 | | | ft ² /day |
| Cement content | 600 | | | lb/yd ³ |
| Base Elastic modulus | 1,300,000 | | | psi |
| Base Thickness | 4 | | | inches |
| Base/subbase type | ATB | | | |
| Subbase friction coefficient | 7.5 | | | |
| Base load transfer efficiency | 30 | | | % |
| Construction season | summer | | | |
| PCC temperature at set time at depth of steel | 106 | | | °F |
| Relative humidity in the concrete at depth of steel | 85 | | | % |
| Total stress correction factor | 0.8 | | | |
| Modulus of subgrade reaction for loading | 50, 100, 200 | | | psi/in. |
| Modulus of subgrade reaction for curling | 100 | | | psi/in. |
| Fatigue equation | Zero Maintenance | | | |
| Reliability | 50 or 95 | | | % |
| Failure criterion (number of punchouts per mile) | 10 | | | |

Table 15. 20-Year CRCP Design Thicknesses for Updated CRCP Design Framework

| Shoulder Type = | | | AC | PCC Tied Separate | Monolithic |
|------------------|-------------|----------------|----------------|----------------------|----------------|
| k-value, psi/in. | Reliability | Millions ESALs | Thickness, in. | Thickness, in. | Thickness, in. |
| 50 | 50 | 10 | 9.75 | 9.75 | 9.75 |
| 50 | 50 | 35 | 10.50 | 10.5 | 10.25 |
| 50 | 50 | 70 | 10.75 | 11.00 | 10.50 |
| 50 | 50 | 100 | 11.00 | 11.00 | 10.75 |
| 50 | 50 | 150 | 11.25 | 11.50 | 11.00 |
| 50 | 50 | 200 | 11.25 | 11.50 | 11.25 |
| 50 | 50 | 300 | 11.75 | 12.00 | 11.50 |
| 50 | 95 | 10 | 10.50 | 10.50 | 10.25 |
| 50 | 95 | 35 | 11.25 | 11.25 | 11.00 |
| 50 | 95 | 70 | 11.50 | 12.00 | 11.50 |
| 50 | 95 | 100 | 11.75 | 12.25 | 11.75 |
| 50 | 95 | 150 | 12.00 | 12.50 | 12.25 |
| 50 | 95 | 200 | 12.25 | 12.75 | 12.50 |
| 50 | 95 | 300 | 12.50 | 13.25 | 13.00 |
| 100 | 50 | 10 | 9.50 | 9.50 | 9.25 |
| 100 | 50 | 35 | 10.00 | 10.00 | 9.75 |
| 100 | 50 | 70 | 10.50 | 10.50 | 10.25 |
| 100 | 50 | 100 | 10.50 | 10.75 | 10.25 |
| 100 | 50 | 150 | 10.75 | 11.00 | 10.50 |
| 100 | 50 | 200 | 11.00 | 11.25 | 10.75 |
| 100 | 50 | 300 | 11.25 | 11.50 | 11.00 |
| 100 | 95 | 10 | 10.25 | 10.25 | 9.75 |
| 100 | 95 | 35 | 10.75 | 11.00 | 10.50 |
| 100 | 95 | 70 | 11.25 | 11.50 | 11.00 |
| 100 | 95 | 100 | 11.50 | 11.75 | 11.25 |
| 100 | 95 | 150 | 11.75 | 12.00 | 11.75 |
| 100 | 95 | 200 | 12.00 | 12.25 | 12.00 |
| 100 | 95 | 300 | 12.25 | 12.75 | 12.50 |
| 200 | 50 | 10 | 9.00 | 9.00 | 8.75 |
| 200 | 50 | 35 | 9.50 | 9.50 | 9.25 |
| 200 | 50 | 70 | 10.00 | 10.00 | 9.50 |
| 200 | 50 | 100 | 10.00 | 10.25 | 9.75 |
| 200 | 50 | 150 | 10.25 | 10.50 | 10.00 |
| 200 | 50 | 200 | 10.50 | 10.75 | 10.25 |
| 200 | 50 | 300 | 10.75 | 11.00 | 10.50 |
| 200 | 95 | 10 | 9.75 | 9.75 | 9.25 |
| 200 | 95 | 35 | 10.25 | 10.50 | 10.00 |
| 200 | 95 | 70 | 10.75 | 11.00 | 10.50 |
| 200 | 95 | 100 | 11.00 | 11.25 | 10.75 |
| 200 | 95 | 150 | 11.25 | 11.50 | 11.00 |
| 200 | 95 | 200 | 11.50 | 11.75 | 11.25 |
| 200 | 95 | 300 | 11.75 | 12.25 | 11.75 |

Table 16. 30-Year CRCP Design Thicknesses for Updated CRCP Design Framework

| Shoulder Type = | | | AC | PCC Tied Separate | Monolithic |
|------------------|-------------|----------------|----------------|-------------------|----------------|
| k-value, psi/in. | Reliability | Millions ESALs | Thickness, in. | Thickness, in. | Thickness, in. |
| 50 | 50 | 10 | 9.75 | 9.50 | 9.50 |
| 50 | 50 | 35 | 10.25 | 10.25 | 10.00 |
| 50 | 50 | 70 | 10.75 | 10.50 | 10.50 |
| 50 | 50 | 100 | 11.00 | 10.75 | 10.50 |
| 50 | 50 | 150 | 11.25 | 11.00 | 10.75 |
| 50 | 50 | 200 | 11.25 | 11.25 | 11.00 |
| 50 | 50 | 300 | 11.50 | 11.50 | 11.25 |
| 50 | 95 | 10 | 10.50 | 10.25 | 10.00 |
| 50 | 95 | 35 | 11.00 | 11.00 | 10.75 |
| 50 | 95 | 70 | 11.50 | 11.50 | 11.25 |
| 50 | 95 | 100 | 11.75 | 11.75 | 11.50 |
| 50 | 95 | 150 | 12.00 | 12.25 | 11.75 |
| 50 | 95 | 200 | 12.25 | 12.50 | 12.00 |
| 50 | 95 | 300 | 12.50 | 13.00 | 12.50 |
| 100 | 50 | 10 | 9.25 | 9.00 | 8.75 |
| 100 | 50 | 35 | 10.00 | 9.75 | 9.50 |
| 100 | 50 | 70 | 10.25 | 10.00 | 9.75 |
| 100 | 50 | 100 | 10.50 | 10.25 | 10.00 |
| 100 | 50 | 150 | 10.75 | 10.50 | 10.25 |
| 100 | 50 | 200 | 11.00 | 10.75 | 10.50 |
| 100 | 50 | 300 | 11.25 | 11.25 | 10.75 |
| 100 | 95 | 10 | 10.00 | 9.75 | 9.50 |
| 100 | 95 | 35 | 10.75 | 10.50 | 10.25 |
| 100 | 95 | 70 | 11.00 | 11.00 | 10.75 |
| 100 | 95 | 100 | 11.25 | 11.25 | 11.00 |
| 100 | 95 | 150 | 11.75 | 11.75 | 11.25 |
| 100 | 95 | 200 | 11.75 | 12.00 | 11.50 |
| 100 | 95 | 300 | 12.25 | 12.25 | 12.00 |
| 200 | 50 | 10 | 8.75 | 8.50 | 8.50 |
| 200 | 50 | 35 | 9.00 | 9.25 | 8.75 |
| 200 | 50 | 70 | 9.75 | 9.50 | 9.25 |
| 200 | 50 | 100 | 10.00 | 9.75 | 9.50 |
| 200 | 50 | 150 | 10.25 | 10.00 | 9.75 |
| 200 | 50 | 200 | 10.25 | 10.25 | 10.00 |
| 200 | 50 | 300 | 10.50 | 10.50 | 10.25 |
| 200 | 95 | 10 | 9.25 | 9.25 | 9.00 |
| 200 | 95 | 35 | 10.00 | 10.00 | 9.75 |
| 200 | 95 | 70 | 10.50 | 10.50 | 10.00 |
| 200 | 95 | 100 | 10.75 | 10.75 | 10.25 |
| 200 | 95 | 150 | 11.00 | 11.25 | 10.75 |
| 200 | 95 | 200 | 11.25 | 11.50 | 11.00 |
| 200 | 95 | 300 | 11.50 | 11.75 | 11.25 |

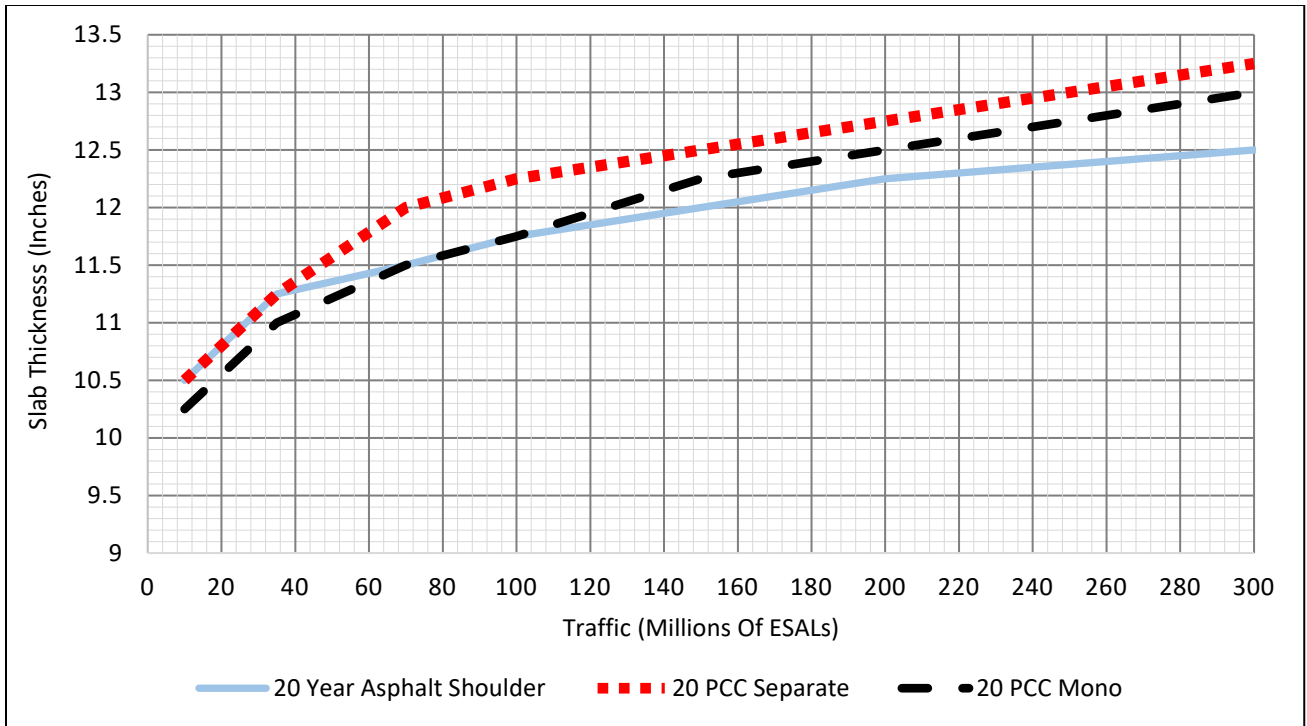


Figure 34. Graph. CRCP slab thickness at 95% reliability, K-value = 50 psi/in., and three shoulder types for a 20-year design.

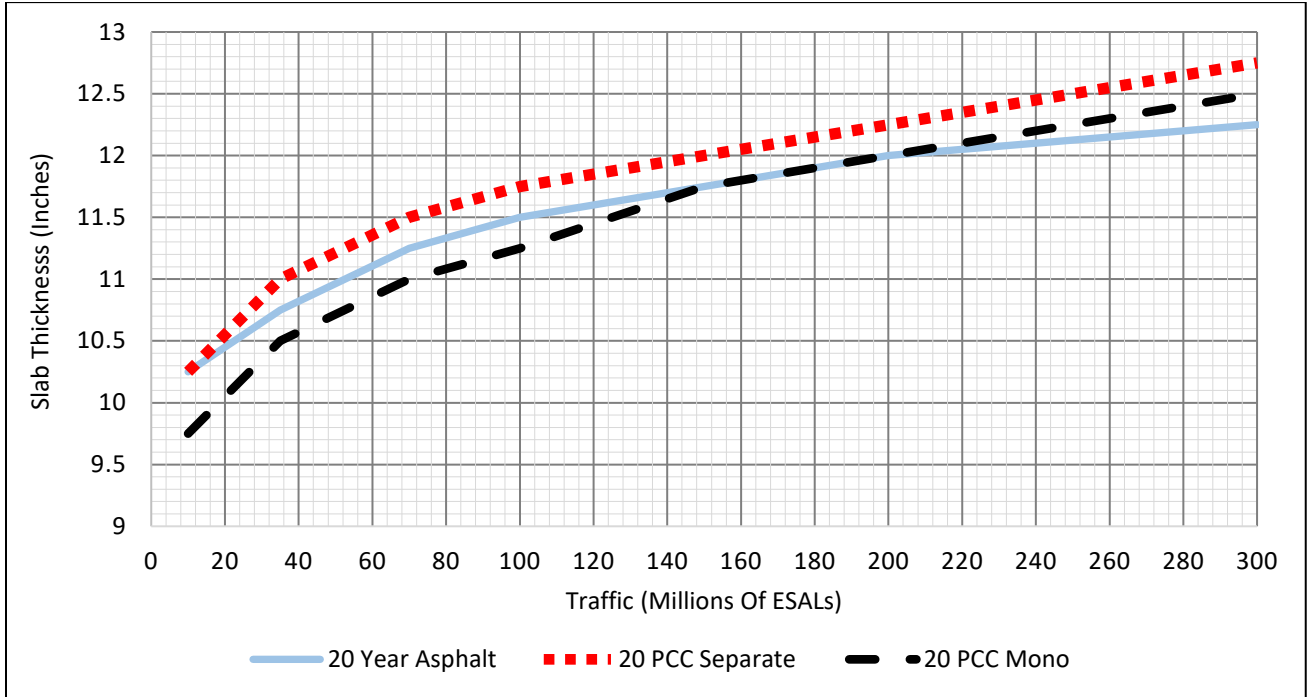


Figure 35. Graph. CRCP slab thickness at 95% reliability, K-value = 100 psi/in., and three shoulder types for a 20-year design.

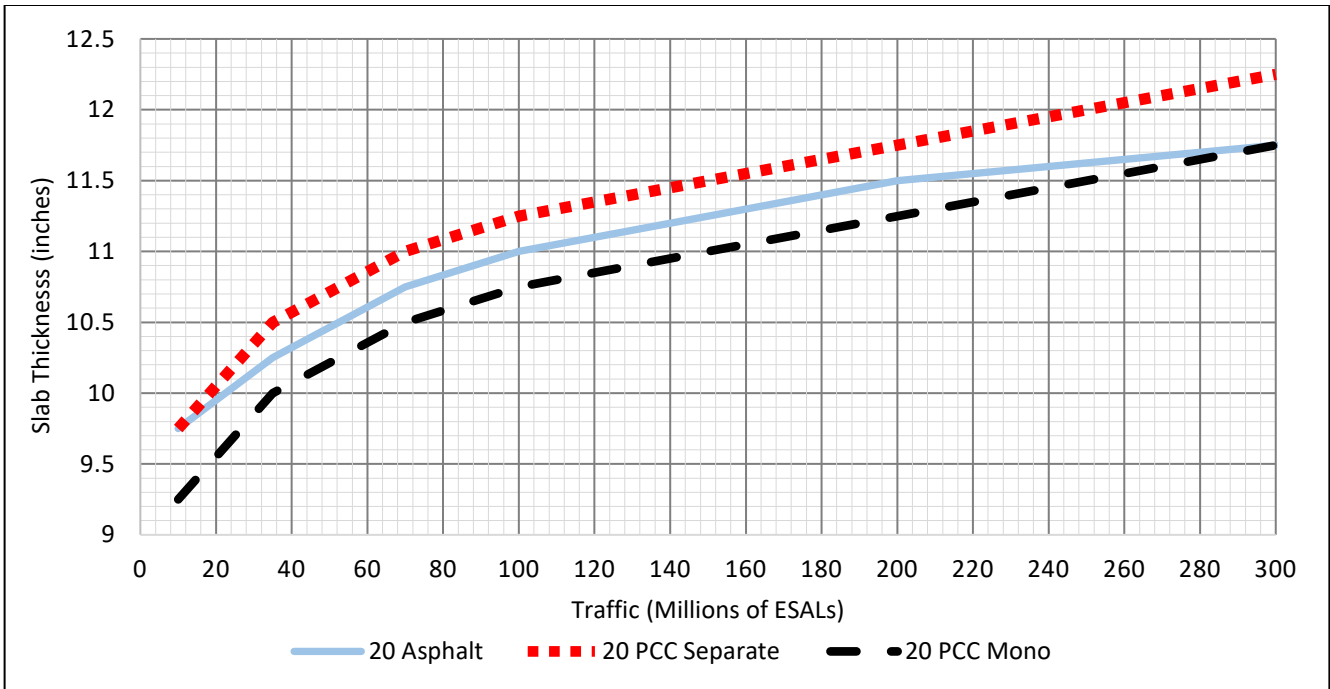


Figure 36. Graph. CRCP slab thickness at 95% reliability, K-value = 200 psi/in., and three shoulder types for a 20-year design.

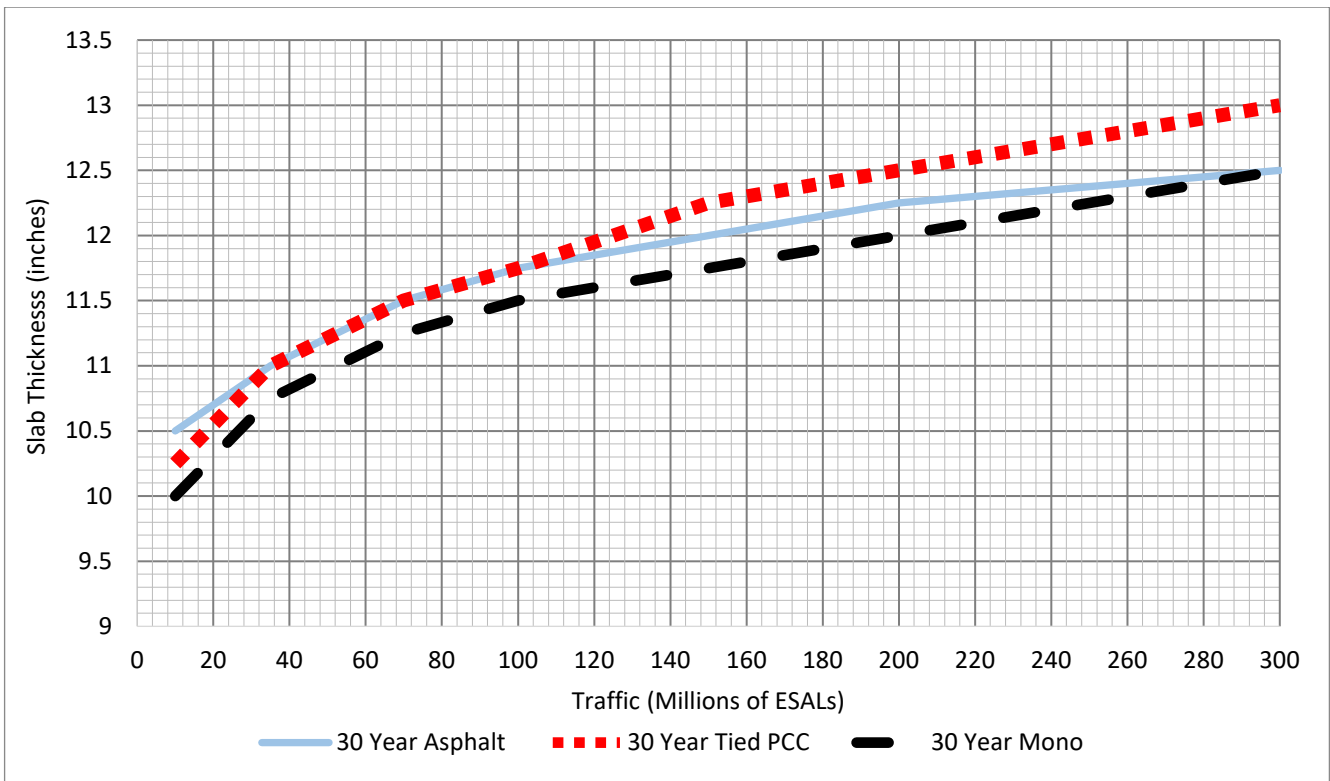


Figure 37. Graph. CRCP slab thickness at 95% reliability, K-value = 50 psi/in., and three shoulder types for a 30-year design.

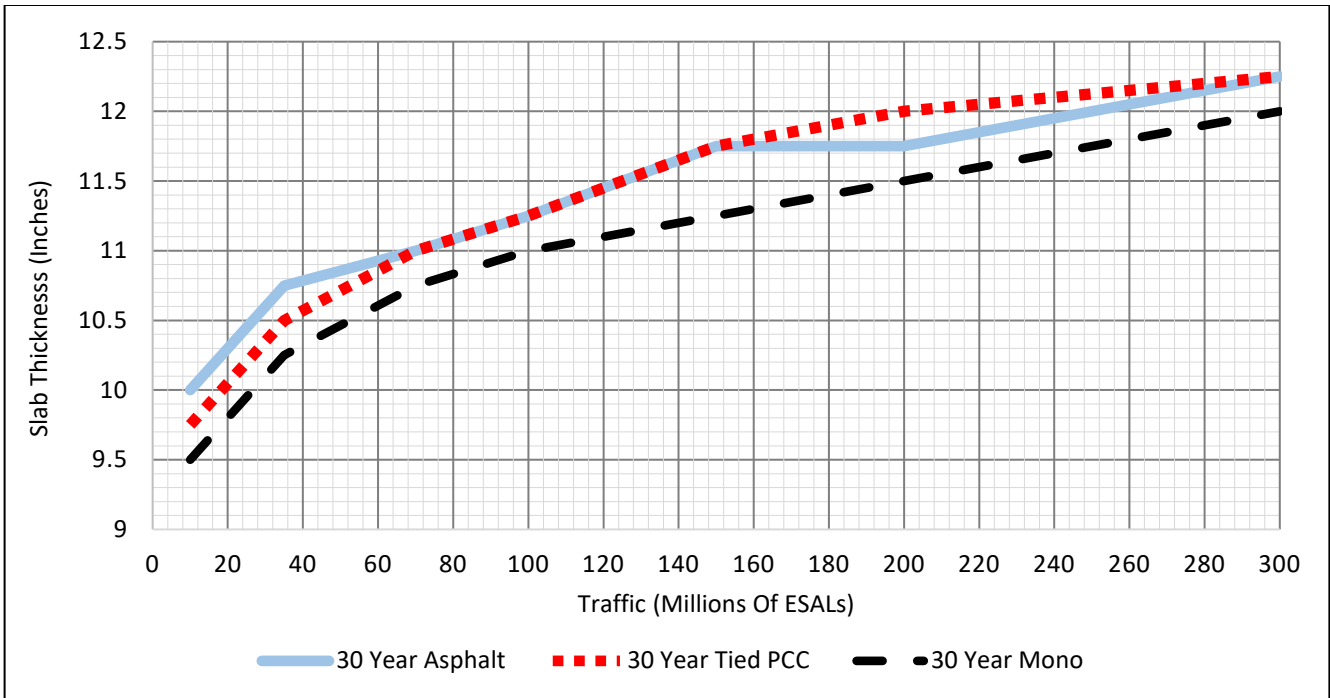


Figure 38. Graph. CRCP slab thickness at 95% reliability, K-value = 100 psi/in., and three shoulder types for a 30-year design.

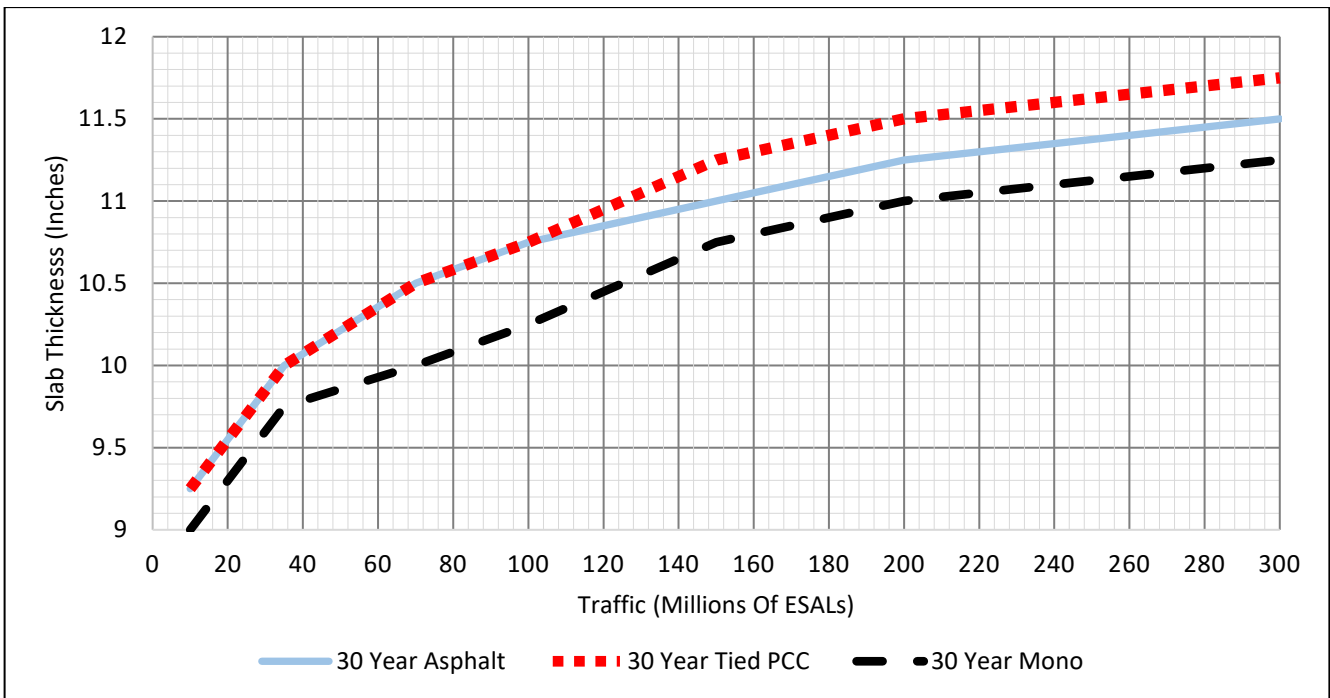


Figure 39. Graph. CRCP slab thickness at 95% reliability, K-value = 200 psi/in., and three shoulder types for a 30-year design.

CRCP DESIGN COMPARISON OF UIUC'S UPDATED CRCP DESIGN FRAMEWORK VS. AASHTOWARE PAVEMENT ME DESIGN

A comparative analysis was performed between the AASHTOWare Pavement ME Design software and the current recalibrated CRCP design software in Excel for this project to determine the reasonableness and sensitivity of the proposed Excel design software relative to AASHTOWare. As noted in this chapter, AASHTOWare Pavement ME Design for CRCP used a nationally calibrated punchout-damage model (AASHTO, 2024). The UIUC CRCP Excel Design software was calibrated specifically to existing Illinois CRCP sections (new and overlays). There are many similarities between the AASHTOWare Pavement ME Design and proposed CRCP design framework, but the main differences are the fatigue equations, punchout-to-damage function, and consideration of void development in the tensile stress calculations with the MEPDG model.

The two different design methods were compared over ESALs from 10 million to 300 million and K-values of 50, 100, and 200 psi/in. For the AASHTO Pavement ME Design program, it is not possible to directly input the supporting K-value. Therefore, pavement structures were built with various thicknesses and moduli to create estimated composite (support) K-values of 50, 100, and 200 psi/in. comparable to the proposed CRCP method. The ACPA combined K-value calculator (American Concrete Pavement Association, n.d.) was used to build layers to a desired K-value. The layers and respective thickness and stiffness inputs for the AASHTO Pavement Design ME software are shown in Table 17 through Table 19. The concrete properties in the AASHTO Pavement ME Design software were also changed to match UIUC CRCP default concrete properties (Table 14).

For each design life in the AASHTOWare Pavement ME Design, an analysis was performed to convert the AADTT to ESALs given the TTC1 traffic option, as shown in Table 20. For the same amount of ESALs over the design life, a 30-year pavement will receive 60% of the AADTT of the 20-year pavement (i.e., 20-year pavement designs receive more traffic per day). For a 20-year design, more traffic and damage occur earlier in the concrete pavement life. Table 21 and 22 illustrated the inputs for CRCP design properties required by the AASHTOWare Pavement ME software.

Appendix E shows the complete set of thickness comparison tables for 20- and 30-year new CRCP designs for asphalt, tied separate, and monolithic shoulders at K-values of 50, 100, and 200 psi/in. at 50% and 95% reliability between the updated CRCP design framework and the AASHTOWare Pavement ME Design. A summary of the comparison of CRCP slab thickness for 20- and 30-year designs between the proposed CRCP method and the AASHTO Pavement ME Design software for different types of shoulders and K-values, and variable traffic are presented in Table 23 and 24.

The trends of the CRCP thickness calculations by both methods showed that AASHTOWare Pavement ME Design was more sensitive to the increase in accumulated traffic than the proposed CRCP design framework, as illustrated in Figures 40 to 48. Under lower traffic conditions, AASHTOWare Pavement ME Design recommended thinner design slabs compared to the proposed CRCP design framework. However, as traffic increased, the rate of increase in required thickness for AASHTOWare Pavement ME Design was significantly higher. As seen in Figures 40 to 48, the two methods' results intersected at moderate traffic levels, and beyond this intersection, AASHTOWare Pavement ME Design specified thicker slabs for high traffic volumes. Moreover, the crossing points of design thickness from both

methods were noticeably affected by the modulus of subgrade reaction (k-value), with the crossing points shifting to intersect at lower traffic volumes as the k-value increased. The observed greater variations in slab thickness calculated by the AASHTOWare Pavement ME design is attributed to the inclusion of base erosion in the stress calculations whereas the proposed CRCP design framework does not directly account for erosion in design calculations.

Table 17. Layer Inputs for AASHTOWare for Composite K = 200 psi/in.

| Material | MR (psi) | Thickness (in.) |
|----------------------------|----------|-----------------|
| A-7-6 | 4,000 | Subgrade |
| Unstabilized Granular Base | 15,000 | 4 |
| Asphalt-Treated Base | 350,000 | 4 |

Table 18. Layer Inputs for AASHTOWare for Composite K = 100 psi/in.

| Material | MR (psi) | Thickness |
|----------------------------|----------|-----------|
| A-7-6 | 2,000 | Subgrade |
| Unstabilized Granular Base | 15,000 | 4 |
| Asphalt-Treated Base | 350,000 | 4 |

Table 19. Layer Inputs for AASHTOWare for Composite K = 50 psi/in.

| Material | MR (psi) | Thickness |
|----------------------------|----------|-----------|
| A-7-6 | 850 | Subgrade |
| Unstabilized Granular Base | 15,000 | 4 |
| Asphalt-Treated Base | 350,000 | 4 |

Table 20. Comparison of 20- and 30-Year AADTT versus ESALs for AASHTO Traffic Input

| AADTT (20 Year) | AADTT (30 Year) | Traffic (Millions of ESALs) |
|-----------------|-----------------|-----------------------------|
| 1,326 | 792 | 10 |
| 4,643 | 2,772 | 35 |
| 9,286 | 5,544 | 70 |
| 13,266 | 7,920 | 100 |
| 19,898 | 11,879 | 150 |
| 26,531 | 15,839 | 200 |
| 39,797 | 23,759 | 300 |

Table 21. AASHTO Pavement ME Inputs for 20-Year CRCP Designs

| AASHTO Layer | Thickness (in.) | Modulus (ksi) | MOR28 (psi) | Poisson | Unit Weight (pcf) | Bar Diameter (in.) | Steel % | Depth (in.) | SSA | CoTE x10 ⁻⁶ (1/°F) | Heat Capacity (BTU/lb-°F) | Conductivity (BTU/hr-ft-°F) | Aggregate Type |
|--------------|-----------------|---------------|-------------|---------|-------------------|--------------------|---------|-------------|------|-------------------------------|---------------------------|-----------------------------|----------------|
| CRCP | Varies | 4,400 | 675 | 0.15 | 150 | 0.75 | 0.7 | Varies | 0.85 | 5.5 | 0.28 | 1.25 | Limestone |

*MOR28 is flexural strength at 28 days, SSA is short-wave surface absorptivity, and CoTE is concrete coefficient of thermal expansion.

Table 22. AASHTO Pavement ME Inputs for 30-Year CRCP Designs

| AASHTO Layer | Thickness (in.) | Modulus (ksi) | MOR28 (psi) | Poisson | Unit Weight (pcf) | Bar Diameter (in.) | Steel% | Depth (in.) | SSA | CoTE x10 ⁻⁶ (1/°F) | Heat Capacity (BTU/lb-°F) | Conductivity (BTU/hr-ft-°F) | Aggregate Type |
|--------------|-----------------|---------------|-------------|---------|-------------------|--------------------|--------|-------------|------|-------------------------------|---------------------------|-----------------------------|----------------|
| CRCP | Varies | 4,400 | 675 | 0.15 | 150 | 0.875 | 0.8 | Varies | 0.85 | 5.5 | 0.28 | 1.25 | Limestone |

*MOR28 is flexural strength at 28 days, SSA is short-wave surface absorptivity, and CoTE is concrete coefficient of thermal expansion.

**Table 23. AASHTOWare Pavement ME Design versus Proposed CRCP Design Thickness
Comparisons for Tied Shoulder and 20-Year Design Life**

| K-value (psi/in.) | Traffic (Millions of ESALs) | R% | Proposed CRCP Design Thickness (in.) | | | AASHTOWARE Pavement ME Design Thickness (in.) | | |
|----------------------|-----------------------------------|----|--------------------------------------|------------|---------------|--|------------|---------------|
| | | | AC | Monolithic | Tied Separate | AC | Monolithic | Tied Separate |
| 50 | 10 | 95 | 10.50 | 10.25 | 10.50 | 8.50 | 7.50 | 8.00 |
| 50 | 35 | 95 | 11.25 | 11.00 | 11.25 | 10.00 | 8.50 | 9.00 |
| 50 | 70 | 95 | 11.50 | 11.50 | 12.00 | 11.00 | 9.50 | 10.50 |
| 50 | 150 | 95 | 12.00 | 12.25 | 12.50 | 12.50 | 11.50 | 12.00 |
| 50 | 300 | 95 | 12.50 | 13.00 | 13.25 | 14.00 | 13.50 | 13.50 |
| 100 | 10 | 95 | 10.25 | 9.75 | 10.25 | 8.50 | 7.50 | 7.50 |
| 100 | 35 | 95 | 10.75 | 10.50 | 11.00 | 10.00 | 8.50 | 9.00 |
| 100 | 70 | 95 | 11.25 | 11.00 | 11.50 | 11.00 | 10.00 | 10.50 |
| 100 | 150 | 95 | 11.75 | 11.75 | 12.00 | 13.00 | 11.50 | 12.00 |
| 100 | 300 | 95 | 12.25 | 12.50 | 12.75 | 14.50 | 13.50 | 14.00 |
| 200 | 10 | 95 | 9.75 | 9.25 | 9.75 | 8.00 | 8.00 | 7.50 |
| 200 | 35 | 95 | 10.25 | 10.00 | 10.50 | 9.50 | 8.50 | 9.00 |
| 200 | 70 | 95 | 10.75 | 10.50 | 11.00 | 11.00 | 10.00 | 10.50 |
| 200 | 150 | 95 | 11.25 | 11.00 | 11.50 | 13.00 | 12.00 | 12.00 |
| 200 | 300 | 95 | 11.75 | 11.75 | 12.25 | 15.00 | 13.50 | 14.00 |

**Table 24. AASHTOWare Pavement ME Design versus Proposed CRCP Design Thickness
Comparisons for Tied Shoulder and 30-Year Design Life**

| K-value | Traffic (Millions of ESALs) | R% | Proposed CRCP Design Thickness (in.) | | | AASHTOWARE Pavement ME Design Thickness (in.) | | |
|---------|-----------------------------------|----|--------------------------------------|------------|---------------|---|------------|---------------|
| | | | AC | Monolithic | Tied Separate | AC | Monolithic | Tied Separate |
| 50 | 10 | 95 | 10.50 | 10.00 | 10.25 | 8.50 | 7.50 | 8.00 |
| 50 | 35 | 95 | 11.00 | 10.75 | 11.00 | 10.00 | 8.50 | 9.00 |
| 50 | 70 | 95 | 11.50 | 11.25 | 11.50 | 11.00 | 10.00 | 10.50 |
| 50 | 150 | 95 | 11.75 | 11.50 | 11.75 | 12.50 | 11.50 | 12.00 |
| 50 | 300 | 95 | 12.00 | 11.75 | 12.25 | 14.50 | 13.50 | 13.50 |
| 100 | 10 | 95 | 10.00 | 9.50 | 9.75 | 8.50 | 7.50 | 7.50 |
| 100 | 35 | 95 | 10.75 | 10.25 | 10.50 | 10.00 | 8.50 | 9.00 |
| 100 | 70 | 95 | 11.00 | 10.75 | 11.00 | 11.00 | 10.00 | 10.50 |
| 100 | 150 | 95 | 11.25 | 11.00 | 11.25 | 13.00 | 12.50 | 12.50 |
| 100 | 300 | 95 | 11.75 | 11.25 | 11.75 | 14.50 | 13.50 | 14.00 |
| 200 | 10 | 95 | 9.25 | 9.00 | 9.25 | 8.00 | 7.50 | 7.50 |
| 200 | 35 | 95 | 10.00 | 9.75 | 10.00 | 10.00 | 8.50 | 9.00 |
| 200 | 70 | 95 | 10.50 | 10.00 | 10.50 | 11.50 | 10.00 | 10.50 |
| 200 | 150 | 95 | 10.75 | 10.25 | 10.75 | 13.00 | 13.00 | 13.00 |
| 200 | 300 | 95 | 11.00 | 10.75 | 11.25 | 15.00 | 14.00 | 14.50 |

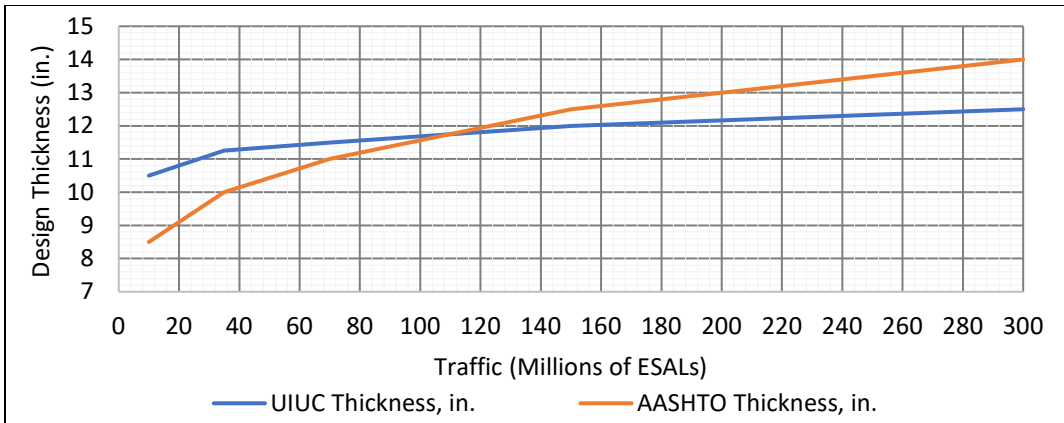


Figure 40. Graph. Comparison of CRCP thickness between proposed CRCP design framework and AASHTOWare Pavement ME Design (20-year design, K = 50 psi/in., asphalt shoulder).

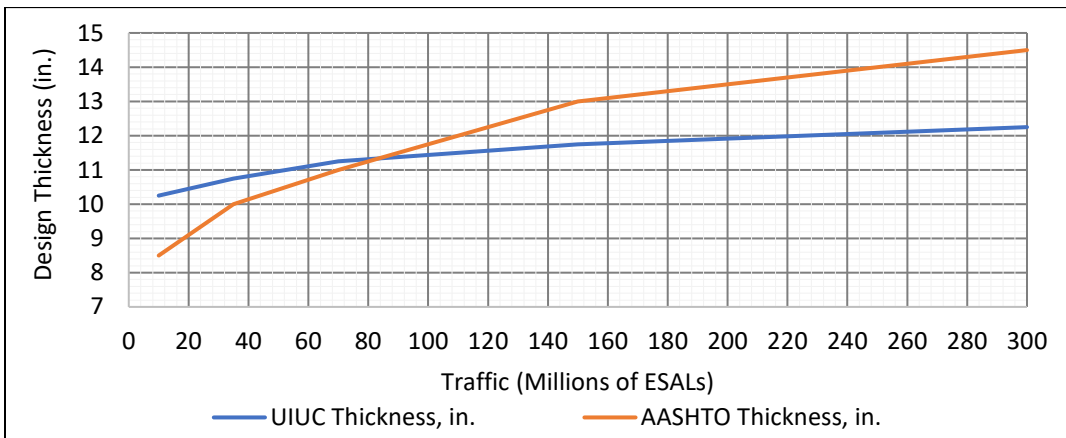


Figure 41. Graph. Comparison of CRCP thickness between proposed CRCP design framework and AASHTOWare Pavement ME Design (20-year design, K = 100 psi/in., asphalt shoulder).

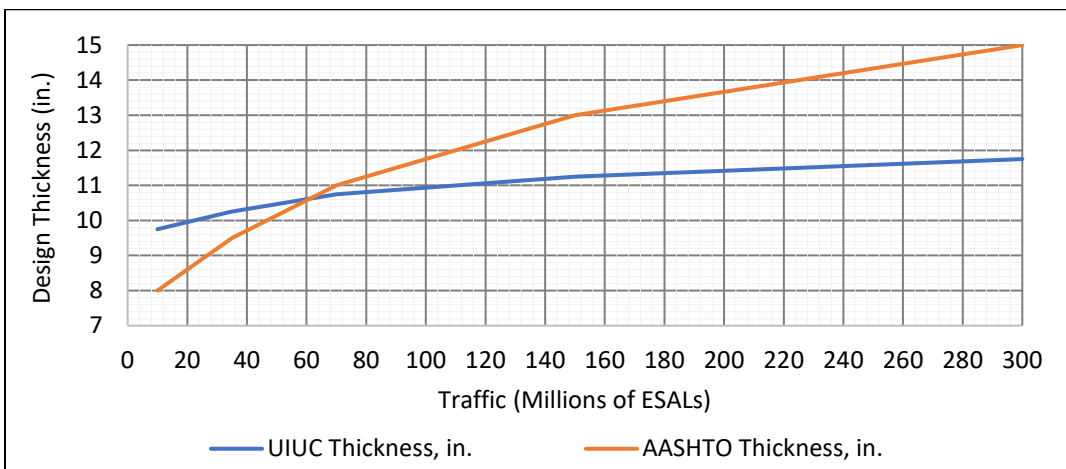


Figure 42. Graph. Comparison of CRCP thickness between proposed CRCP design framework and AASHTOWare Pavement ME Design (20-year design, K = 200 psi/in., asphalt shoulder).

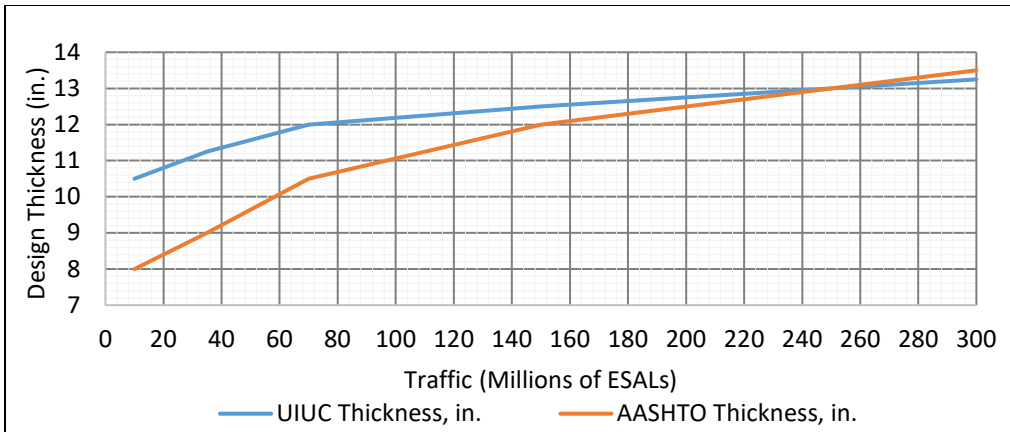


Figure 43. Graph. Comparison of CRCP thickness between proposed CRCP design framework and AASHTOWare Pavement ME Design (20-year design, K = 50 psi/in., PCC tied separate shoulder).

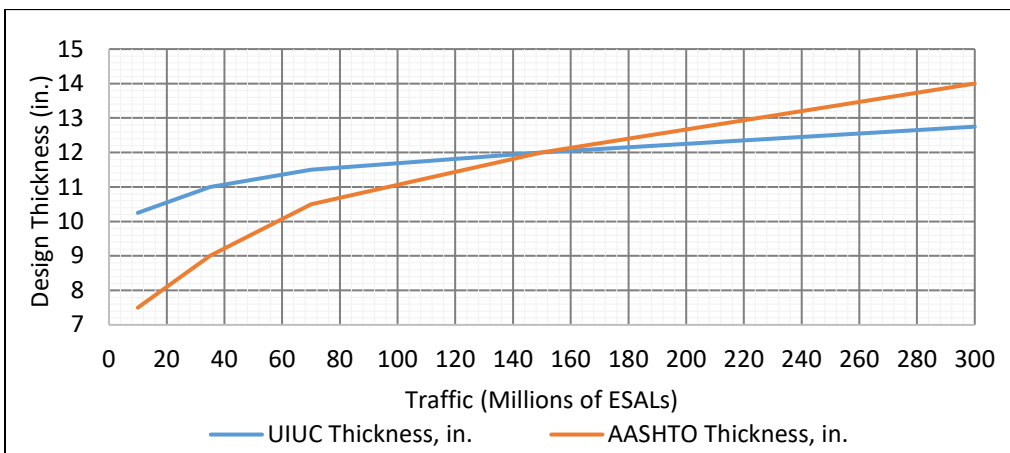


Figure 44. Graph. Comparison of CRCP thickness between proposed CRCP design framework and AASHTOWare Pavement ME Design (20-year design, K = 100 psi/in., PCC tied separate shoulder).

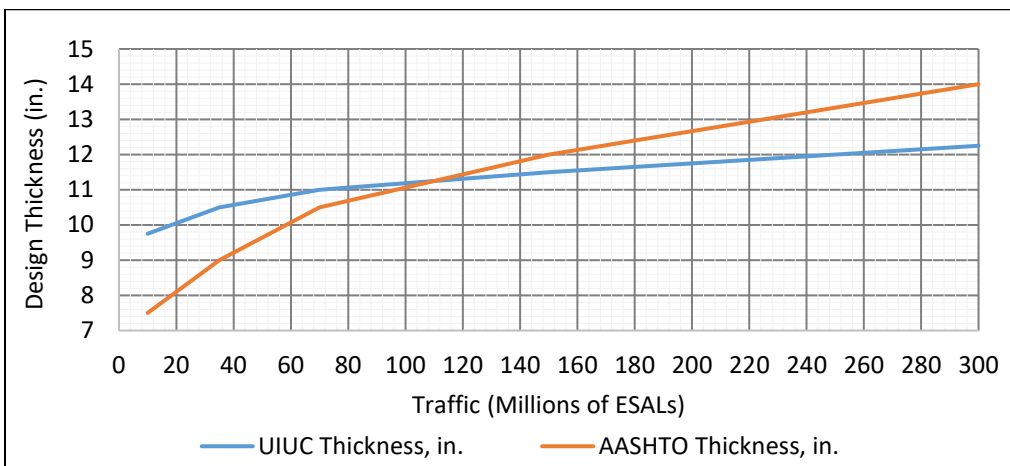


Figure 45. Graph. Comparison of CRCP thickness between proposed CRCP design framework and AASHTOWare Pavement ME Design (20-year design, K = 200 psi/in., PCC tied separate shoulder).

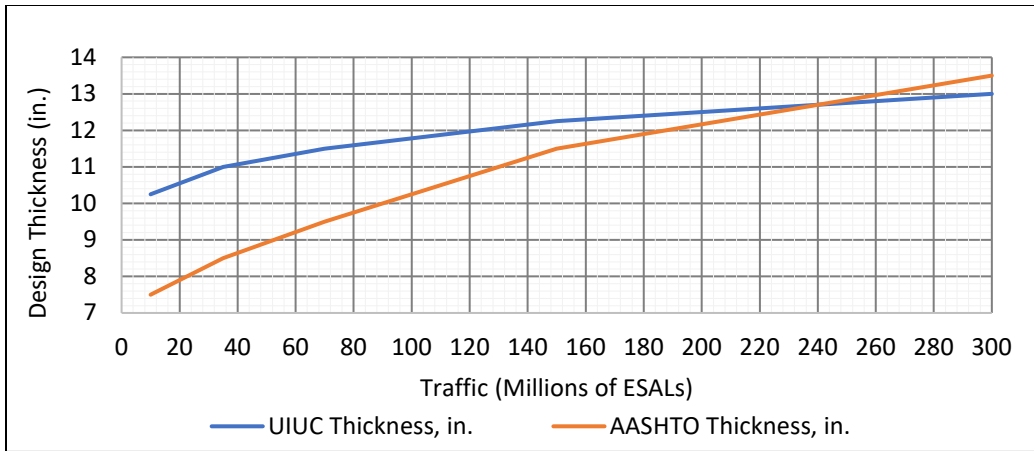


Figure 46. Graph. Comparison of CRCP thickness between proposed CRCP design framework and AASHTOWare Pavement ME Design (20-year design, K = 50 psi/in., PCC tied monolithic shoulder).

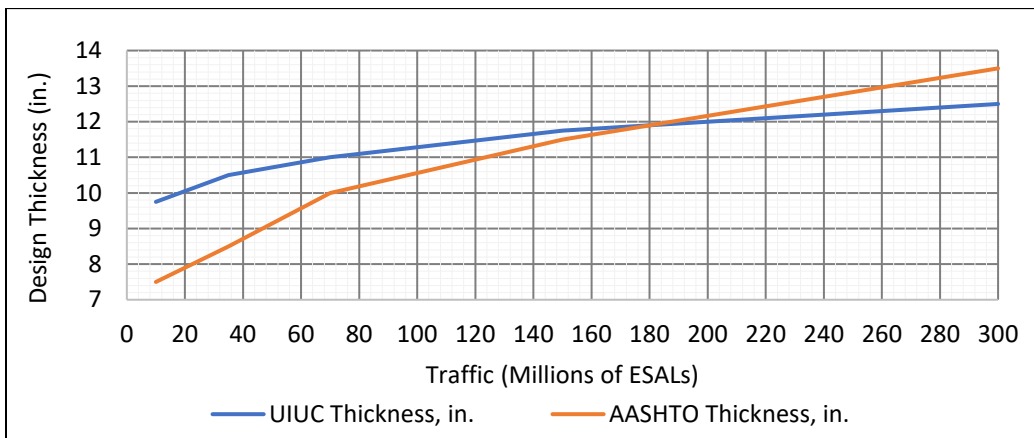


Figure 47. Graph. Comparison of CRCP thickness between proposed CRCP design framework and AASHTOWare Pavement ME Design (20-year design, K = 100 psi/in., PCC tied monolithic shoulder).

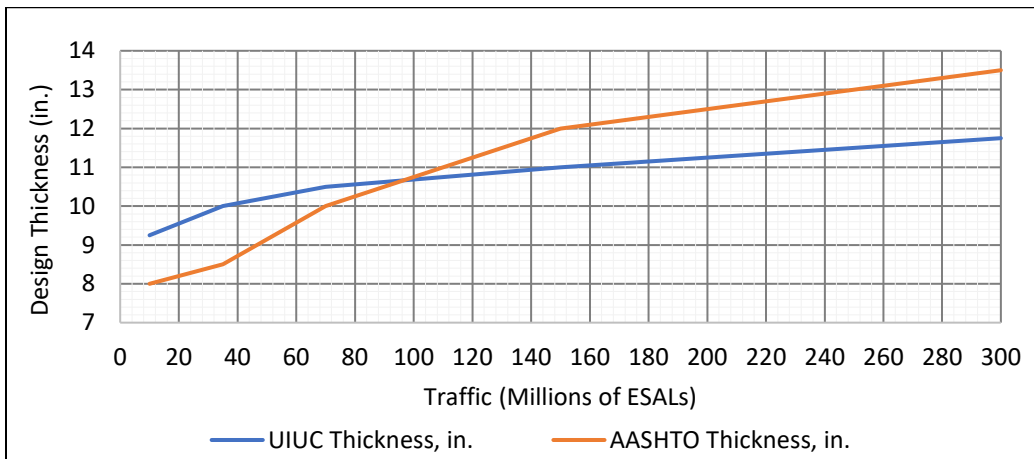


Figure 48. Graph. Comparison of CRCP thickness between proposed CRCP design framework and AASHTOWare Pavement ME Design (20-year design, K = 200 psi/in., PCC tied monolithic shoulder).

CHAPTER 6: DEVELOPMENT OF CRCP OVERLAY DESIGN PROCESS FOR ILLINOIS

The CRCP overlay rehabilitation design procedure within the AASHTOWare Pavement ME Design is capable of designing unbonded CRCP overlays on existing rigid pavements as well as on existing flexible pavements. This overlay design procedure employs a similar punchout prediction model that is applicable across various CRCP rehabilitation strategies and integrated with the new CRCP design module. To determine the most effective method for a CRCP overlay, the choices were either to extend the capabilities of the proposed CRCP Excel software or to verify and, if necessary, calibrate the AASHTOWare Pavement ME Design module specific to CRCP overlays. The initial step involved evaluating the AASHTOWare module’s accuracy for CRCP overlay against the actual performance data of CRCP overlay sections in Illinois. This CRCP overlay method utilized the MEPDG concrete fatigue equation (Figure 49). Subsequently, the total predicted number of medium- to high-severity punchouts was calculated using the equation in Figure 50, where the calibration constants for the CRCP punchout-damage relationship are provided in Table 25.

$$\text{Log}(N_{i,j}) = C_1 * \left(\frac{M_{Ri}}{\sigma_{i,j}}\right)^{C_2} - 1$$

Figure 49. Equation. AASHTOWare fatigue model.

Source: AASHTO (2024)

- Where:
- $N_{i,j}$ = Allowable number load repetitions
 - M_{Ri} = PCC modulus of rupture at age i, psi
 - $\sigma_{i,j}$ = Applied stress at time increment i due to load magnitude j, psi
 - C_i = Calibration constants (Table 25)

$$PO = \frac{C_3}{1 + C_4(DI_{PO})^{C_5}}$$

Figure 50. Equation. AASHTOWare punchout model.

Source: AASHTO (2024)

- Where:
- PO = Total predicted number of medium and high severity punchouts per mile
 - C_i = Calibration constants (Table 25)
 - DI_{PO} = Accumulated fatigue damage (due to slab bending in the transverse direction) at the end of y^{th} year

**Table 25. Values of Coefficients in AASHTOWare
Pavement ME Punchout Models**

| Coefficient | Value |
|--------------------|--------------|
| C ₁ | 2 |
| C ₂ | 1.22 |
| C ₃ | 107.73 |
| C ₄ | 2.475 |
| C ₅ | -0.785 |

A sensitivity analysis has been performed previously on the key CRCP design inputs within the AASHTOWare Pavement ME Design for new CRCPs by Roesler and Hiller (2016). This CRCP overlay module in the AASHTO Pavement ME Design software was used previously to analyze overlay options for the I-57/I-64 section in Jefferson County (Roesler, 2010). Seven unbonded concrete overlays constructed in Illinois were used to determine how the AASHTO Pavement ME Design software predicts performance of unbonded CRCP overlays. Heckel and Wienrank (2018) completed a performance study at IDOT on concrete overlays from 1967 to 2016, shown in Table 26. The seven unbonded overlay sections and their performance are summarized in Table 27. The most recently designed and constructed CRCP overlay project was I-57/I-64 in Jefferson County, Illinois.

Illinois CRCP overlay sections were entered into the AASHTO Pavement ME Design software for an assessment of actual versus predicted CRCP overlay performance. The Illinois inputs for the AASHTOWare analysis of the CRCP overlays are shown in Tables 30 and 31. To estimate the cumulative ESALs throughout the pavement’s service life, AADTT to ESALs correlations for the TTC1 traffic option (see Table 20) was again used. Appendix E has a full summary of the 20- and 30-year overlay design with the AASHTO Pavement ME Design software.

In Table 28, the AASHTOWare Pavement ME punchout predictions were based on the actual CRCP slab thickness and the accumulated traffic (ESALs) for each section up to 2021, the year of the punchout visual observation. The traffic data originally from Heckel and Wienrank’s study (2018), were projected forward with a constant growth rate to the year 2021. The observed punchouts on most sections did not exceed the predicted punchouts with AASHTOWare. This suggested the original designs were likely too conservative. Table 29 summarizes the AASHTOWare derived thickness for a 20-year CRCP overlay design given the same Illinois inputs from the projects. The results of the AASHTOWare indicate that the minimum overlay thicknesses calculated by the software did not exceed the as-built thicknesses of the CRCP overlay sections. This confirms the existing CRCP overlay design by IDOT is conservative in its predictions relative to the AASHTOWare.

Given the AASHTO Pavement ME Design software’s capability to produce reasonable performance predictions for existing CRCP overlays in Illinois, the program was used to develop a set of proposed CRCP overlay design charts. The inputs for these charts are listed in Tables 30 and 31, which cover cases with either intact or rubblized concrete pavement, respectively. Traffic projections ranged from 10 to 300 million ESALs, with AADTT varied for the 20- and 30-year design life charts to ensure the total ESALs at the end of the design period remain the same. The design tables for 20- and 30-year slab thicknesses for unbonded CRCP overlays on intact and rubblized concrete pavements, for

asphalt, tied, and monolithic shoulders at 95% reliability, are presented in Tables 32 through 43 and plotted in Figures 51 to 55. As shown in Tables 32–43 and Figures 51–55, the AASHTOWare CRCP overlay thickness produced reasonable slab thickness values for different traffic levels and shoulder types as well as whether the existing concrete pavement was left intact or rubblized. As noted, the AASHTOWare CRCP overlay thickness was most sensitive to traffic level. The choice of shoulder type affected the CRCP overlay thickness by up to 1 inch. Rubblizing the existing concrete pavement prior to the CRCP overlay also increased the CRCP overlay thickness by as much as 1 inch.

Table 26. Unbonded Concrete Overlays (JPCP and CRCP) in Illinois

| Table 1. Concrete Overlay Locations, Original Construction, and New Construction | | | | | | |
|---|----------------|------------------------|------------------------|-----------------------|------------------|-------------|
| Route | County | Original pavement type | Original pavement year | New overlay type | New overlay year | In service? |
| Bonded concrete overlays | | | | | | |
| I-80 | Rock Island | 8" CRCP | 1965 | 4" concrete | 1994–1995 | No – 2010 |
| I-88 | Whiteside | 8" CRCP | 1976 | 3" concrete | 1996 | Yes |
| Unbonded concrete overlays | | | | | | |
| I-70 WB | Bond | 8" JRCP | 1939 | 6", 7", 8" CRCP | 1967 | No – 1987 |
| I-55 | South Sangamon | 7" JRCP | 1933 | 8" CRCP | 1970 | No – 2001 |
| I-55 NB | North Sangamon | 10" JRCP | mid 1950s | 9" CRCP | 1976 | No – 1997 |
| I-74 WB | Knox | 7" CRCP | 1969 | 9" CRCP | 1995 | Yes |
| I-88 | Whiteside | 8" CRCP | 1975 | 9" CRCP | 2001 | Yes |
| I-70 | Clark | 8" CRCP | 1969 | 12" CRCP | 2002 | Yes |
| I-57 | Jefferson | 8" CRCP | 1969 | 10" CRCP | 2014 | Yes |
| I-57 | Union/Johnson | 10" JRCP | 1960–1961 | 9.75" JPCP | 2016 | Yes |
| Thin unbonded concrete overlay | | | | | | |
| I-72 | Sangamon | 8" CRCP | 1976 | 6' × 6' × 6" concrete | 2015 | Yes |

Note: CRCP = continuously reinforced concrete pavement; JRCP = jointed reinforced concrete pavement; JPCP = jointed plain concrete pavement; 1 in. (") = 25.4 mm; 1 ft (') = 0.305 m.

Source: Heckel & Wienrank (2018)

Table 27. Unbonded Concrete Overlays Traffic Data in Illinois

| Table 4. Unbonded Concrete Overlay Traffic Data | | | | | | |
|--|------------------|-------------------|----------------|---------------------|-----------------------|------------------|
| Route | Traffic years | Cumulative MESALs | Percent trucks | Design life (years) | Design traffic factor | Percent consumed |
| I-70 Bond Co. | 1967–1987 | 23.4 | 37.6 | 20 | 13.4 | 174.7 |
| I-55 S. Sangamon Co. | 1970–2001 | 38.1 | 21.5 | 20 | 17.1 | 222.0 |
| I-55 N. Sangamon Co. | 1976–1997 | 27.5 | 25.6 | 20 | 15.8 | 174.1 |
| I-74 Knox Co. | 1995–2016 | 25.3 ^a | 29.1 | 20 | 24.0 | 104.7 |
| I-88 Whiteside Co. | 2001–2016 | 13.7 ^a | 35.1 | 20 | 16.2 ^b | 84.7 |
| I-70 Clark Co. | 2002–2016 | 45.3 ^a | 49.8 | 30 | 116.6 | 38.8 |
| I-57 Jefferson Co. | 2014–2016 | 9.6 ^a | 30.7 | 20 | 80.0 | 12.0 |
| I-57 Union/Johnson Co. | N/A ^c | N/A ^c | 19.1 | 20 | 32.8 | N/A ^c |

Note: MESALs = millions of equivalent single axle loads.

^aCumulative MESALs as of 2016, as the pavement section is still in service.

^bEstimated from 1995 traffic data with a 0.5% growth rate.

^cConstructed in 2016, so no traffic had accumulated in 2016.

Source: Heckel & Wienrank (2018)

Table 28. Summary of Unbonded CRCP Overlays in Illinois

| Location (County) | Overlay Type | Overlay Construction Year | Status | Cumulative Millions of ESALs (Traffic Years) | IRI Value | 20-year AADTT Equivalent | 2021 Observed Punchouts/Mile | AASHTO Predicted Punchouts/Mile |
|--------------------------|-------------------------|---------------------------|---------------------------|--|-----------|--------------------------|------------------------------|---------------------------------|
| I-70 WB (Bond County) | 6-, 7-, and 8-inch CRCP | 1967 | Removed from service 1987 | 23.4 (1967–1987) | – | 3104 | N/A | 11.52, 5.30, 1.56 |
| I-55 (South Sangamon) | 8-inch CRCP | 1970 | Removed from service 2001 | 38.1 (1970–2001) | – | 5054 | N/A | 3.16 |
| I-55 NB (North Sangamon) | 9-inch CRCP | 1976 | Removed from service 1997 | 27.5 (1976–1997) | – | 3648 | N/A | 0.96 |
| I-74 (Knox) | 9-inch CRCP | 1995 | In service 2021 | 31.1 (1995–2021) | 68 | 4119 | 0 | 1.16 |
| I-88, (Whiteside) | 9-inch CRCP | 2001 | In service 2021 | 15.1 (2001–2021) | 60 | 2009 | 0 | 0.82 |
| I-70 (Clark) | 12-inch CRCP | 2002 | In service 2021 | 60.4 (2002–2021) | 69 | 8012 | 0.3 | 0.27 |
| I-57 (Jefferson) | 10-inch CRCP | 2014 | In service 2021 | 25.6 (2014–2021) | 70 | 3396 | 0 | 0.58 |

Table 29. AASHTOWare Predicted Unbonded CRCP Overlay Thickness in Illinois

| Location (County) | Overlay Type | Original Pavement Type | Overlay Construction Year | Status | IRI Value | Overlay Design Life (Years) | Design Traffic Factor | Equivalent AADTT for Design Period | AASHTO Required Thickness (in.) |
|--------------------------|-------------------------|-------------------------|---------------------------|---------------------------|-----------|-----------------------------|-----------------------|------------------------------------|---------------------------------|
| I-70 WB (Bond County) | 6-, 7-, and 8-inch CRCP | 8-inch JRCP | 1967 | Removed from service 1987 | – | 20 | 13.4 | 1777 | 6.0 |
| I-55 (South Sangamon) | 8-inch CRCP | 7-inch JRCP | 1970 | Removed from service 2001 | – | 20 | 17.1 | 2268 | 6.0 |
| I-55 NB (North Sangamon) | 9-inch CRCP | 10-inch JRCP | 1976 | Removed from service 1997 | – | 20 | 15.8 | 2096 | 6.0 |
| I-74 (Knox) | 9-inch CRCP | 7-inch CRCP | 1995 | In service 2021 | 68 | 20 | 24 | 3184 | 7.0 |
| I-88, (Whiteside) | 9-inch CRCP | 8-inch CRCP | 2001 | In service 2021 | 60 | 20 | 16.2 | 2149 | 7.0 |
| I-70 (Clark) | 12-inch CRCP | 8-inch CRCP | 2002 | In service 2021 | 69 | 30 | 116.6 | 9234 | 9.5 |
| I-57 (Jefferson) | 10-inch CRCP | 8-inch CRCP (Rubblized) | 2014 | In service 2021 | 70 | 20 | 80 | 10612 | 10.0 |

Table 30. AASHTO Pavement ME Inputs for Unbonded CRCP Overlays in Illinois

| AASHTO Layer | Thickness (in) | Modulus (psi) | MOR 28d (psi) | Binder % | Poisson Ratio | Coef. Lat. Earth Pres | Unit Weight (pcf) | Bar Diameter (in.) | Steel % | Steel Depth (in.) | SSA | CoTE _{10⁶} (1/°F) | Heat Capacity (BTU/lb-°F) | Conduc-tivity (BTU/hr -ft-°F) | Aggregate Type |
|-----------------------|----------------|--|---------------|----------|---------------|-----------------------|-------------------|--------------------|------------|-------------------|------|---------------------------------------|---------------------------|-------------------------------|----------------|
| CRCP (monolithic) | Varies | 4,400,000 | 675 | – | 0.2 | – | 150 | 0.75 or 0.875 | 0.7 or 0.8 | Varies | 0.85 | 5.5 | 0.28 | 1.25 | Limestone |
| HMA | 4 | Input Level 3 (76-22 binder, ref temp =70) | – | 11.6 | 0.35 | – | 150 | – | – | – | – | – | – | – | |
| Existing PCC (intact) | 8 | 2,000,000 | – | – | 0.2 | – | 150 | – | – | – | – | – | 0.28 | 1.25 | |
| A-1-A Granular Base | 4 | 30,000 | – | – | 0.35 | 0.5 | | | | | | | | | |
| A-7-6 | Semi Infinite | 13,000 | – | – | 0.35 | 0.5 | | | | | | | | | |

*MOR28 is flexural strength at 28 days, SSA is short-wave surface absorptivity, and CoTE is concrete coefficient of thermal expansion.

Table 31. Unbonded CRCP Overlay Inputs (Existing PCC Rubbilized) for AASHTOWare in Illinois

| AASHTO Layer | Thickness | Modulus (psi) | MOR 28d (psi) | Binder % | Poisson Ratio | Coef. Lat. Earth Pres | Unit Weight (pcf) | Bar Diameter (in.) | Steel % | Steel Depth (in.) | SSA | CoTE _{x10⁻⁶} (1/°F) | Heat Capacity (BTU/lb-°F) | Conductivity (BTU/hr-ft-°F) | Aggregate Type |
|---------------------|---------------|--|---------------|----------|---------------|-----------------------|-------------------|--------------------|------------|-------------------|------|---|---------------------------|-----------------------------|----------------|
| CRCP (monolithic) | Varies | 4,400,000 | 675 | — | 0.2 | — | 150 | 0.75 | 0.7 or 0.8 | Varies | 0.85 | 5.5 | 0.28 | 1.22 | limestone |
| HMA | 2 | Input Level 3 (76-22 binder, ref temp =70) | — | 11.6 | 0.35 | — | 150 | — | — | — | — | — | — | — | |
| Existing PCC | 9 | Rubbilized =200,000) | — | — | 0.2 | — | 150 | — | — | — | — | — | 0.28 | 1.25 | |
| A-1-A Granular Base | 4 | 30,000 | — | — | 0.35 | 0.5 | | | | | | | | | |
| A-7-6 | Semi Infinite | 13,000 | — | — | 0.35 | 0.5 | | | | | | | | | |

*MOR28 is flexural strength at 28 days, SSA is short-wave surface absorptivity, and CoTE is concrete coefficient of thermal expansion (1/°F).

CRCP OVERLAY DESIGN TABLES

20-Year Overlays on Existing CRCP/JPCP/JRCP

Table 32. Slab Thickness for 20-Year Unbonded CRCP Overlays on Existing PCC with Asphalt Shoulder

| AADTT | Millions ESALs | Reliability % | AASHTO Thickness |
|--------|----------------|---------------|------------------|
| 1,326 | 10 | 95 | 6.00 |
| 4,643 | 35 | 95 | 8.50 |
| 9,286 | 70 | 95 | 10.00 |
| 19,898 | 150 | 95 | 11.50 |
| 39,797 | 300 | 95 | 13.00 |

Table 33. Slab Thickness for 20-Year Unbonded CRCP Overlays on Existing PCC with PCC Tied Separate Concrete Shoulder

| AADTT | Millions ESALs | Reliability % | AASHTO Thickness |
|--------|----------------|---------------|------------------|
| 1,326 | 10 | 95 | 6.00 |
| 4,643 | 35 | 95 | 8.00 |
| 9,286 | 70 | 95 | 9.50 |
| 19,898 | 150 | 95 | 11.00 |
| 39,797 | 300 | 95 | 12.50 |

Table 34. Slab Thickness for 20-Year Unbonded CRCP Overlays on Existing PCC with Monolithic Tied Concrete Shoulder

| AADTT | Millions ESALs | Reliability % | AASHTO Thickness |
|--------|----------------|---------------|------------------|
| 1,326 | 10 | 95 | 6.00 |
| 4,643 | 35 | 95 | 7.00 |
| 9,286 | 70 | 95 | 9.00 |
| 19,898 | 150 | 95 | 10.50 |
| 39,797 | 300 | 95 | 12.00 |

30-Year Overlays on Existing CRCP/JPCP/JRCP

Table 35. Slab Thickness for 30-Year Unbonded CRCP Overlays on Existing PCC with Asphalt Shoulder

| AADTT | Millions ESALs | Reliability % | AASHTO Thickness |
|--------|----------------|---------------|------------------|
| 792 | 10 | 95 | 6.00 |
| 2,772 | 35 | 95 | 8.00 |
| 5,544 | 70 | 95 | 10.00 |
| 11,879 | 150 | 95 | 11.50 |
| 23,759 | 300 | 95 | 12.50 |

Table 36. Slab Thickness for 30-Year Unbonded CRCP Overlays on Existing PCC with PCC Tied Separate Concrete Shoulder

| AADTT | Millions ESALs | Reliability % | AASHTO Thickness |
|--------|----------------|---------------|------------------|
| 792 | 10 | 95 | 6.00 |
| 2,772 | 35 | 95 | 7.00 |
| 5,544 | 70 | 95 | 9.00 |
| 11,879 | 150 | 95 | 10.50 |
| 23,759 | 300 | 95 | 12.00 |

Table 37. Slab Thickness for 30-Year Unbonded CRCP Overlays on Existing PCC with Monolithic Tied Concrete Shoulder

| AADTT | Millions ESALs | Reliability % | AASHTO Thickness |
|--------|----------------|---------------|------------------|
| 792 | 10 | 95 | 6.00 |
| 2,772 | 35 | 95 | 6.00 |
| 5,544 | 70 | 95 | 8.50 |
| 11,879 | 150 | 95 | 10.00 |
| 23,759 | 300 | 95 | 11.00 |

20-Year Overlay on Rubblized CRCP/JPCP/JRCP

Table 38. Slab Thickness for 20-Year Unbonded CRCP Overlays on Rubblized PCC with Asphalt Shoulder

| AADTT | Millions ESALs | Reliability % | AASHTO Thickness |
|--------|----------------|---------------|------------------|
| 1,326 | 10 | 95 | 8.00 |
| 4,643 | 35 | 95 | 9.00 |
| 9,286 | 70 | 95 | 10.50 |
| 19,898 | 150 | 95 | 12.50 |
| 39,797 | 300 | 95 | 14.00 |

Table 39. Slab Thickness for 20-Year Unbonded CRCP Overlays on Rubblized PCC with PCC Tied Separate Concrete Shoulder

| AADTT | Millions ESALs | Reliability % | AASHTO Thickness |
|--------|----------------|---------------|------------------|
| 1,326 | 10 | 95 | 7.50 |
| 4,643 | 35 | 95 | 8.50 |
| 9,286 | 70 | 95 | 10.00 |
| 19,898 | 150 | 95 | 12.00 |
| 39,797 | 300 | 95 | 13.50 |

Table 40. Slab Thickness for 20-Year Unbonded CRCP Overlays on Rubblized PCC with Monolithic Tied Concrete Shoulder

| AADTT | Millions ESALs | Reliability % | AASHTO Thickness |
|--------------|-----------------------|----------------------|-------------------------|
| 1,326 | 10 | 95 | 7.50 |
| 4,643 | 35 | 95 | 8.00 |
| 9,286 | 70 | 95 | 9.50 |
| 19,898 | 150 | 95 | 11.50 |
| 39,797 | 300 | 95 | 13.00 |

30-Year Overlay on Rubblized CRCP/JPCP/JRCP

Table 41. Slab Thickness for 30-Year Unbonded CRCP Overlays on Rubblized PCC with Asphalt Shoulder

| AADTT | Millions ESALs | Reliability % | AASHTO Thickness |
|--------------|-----------------------|----------------------|-------------------------|
| 792 | 10 | 95 | 7.50 |
| 2,772 | 35 | 95 | 9.00 |
| 5,544 | 70 | 95 | 11.00 |
| 11,879 | 150 | 95 | 12.50 |
| 23,759 | 300 | 95 | 14.00 |

Table 42. Slab Thickness for 30-Year Unbonded CRCP Overlays on Rubblized PCC with PCC Tied Separate Concrete Shoulder

| AADTT | Millions ESALs | Reliability % | AASHTO Thickness |
|--------------|-----------------------|----------------------|-------------------------|
| 792 | 10 | 95 | 7.50 |
| 2,772 | 35 | 95 | 8.50 |
| 5,544 | 70 | 95 | 10.50 |
| 11,879 | 150 | 95 | 12.00 |
| 23,759 | 300 | 95 | 13.50 |

Table 43. Slab Thickness for 30-Year Unbonded CRCP Overlays on Rubblized PCC with Monolithic Tied Concrete Shoulder

| AADTT | Millions ESALs | Reliability % | AASHTO Thickness |
|--------------|-----------------------|----------------------|-------------------------|
| 792 | 10 | 95 | 7.50 |
| 2,772 | 35 | 95 | 8.50 |
| 5,544 | 70 | 95 | 10.00 |
| 11,879 | 150 | 95 | 11.50 |
| 23,759 | 300 | 95 | 13.00 |

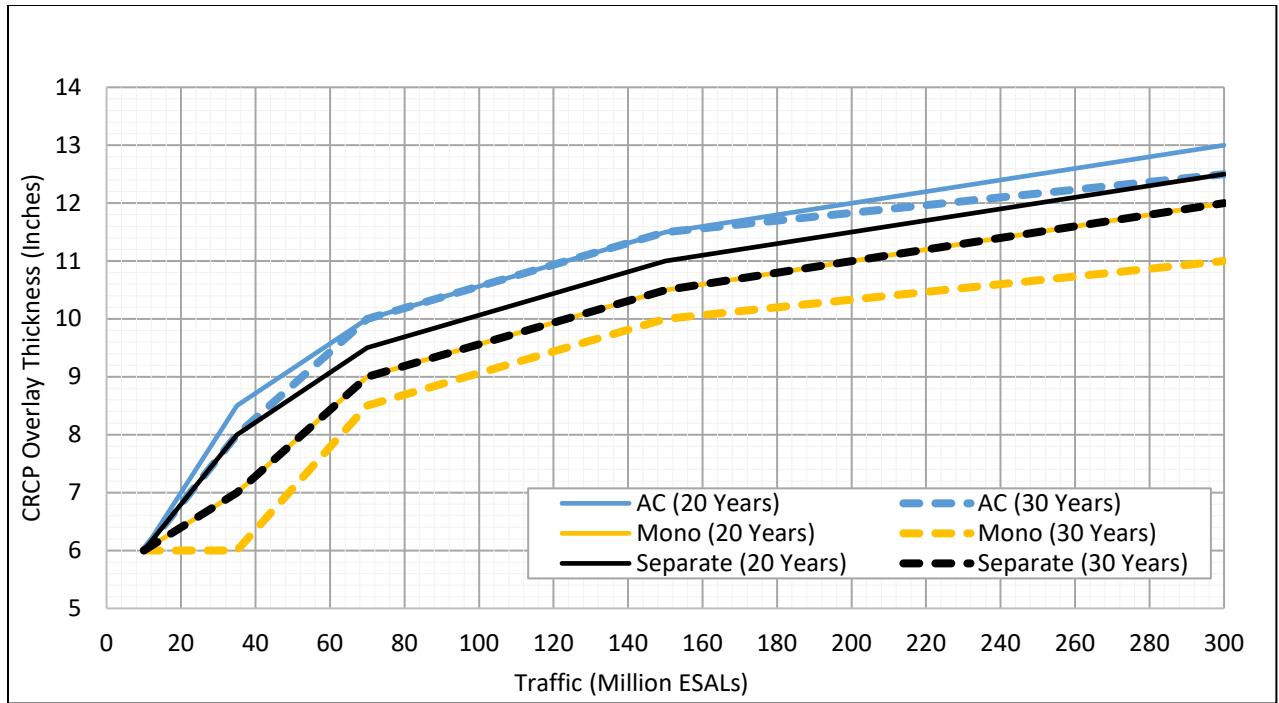


Figure 51. Graph. Comparison of CRCP overlay thickness on intact concrete pavement provided by AASHTOWare Pavement ME Design.

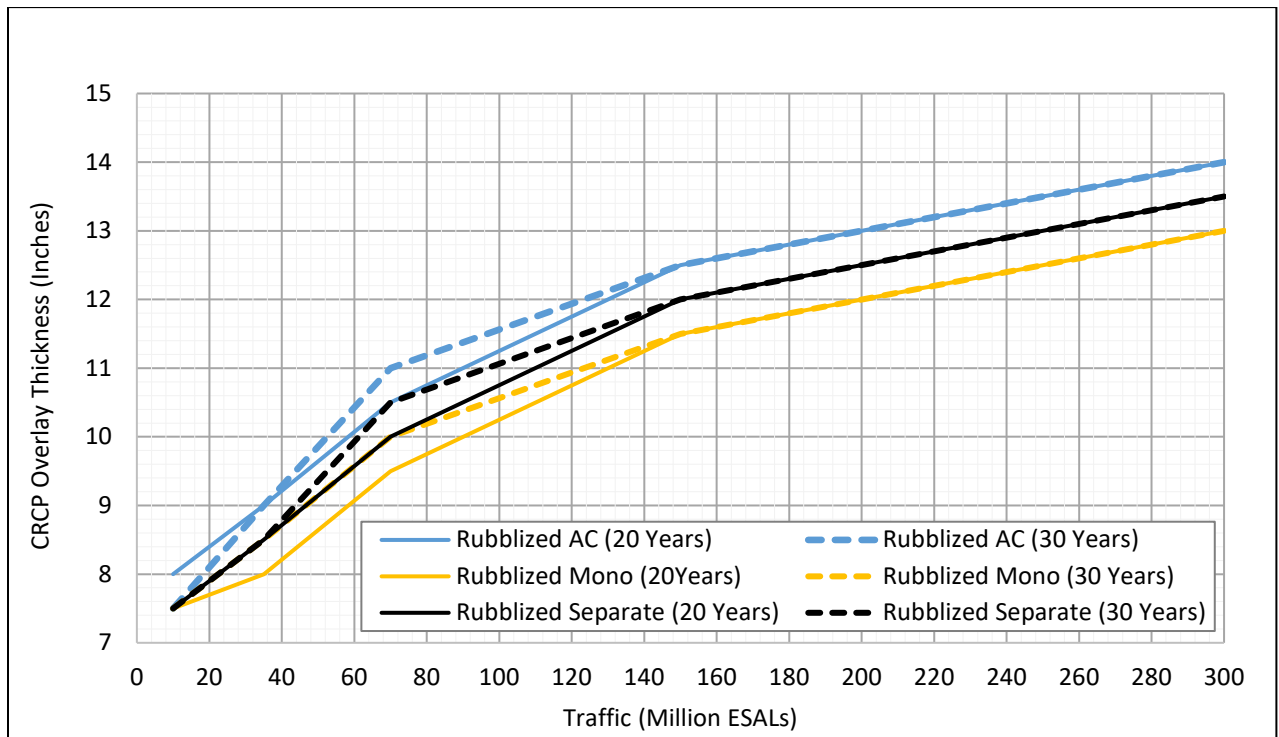


Figure 52. Graph. Comparison of CRCP overlay thickness on rubblized concrete pavement provided by AASHTOWare Pavement ME Design.

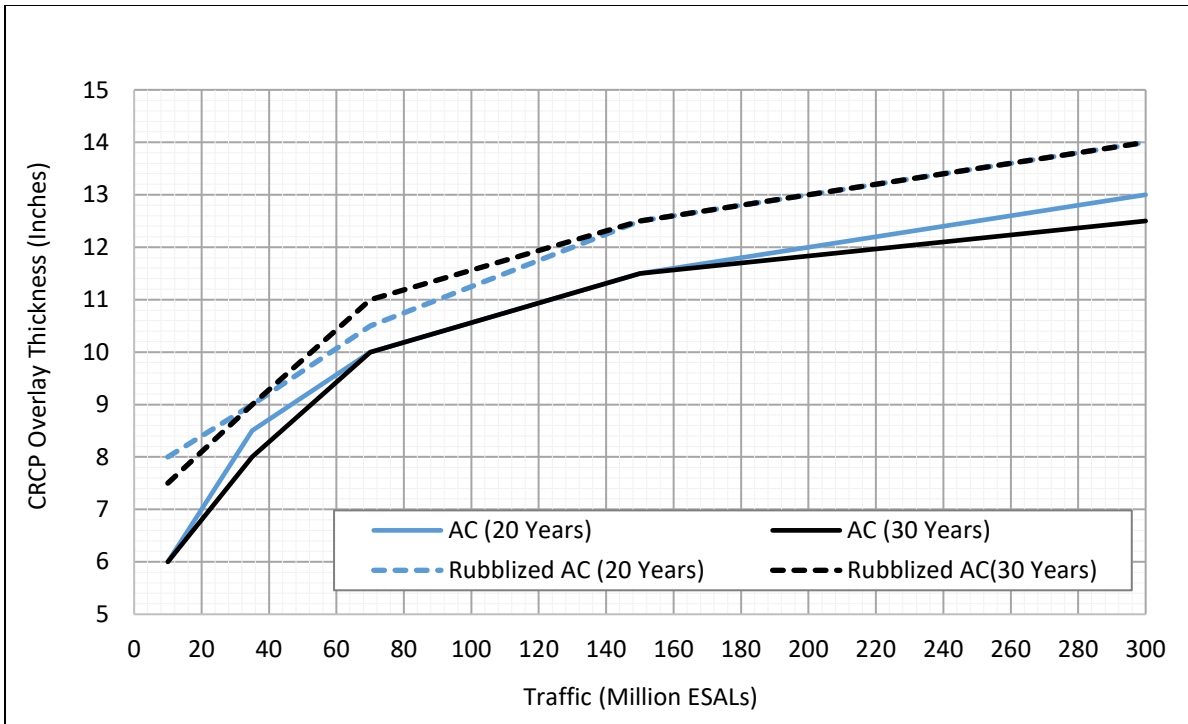


Figure 53. Graph. Comparison of CRCP overlay thickness on intact concrete pavement and rubblized concrete pavement with asphalt shoulder.

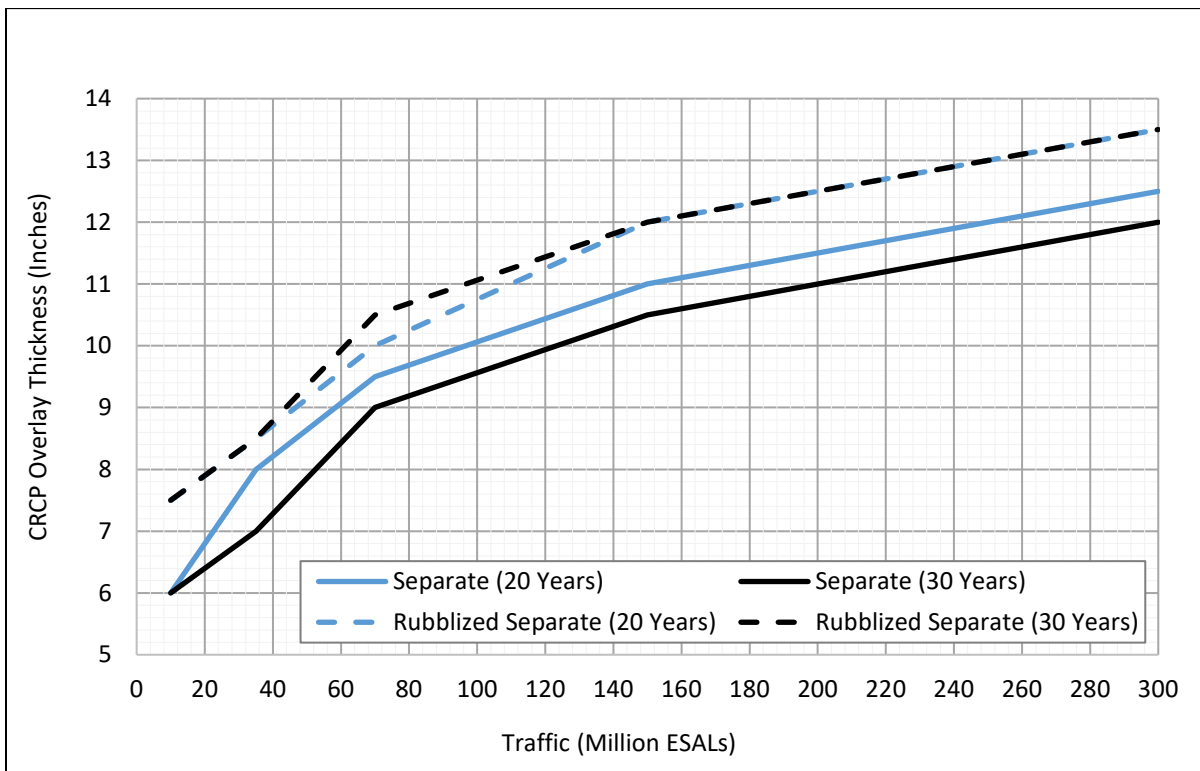


Figure 54. Graph. Comparison of CRCP overlay thickness on intact concrete pavement and rubblized concrete pavement with PCC separate shoulder.

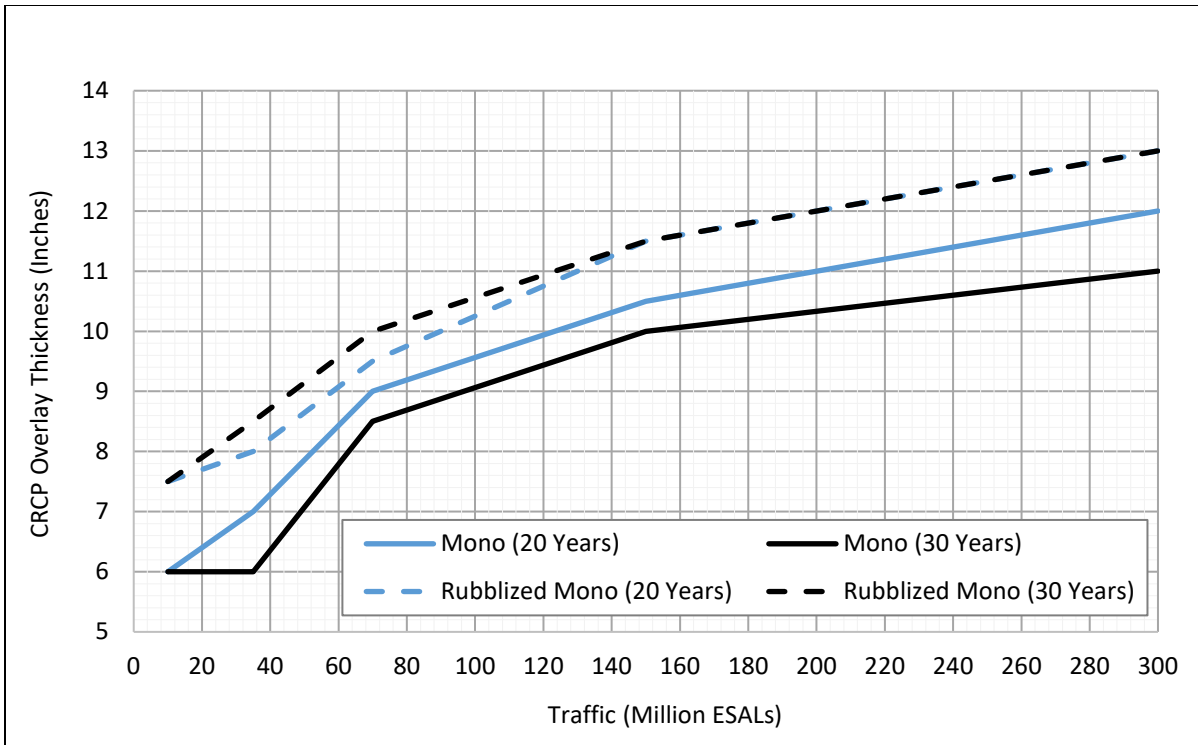


Figure 55. Graph. Comparison of CRCP overlay thickness on intact concrete pavement and rubblized concrete pavement with PCC monolithic shoulder.

CHAPTER 7: SUMMARY AND CONCLUSION

The goals of this research were to update, recalibrate, and finalize a proposed CRCP design framework for Illinois by incorporating more comprehensive field performance data. A review of recent CRCP studies across the U.S. and other countries found multiple field studies on the performance of CRCP (e.g., California, Illinois Tollway, and Belgium). A CRCP performance study was also completed on IDOT interstates with the IROADS software. This visual observation of approximately 100 miles of CRCP on IROADS enabled assessment of the performance of current CRCP sections in Illinois for the number of punchouts per mile. The results of the current performance study showed only 3 out of 28 sections containing visible punchouts, which were located on I-80 and I-94 in Cook County, and I-70 in Clark County.

The proposed CRCP design framework in Excel was verified against the outputs of the 2009 original version by comparing punchout prediction results. A sensitivity analysis was then conducted by comparing the proposed framework's CRCP slab thicknesses with the JPCP design charts in Chapter 54 of IDOT's *BDE Manual*. The results confirmed that the updated framework aligned with the IDOT JPCP design charts and offered a broader range of design traffic. Under poor subgrade conditions and traffic volumes below 50 million ESALs, JPCP with AC shoulders required thinner slabs than CRCP. However, when traffic volumes increased from 50 to 100 million ESALs, JPCP with AC shoulders needed thicker slabs compared to CRCP. This pattern was also observed under granular subgrade conditions for traffic volumes from 30 to 100 million ESALs. For tied concrete shoulders under poor subgrade support, JPCP thickness was slightly less than CRCP thickness for both 0.7% and 0.8% steel contents, whereas under granular conditions, JPCP thickness fell between CRCP thicknesses for 0.7% and 0.8% steel content.

The Illinois CRCP performance data were used to successfully recalibrate the punchout-to-fatigue damage model in the Excel design software. The punchout prediction model coefficients were updated to better reflect the field performance data, which reduced the SSE and resulted in an R^2 value of 95% for actual versus predicted punchouts. Based on the updated CRCP design framework, proposed CRCP slab thickness tables and charts were generated for two reliability levels, three shoulder types, three support conditions, and traffic levels from 10–300 million ESALs. The results showed that under weak subgrade conditions with traffic volumes below 100 million ESALs, 20-year CRCP designs with monolithic PCC shoulders required thinner slabs than those with asphalt and separate PCC shoulders. However, beyond 140 million ESALs, asphalt shoulders required the thinnest slabs, especially as volumes exceeded 200 million ESALs. In strong subgrade conditions, CRCP with monolithic PCC shoulders consistently required less thickness across all traffic levels up to 300 million ESALs. The 30-year design trends showed more consistency, with monolithic PCC shoulders consistently requiring the least slab thickness, while differences between asphalt and separate PCC shoulders were minor. Notably, the gap in required thickness between monolithic PCC shoulders and the other two cases widened as the k-value increased.

The updated CRCP design method was then compared with the AASHTOWare Pavement ME Design (V2.6.2.2) for a similar set of inputs. The analysis revealed AASHTOWare Pavement ME Design for new CRCP was significantly more sensitive to traffic increases than the proposed CRCP design

framework in Excel. AASHTOWare Pavement ME Design also produced thinner slabs at low traffic levels and significantly thicker ones as traffic increased.

Finally, a CRCP overlay design method was developed for both intact and rubblized (existing) concrete pavements, leveraging performance data from seven unbonded CRCP overlays constructed in Illinois. The proposed CRCP overlay charts and tables were created by comparing the actual CRCP overlay performance in Illinois with AASHTOWare Pavement ME Design predictions. The analysis showed the AASHTOWare Pavement ME Design slightly overpredicted punchouts from the Illinois field performance data with the error less than 1.2 punchouts per mile, which indicated that it was sufficient for generating CRCP overlay designs for 20- and 30-year design lives. A set of design tables were generated for CRCP overlay thicknesses with different traffic levels (10 to 300 million ESALs), shoulder types, and condition of the existing concrete pavement (intact or rubblized). Traffic levels were again the most sensitive factor in the slab thickness followed by shoulder type and condition of the existing concrete pavement. According to the assigned inputs in this study, for 20-year CRCP overlays on existing concrete, AASHTOWare Pavement ME Design recommended thickness ranges from 6 inches for lower traffic levels up to 13 inches for the highest traffic projections for overlays with asphalt shoulders. The CRCP slab thickness ranges from 6 to 12.5 inches for tied separate concrete shoulders and from 6 to 12 inches for monolithic tied concrete shoulders. The 30-year CRCP overlay thicknesses were slightly thinner for similar traffic levels with a ranged between 0 to 0.5 inches compared with the 20-year CRCP overlay thicknesses.

REFERENCES

- American Concrete Pavement Association. (n.d.). *Subgrade K Value Calculator*. Retrieved from <http://www.apps.acpa.org/apps/kvalue.aspx>
- AASHTO. (2024). January 2024 ERRATA for Mechanistic-Empirical Pavement Design Guide, 3rd Edition (MEPDG-3). American Association of State Highway and Transportation Officials. Retrieved from <https://downloads.transportation.org/MEPDG-3-Errata.pdf>
- ARA, Inc. (2003). *Guide for mechanistic empirical design of new and rehabilitated pavement structures*. National Cooperative Highway Research Program, Transportation Research Board National Research Council.
- Beyer, M., & Roesler, J. (2009). *Mechanistic-empirical design concepts for continuously reinforced concrete pavements in Illinois* (Report No. FHWA-ICT-09-040). Illinois Center for Transportation.
- Choi, P., Poudyal, L., Rouzmehr, F., & Won, M. (2020). Spalling in continuously reinforced concrete pavement in Texas. *Transportation Research Record*, 2674(11). <https://doi.org/10.1177/0361198120948509>
- Dahal, S., & Roesler, J. R. (2021). Continuously reinforced concrete pavement cracking patterns and properties with internal curing and active cracking. *Transportation Research Record*, 2676(2). <https://doi.org/10.1177/03611981211041601>
- Dahal, S., Roesler, J., Gupta, P., & Zhang, Y. (2020). *Performance monitoring of re-engineered continuously reinforced concrete pavement test sections: Volume 2* (Report No. ICT-21-012). Illinois State Tollway Authority. <https://doi.org/10.36501/0197-9191/21-012>
- Darter, M. I., (1977). *Design of zero-maintenance plain jointed pavements* (Report No. FHWA-RD-77-111). Federal Highway Administration.
- Darter, M., & Rao, C. (2015). *Long Life CRCP*. Applied Research Associates, Inc.
- Fick, G., Gross, J., Snyder, M. B., Harrington, D., Roesler, J., & Cackler, T. (2021). *Guide to concrete overlays, Fourth Edition*. National Concrete Pavement Technology Center.
- Heckel, L. B., & Wienrank, C. J. (2018). Performance of concrete overlays on Illinois interstates, 1967 through 2016. *Transportation Research Record: Journal of the Transportation Research Board*, 2672, 282–290. <https://doi.org/10.1177/0361198118781146>
- Illinois Department of Transportation. (n.d.). *Highway System*. Retrieved from <https://idot.illinois.gov/transportation-system/Network-Overview/highway-system/index>
- Illinois Department of Transportation. (2023). *Bureau of design and environment manual*. <https://idot.illinois.gov/Assets/uploads/files/Doing-Business/Manuals-Guides-&-Handbooks/Highways/Design-and-Environment/Design%20and%20Environment%20Manual,%20Bureau%20of.pdf>
- Kim, S. M., & Won, M. C. (2004). Horizontal cracking in continuously reinforced concrete pavements. *ACI Structural*, 101, 784–791.
- Kohler, E. R., & Roesler, J. R. (2004). Active crack control for continuously reinforced concrete pavements. *Transportation Research Record*, 19–29.

- McCullough, B. F., & Dossey, T. (1999). Considerations for high-performance concrete paving: Recommendations from 20 years of field experience in Texas. *Transportation Research Record: Journal of the Transportation Research Board*, 1684, 17–24.
- Miller, J. S., & Bellinger, W. Y. (2014). *Distress identification manual for the long-term pavement performance program*. Federal Highway Administration.
- Moderie, J., & Burch, P. (2019). *ODOT pavement design guide*. Oregon DOT Pavement Services Unit.
- Plei, M., & Tayabji, S. (2012). *Continuously reinforced concrete pavement performance and best practices* (No. FHWA-HIF-12-039). Federal Highway Administration.
- Ren, D., Houben, L., & Rens, L. (2014a). Cracking behavior of continuously reinforced concrete pavements in Belgium. *Transportation Research Record: Journal of the Transportation Research Board*, 2367(1), 97–106. <https://doi.org/10.3141/2367-10>
- Rens, L., Beeldens, A., Ren, D., & Houben, L. (2014b). Active crack control for continuously reinforced concrete pavements in Belgium through partial surface notches. *Transportation Research Record: Journal of the Transportation Research Board*, 2456(1), 33–41. <https://doi.org/10.3141/2456-04>
- Rens, L., Winnie, P., & Beeldens, A. (2014c) Recent Developments in the Design and Construction of CRCP Towards a More Durable Concept. Prague, Czech Republic: 12th International Symposium of Concrete Roads.
- Roesler, J. (2010). *I-57/ I-64 Mt. Vernon Overlay Options*. University of Illinois Urbana-Champaign.
- Roesler, J., Dahal, S., Zollinger, D., & Weiss, W. J. (2020). *Summary of findings of re-engineered CRCP test sections: Volume 1* (Report No. ICT-21-011). Illinois State Tollway Authority. <https://doi.org/10.36501/0197-9191/21-011>
- Roesler, J., Hiller, J., & Brand, A. (2016) *Continuously reinforced concrete pavement manual: Guidelines for design, construction, maintenance, and rehabilitation* (No. FHWA-HIF-16-026). Federal Highway Administration.
- Stempihar, J., Weitzel, N., Van Dam, T., Schmalzer, P., & Pierce, L. (2020). Assessment of California’s continuously reinforced concrete pavement practice and performance. *Transportation Research Record*, 2674(9), <https://doi.org/10.1177/03611981209325>
- Tayabji, S. D., Stephanos, P. J., Gagnon, J. S., & Zollinger, D. G. (1998a). *Performance of continuously reinforced concrete pavements. Volume 2—Field investigations of CRC pavements* (Report No. FHWA-RD-94-179). Federal Highway Administration.
- Tayabji, S. D., Zollinger, D. G., Vederey, J. R., & Gagnon, J. S. (1998b). *Performance of continuously reinforced concrete pavements. Volume III—Analysis and evaluation of field test data* (Report No. FHWA-RD-94-180). Federal Highway Administration.
- Titus-Glover, L., Mallela, J., & Darter, M. I. (2004). *Enhanced PCC fatigue model for streetpave*. American Concrete Pavement Association.
- Won, M., & Choi, P. (2017). Factors influencing CRCP performance in Texas. Conference on Australian Society for Concrete Pavements, Kingscliff, New South Wales.
- Won, M., Medina-Chavez, C., & Choi, S. (2008). *Concrete pavement overlays and failure mechanism*.

Texas Department of Transportation.

Zhang, Y., & Roesler, J. (2020). *Enhanced CRCP backcalculation procedure and interface bond assessment: Volume 3*. (Report No. ICT-21-013). Illinois State Tollway Authority.
<https://doi.org/10.36501/0197-9191/21-013>

Zollinger, D. G., & Barenberg, E. J. (1989). *Proposed mechanistic based design procedure for jointed concrete pavements* (Report No. FHWA/IL/UI 225). Illinois Cooperative Highway Research Program, University of Illinois at Urbana-Champaign.

Zollinger, D. G., Buch, N., Xin, D., & Soares, J. (1999). *Performance of continuously reinforced concrete pavements volume VI-CRC pavement design, construction, and performance*. (Report No. FMWA-HD-97-151). Federal Highway Administration.

APPENDIX A: CRCP AND CRCP OVERLAY PERFORMANCE DATA FROM ILLINOIS

AVERAGE DAILY TRAFFIC TO ESALS CALCULATIONS

Table 44. ESALs Calculated Based on AADT

| County | Road | County-Inventory No. | Begin KR | End KR | 2-way Traffic Data from [Annual Average Daily Traffic - 2021, IDOT] | | | | | Traffic Opening year | Service Period until 2021 | Backward AADT due to %growth factor (i) | Actual Traffic Factor (TF) for Different Growth Rate (i) until 2021 |
|-------------|-----------------|----------------------|----------|--------|---|---------|-----|-----|------|----------------------|---------------------------|---|---|
| | | | | | Traffic Counting Year | AADT | PV | MU | SU | | | 1% | 1% |
| Cook | I-55 | 16 10055 000000 | 12.2 | 16.3 | 2022 | 157,700 | 93% | 5% | 3% | 2000 | 21 | 126,696 | 44.1 |
| | I-57 | 16 10057 000000 | 19.2 | 20.4 | 2022 | 153,700 | 95% | 3% | 2% | 2008 | 13 | 133,713 | 17.0 |
| | I-80 | 16 10080 000000 | 11.4 | 14.6 | 2022 | 193,600 | 75% | 22% | 3% | 2006 | 15 | 165,106 | 178.9 |
| | I-94 | 16 10094 000000 | 18.2 | 25.3 | 2022 | 246,100 | 95% | 3% | 2% | 1993 | 28 | 184,413 | 53.6 |
| | | 16 10094 000000 | 29.6 | 37.7 | 2022 | 315,700 | 92% | 6% | 2% | 1993 | 28 | 236,567 | 134.3 |
| I-290 | 16 10290 000000 | 1.4 | 4.6 | 2022 | 158,100 | 91% | 6% | 3% | 2003 | 18 | 130,866 | 51.2 | |
| Lee | I-39 | 52 10039 000000 | 15.91 | 16.27 | 2021 | 19,400 | 61% | 36% | 4% | 2012 | 9 | 17,738 | 18.2 |
| Henry | I-80 | 37 10080 000000 | 1.77 | 2.23 | 2021 | 20,400 | 62% | 34% | 4% | 2016 | 5 | 19,410 | 10.5 |
| Rock Island | I-80 | 81 10080 000000 | 4.51 | 5.02 | 2021 | 23,000 | 65% | 32% | 3% | 2009 | 12 | 20,411 | 24.9 |
| Rock Island | I-80 | 81 10080 000000 | 4.51 | 5.02 | 2021 | 23,000 | 65% | 32% | 3% | 2015 | 6 | 21,667 | 13.2 |
| Whiteside | I-88 | 98 10088 000000 | 13.42 | 22.01 | 2022 | 11,600 | 66% | 30% | 4% | 2001 | 20 | 9,413 | 18.1 |
| Winnebago | I-90/I-39 | 101 10090 000000 | 0.00 | 2.71 | 2022 | 56,300 | 69% | 28% | 3% | 2012 | 9 | 50,968 | 41.5 |
| Livingston | I-55 | 53 10055 000000 | 15.68 | 15.88 | 2019 | 16,500 | 64% | 33% | 3% | 2017 | 4 | 16,175 | 6.9 |
| | | 53 10055 000000 | 27.55 | 27.84 | 2021 | 20,600 | 65% | 32% | 4% | 2019 | 2 | 20,194 | 4.1 |
| Bureau | I-80 | 6 10080 000000 | 21.98 | 22.71 | 2021 | 21,000 | 77% | 18% | 5% | 2012 | 9 | 19,201 | 10.4 |
| Grundy | I-80 | 32 10080 000000 | 8.67 | 19.56 | 2021 | 50,300 | 74% | 20% | 6% | 2002 | 19 | 41,635 | 53.3 |
| Peoria | I-74 | 72 10074 000000 | 20.0 | 25.3 | 2021 | 50,000 | 94% | 4% | 2% | 2004 | 17 | 42,219 | 10.2 |
| Tazewell | I-74 | 90 10074 000000 | 0.28 | 2.51 | 2021 | 52,800 | 93% | 4% | 2% | 2005 | 16 | 45,029 | 11.1 |
| | I-74 | 90 10074 000000 | 6.03 | 8.77 | 2021 | 49,400 | 86% | 11% | 3% | 2012 | 9 | 45,168 | 15.3 |
| McLean | I-55 | 57 10055 000000 | 15.68 | 25.21 | 2021 | 42,500 | 66% | 31% | 3% | 2003 | 18 | 35,531 | 63.2 |
| Clark | I-70 | 12 10070 000000 | 17.92 | 27.90 | 2021 | 29,300 | 51% | 46% | 3% | 2002 | 19 | 24,253 | 66.9 |
| Effingham | I-57A | 25 10057A000000 | 0.00 | 0.53 | 2021 | 20,700 | 51% | 45% | 3% | 2013 | 8 | 19,116 | 22.1 |
| Effingham | I-70 | 25 10070 000000 | 11.81 | 20.16 | 2022 | 45,100 | 54% | 43% | 3% | 2013 | 8 | 41,237 | 44.8 |
| St. Clair | I-64 | 82 10064 000000 | 0.16 | 0.27 | 2021 | 82,900 | 88% | 9% | 3% | 2012 | 9 | 75,799 | 21.2 |
| St. Clair | I-70A | 82 10070A000000 | 0.76 | 1.97 | 2019 | 44,300 | 86% | 9% | 5% | 2012 | 9 | 41,319 | 12.0 |
| Madison | I-270 | 60 10270 000000 | 1.76 | 2.11 | 2021 | 49,200 | 82% | 15% | 3% | 2011 | 10 | 44,540 | 22.0 |
| Jefferson | I-57 | 41 10057 000000 | 12.47 | 15.18 | 2022 | 45,800 | 57% | 40% | 3% | 2014 | 7 | 42,296 | 37.3 |

Table 45. CRCP Section Details in Illinois

| | Contract_ID | County | Location | Miles | Servicing Period (2021 time of survey) | Traffic Opening Year | Design Life, yrs | Shoulder Type | Base Type | Base Thickness, in. | PCC Thickness, in. | Percent Steel, % | Steel Diameter, in. | Depth to Steel, in. | PCC ft 28 days, psi |
|----|-------------|-------------|-----------|-------|--|----------------------|------------------|---------------|-----------|---------------------|--------------------|------------------|---------------------|---------------------|---------------------|
| 1 | 82989 | Cook | I-55 | 4.16 | 21 | 2000 | 20 | Tied PCC | BAM | 4 | 14 | 0.7 | 0.875 | 4.5 | 566 |
| 2 | 62304 | Cook | I-57 | 1.25 | 13 | 2008 | 30 | Tied PCC | HMA | 6 | 14 | 0.8 | 0.875 | 4.5 | 566 |
| 3 | 62105 | Cook | I-80 | 3.19 | 15 | 2006 | 30 | Tied PCC | BAM | 4 | 14 | 0.8 | 0.875 | 4.5 | 566 |
| 4 | 80954 | Cook | I-94 | 7.17 | 28 | 1993 | 20 | Tied PCC | BAM | 4 | 12 | 0.7 | 0.75 | 3.5 | 566 |
| 5 | 62300 | Cook | I-94 | 8.07 | 14 | 2007 | 30 | Tied PCC | HMA | 6 | 14 | 0.8 | 0.875 | 4.5 | 566 |
| 6 | 60401 | Cook | I-290 | 3.12 | 18 | 2003 | 40 | Tied PCC | HMA | 6 | 14.17 | 0.8 | 0.875 | 4.5 | 566 |
| 7 | 60N87 | Will | I-80 | 1.36 | 3 | 2018 | 20 | Tied PCC | HMA | 4 | 13 | 0.7 | 0.875 | 3.5 | 566 |
| 8 | 64E97 | Lee | I-39 | 0.36 | 9 | 2012 | 20 | Tied PCC | HMA | 4 | 12.25 | 0.7 | 0.875 | 3.5 | 566 |
| 9 | 64B78 | Henry | I-80 | 0.46 | 5 | 2016 | 20 | Tied PCC | BAM | 4 | 12.25 | 0.7 | 0.875 | 3.5 | 566 |
| 10 | 64933 | Rock Island | I-80 | 1.35 | 12 | 2009 | 20 | Tied PCC | HMA | 4 | 12 | 0.7 | 0.875 | 3.5 | 566 |
| 11 | 64B78 | Rock Island | I-80 | 0.51 | 6 | 2015 | 20 | Tied PCC | HMA | 4 | 12.25 | 0.7 | 0.875 | 3.5 | 566 |
| 12 | 64219 | Whiteside | I-88 | 8.59 | 20 | 2001 | 20 | Tied PCC | HMA | 4 | 9 | 0.7 | 0.875 | 3.5 | 566 |
| 13 | 64C29 | Winnebago | I-90/I-39 | 2.71 | 9 | 2012 | 20 | Tied PCC | HMA | 4 | 12.75 | 0.7 | 0.875 | 3.5 | 566 |
| 14 | 66F23 | Livingston | I-55 | 0.2 | 4 | 2017 | 20 | HMA | Granular | 12 | 11 | 0.7 | 0.875 | 3.5 | 566 |
| 15 | 66H50 | Livingston | I-55 | 0.29 | 2 | 2019 | 20 | Tied PCC | HMA | 4 | 10 | 0.7 | 0.875 | 3.5 | 566 |
| 16 | 66686 | Bureau | I-80 | 0.73 | 9 | 2012 | 20 | Tied PCC | HMA | 4 | 10 | 0.7 | 0.875 | 3.5 | 566 |
| 17 | 66044 | Grundy | I-80 | 10.89 | 19 | 2002 | 20 | Tied PCC | HMA | 4 | 14 | 0.7 | 0.875 | 3.5 | 566 |
| 18 | 68200 | Peoria | I-74 | 5.25 | 17 | 2004 | 30 | Tied PCC | HMA | 6 | 11.5 | 0.8 | 0.875 | 4.5 | 566 |
| 19 | 68201 | Tazewell | I-74 | 2.23 | 16 | 2005 | 30 | Tied PCC | HMA | 6 | 11.5 | 0.8 | 0.875 | 4.5 | 566 |
| 20 | 68620 | Tazewell | I-74 | 2.74 | 9 | 2012 | 20 | Tied PCC | HMA | 4 | 11 | 0.7 | 0.875 | 3.5 | 566 |
| 21 | 70757 | McLean | I-55 | 9.53 | 18 | 2003 | 20 | Tied PCC | HMA | 4 | 12.5 | 0.7 | 0.875 | 3.5 | 566 |
| 22 | 70044 | Clark | I-70 | 9.98 | 19 | 2002 | 30 | Tied PCC | HMA | 6 | 13 | 0.8 | 0.875 | 4.5 | 566 |
| 23 | 74295 | Effingham | I-57A | 0.53 | 8 | 2013 | 20 | Tied PCC | HMA | 4 | 13 | 0.7 | 0.875 | 3.5 | 566 |
| 24 | 74296 | Effingham | I-70 | 8.35 | 8 | 2013 | 20 | Tied PCC | HMA | 4 | 13 | 0.7 | 0.875 | 3.5 | 566 |
| 25 | 76C52 | St. Clair | I-64 | 0.11 | 9 | 2012 | 30 | Tied PCC | HMA | 4 | 14 | 0.8 | 0.875 | 4.5 | 566 |
| 26 | 76C43 | St. Clair | I-70A | 1.21 | 9 | 2012 | 20 | Tied PCC | HMA | 4 | 11.25 | 0.7 | 0.875 | 3.5 | 566 |
| 27 | 76A91 | Madison | I-270 | 0.35 | 10 | 2011 | 30 | Tied PCC | HMA | 4 | 12 | 0.8 | 0.875 | 4.5 | 566 |
| 28 | 78172 | Jefferson | I-57 | 2.71 | 7 | 2014 | 20 | Tied PCC | HMA | 4 | 12 | 0.7 | 0.875 | 3.5 | 566 |

Table 46. CRCP Section Performance Data in Illinois

| | Contract_ID | County | Location | Miles | Servicing Period (2021 time of survey) | Traffic Opening Year | ADT | Total of Million ESALs at time of survey | IRI (in/mi) | IDOT CRS | Avg Crack Spacing (ft) | Observed PO (2-way) | Total Punchouts/mile | Longitudinal cracking |
|----|-------------|-------------|-----------|-------|--|----------------------|----------------|--|-------------|----------|------------------------|---------------------|----------------------|-----------------------|
| 1 | 82989 | Cook | I-55 | 4.16 | 21 | 2000 | 157,700 (2022) | 44.1 | 123 | 7.1 | 5.3 | 0 | 0 | Yes |
| 2 | 62304 | Cook | I-57 | 1.25 | 13 | 2008 | 153,700 (2022) | 17.0 | 92 | 8.1 | 12.0 | 0 | 0 | Yes |
| 3 | 62105 | Cook | I-80 | 3.19 | 15 | 2006 | 193,600 (2022) | 178.9 | 84 | 7.8 | 4.3 | 1 | 0.16 | Yes |
| 4 | 80954 | Cook | I-94 | 7.17 | 28 | 1993 | 246,100 (2022) | 53.6 | 136 | 7 | 10.6 | 1 | 0.03 | Yes |
| 5 | 62300 | Cook | I-94 | 8.07 | 14 | 2007 | 315,700 (2022) | 134.3 | 92 | 8.1 | 5.5 | 0 | 0 | No |
| 6 | 60401 | Cook | I-290 | 3.12 | 18 | 2003 | 158,100 (2022) | 51.2 | 148 | 7 | 4.4 | 0 | 0 | No |
| 7 | 60N87 | Will | I-80 | 1.36 | 3 | 2018 | - | - | 137-157 | 5.9 | N/A | - | - | - |
| 8 | 64E97 | Lee | I-39 | 0.36 | 9 | 2012 | 19,400 (2021) | 18.2 | 41 | 7.6 | 6.4 | 0 | 0 | Yes |
| 9 | 64B78 | Henry | I-80 | 0.46 | 5 | 2016 | 20,400 (2021) | 10.5 | 83 | 8.4 | 5.1 | 0 | 0 | No |
| 10 | 64933 | Rock Island | I-80 | 1.35 | 12 | 2009 | 23,000 (2021) | 24.9 | 67 | 8.4 | N/A | 0 | 0 | No |
| 11 | 64B78 | Rock Island | I-80 | 0.51 | 6 | 2015 | 23,000 (2021) | 13.2 | 78 | 7.8 | 19.6 | 0 | 0 | No |
| 12 | 64219 | Whiteside | I-88 | 8.59 | 20 | 2001 | 11,600 (2022) | 18.1 | 60 | 7.8 | 3.3 | 0 | 0 | Yes |
| 13 | 64C29 | Winnebago | I-90/I-39 | 2.71 | 9 | 2012 | 56,300 (2022) | 41.5 | 55 | 8.5 | 5.4 | 0 | 0 | No |
| 14 | 66F23 | Livingston | I-55 | 0.2 | 4 | 2017 | 16,500 (2019) | 6.9 | 46 | 8.6 | 33.0 | 0 | 0 | No |
| 15 | 66H50 | Livingston | I-55 | 0.29 | 2 | 2019 | 20,600 (2021) | 4.1 | 63 | 8.6 | 29.3 | 0 | 0 | No |
| 16 | 66686 | Bureau | I-80 | 0.73 | 9 | 2012 | 21,000 (2021) | 10.4 | 61 | 7.3 | 5.5 | 0 | 0 | No |
| 17 | 66044 | Grundy | I-80 | 10.89 | 19 | 2002 | 50,300 (2021) | 53.3 | 61 | 7.7 | 8.3 | 0 | 0 | Yes |
| 18 | 68200 | Peoria | I-74 | 5.25 | 17 | 2004 | 50,000 (2021) | 10.2 | 64-66 | 8.3 | 5.4 | 0 | 0 | No |
| 19 | 68201 | Tazewell | I-74 | 2.23 | 16 | 2005 | 52,800 (2021) | 11.1 | 97 | 8.3 | 4.4 | 0 | 0 | Yes |
| 20 | 68620 | Tazewell | I-74 | 2.74 | 9 | 2012 | 49,400 (2021) | 15.3 | 69 | 8.5 | 17.6 | 0 | 0 | No |
| 21 | 70757 | McLean | I-55 | 9.53 | 18 | 2003 | 42,500 (2021) | 63.2 | 59-82 | 8.5-9.0 | 3.4 | 0 | 0 | Yes |
| 22 | 70044 | Clark | I-70 | 9.98 | 19 | 2002 | 29,300 (2021) | 66.9 | 68 | 7.9 | 3.1 | 6 | 0.3 | No |
| 23 | 74295 | Effingham | I-57A | 0.53 | 8 | 2013 | 20,700 (2021) | 22.1 | 50 | 7.9 | N/A | - | - | No |
| 24 | 74296 | Effingham | I-70 | 8.35 | 8 | 2013 | 45,100 (2022) | 44.8 | 61 | 8.6 | 4.1 | 0 | 0 | No |
| 25 | 76C52 | St. Clair | I-64 | 0.11 | 9 | 2012 | 82,900 (2021) | 21.2 | 118-119 | 8.3 | | 0 | 0 | No |
| 26 | 76C43 | St. Clair | I-70A | 1.21 | 9 | 2012 | 44,300 (2019) | 12.0 | 145 | 8.0 | 6.4 | 0 | 0 | No |
| 27 | 76A91 | Madison | I-270 | 0.35 | 10 | 2011 | 49,200 (2021) | 22.0 | 82 | 8.4 | N/A | - | - | No |
| 28 | 78172 | Jefferson | I-57 | 2.71 | 7 | 2014 | 45,800 (2022) | 37.3 | 75 | 8.2 | 11.7 | 0 | 0 | No |

| Illinois PAVEMENT DESIGN December 2021 | | |
|--|---|-----------------|
| Facility Class | Traffic Factor Equation | Equation Number |
| Class I | $TF_{-DP} \left[\frac{(0.15 \cdot P \cdot PV) + (143.81 \cdot S \cdot SU) + (696.42 \cdot M \cdot MU)}{1 \times 10^6} \right]$ | Equation 54-4.1 |
| Class II | $TF_{-DP} \left[\frac{(0.15 \cdot P \cdot PV) + (135.78 \cdot S \cdot SU) + (567.21 \cdot M \cdot MU)}{1 \times 10^6} \right]$ | Equation 54-4.2 |
| Class III and Class IV | $TF_{-DP} \left[\frac{(0.15 \cdot P \cdot PV) + (129.58 \cdot S \cdot SU) + (562.47 \cdot M \cdot MU)}{1 \times 10^6} \right]$ | Equation 54-4.3 |

where:
PV, SU, MU = structural design traffic expressed as the number of PV, SU, and MU vehicles.
P, S, M = percent of PV, SU, and MU in the design lane expressed as a decimal.
DP = design period — typically 20 years.

TRAFFIC FACTOR EQUATIONS
(Rigid Pavements)
Figure 54-4.C

Figure 56. Equation. Traffic factor equations.

Source: Chapter 54 of the BDE Manual, section 54-4, IDOT (2023)

Table 47. Percent of Traffic in Design Lane

| Illinois PAVEMENT DESIGN December 2021 | | | | | | |
|--|--|-----|-----|-------|-----|-----|
| Number of Facility Lanes | Percent of Total Vehicular Class Volume (ADT) in Design Lane | | | | | |
| | Rural | | | Urban | | |
| | PV | SU | MU | PV | SU | MU |
| 2 or 3* | 50% | 50% | 50% | 50% | 50% | 50% |
| 4 | 32% | 45% | 45% | 32% | 45% | 45% |
| ≥ 6 | 20% | 40% | 40% | 8% | 37% | 37% |

*One-way roads and streets.

DESIGN LANE DISTRIBUTION FACTORS FOR STRUCTURAL DESIGN TRAFFIC
Figure 54-2.B

Source: Chapter 54 of the BDE Manual, section 54-2, IDOT (2023)

APPENDIX B: CRCP DESIGN FRAMEWORK SENSITIVITY ANALYSIS

CRCP SENSITIVITY ANALYSIS

20 Year, 0.7% Steel

The following table uses the same following parameters and the same inputs used to generate the design charts: design Life = 20 years, $P_s = 0.7\%$, and $R = 95\%$.

Table 48. Inputs for Sensitivity Analysis

| Input | Value | | | Unit |
|---|-----------|------------------|--------------|----------------------|
| Slab thickness | varies | | | inches |
| Design Life (20 or 30) | 20 | | | years |
| Steel content | 0.007 | | | fraction |
| Reinforcing steel bar diameter | 0.75 | | | inches |
| Aggregate type | limestone | | | |
| Shoulder type | Asphalt | Tied Separate | Tied Mono | |
| Stiffness of the shoulder/lane joint | 0.04 | 0.77 | 4 | |
| Shoulder load transfer efficiency | 5 | 40 | 73 | % |
| Total 18 k ESALs - Design Lane | Varies | | | ESALs |
| Annual growth factor | 0 | | | |
| PCC Elastic modulus, 28 days | 4400000 | | | psi |
| PCC Poisson's ratio | 0.15 | | | |
| PCC Coefficient of thermal expansion | 0.0000055 | | | 1/°F |
| PCC Compressive strength, 28 days | 4500 | | | psi |
| PCC Modulus of rupture, 90 days | 750 | | | psi |
| PCC Modulus of rupture, 28 days | 675 | | | psi |
| PCC Top of Slab Strength Reduction Factor | 0.8 | | | |
| PCC Tensile strength, 28 days | 472.5 | | | psi |
| PCC Ultimate drying shrinkage | 0.00078 | | | in/in |
| PCC Thermal diffusivity | 1.22 | | | ft ² /day |
| Cement content | 600 | | | lb/yd ³ |
| Base Elastic modulus | 1300000 | | | psi |
| Base Thickness | 4 | | | inches |
| Base/subbase type | ATB | | | |
| Subbase friction coefficient | 7.5 | | | |
| Base load transfer efficiency | 30 | | | % |
| Construction season | summer | | | |
| PCC temperature at set time at depth of steel | 106 | | | °F |

| Input | Value | Unit |
|---|--------------|---------|
| Relative humidity in the concrete at depth of steel | 85 | % |
| Total stress correction factor | 0.8 | |
| Modulus of subgrade reaction for loading | 50, 100, 200 | psi/in. |
| Modulus of subgrade reaction for curling | 100 | psi/in. |
| Fatigue equation | Zero | |
| Reliability | Maintenance | |
| Failure criterion (number of punchouts per mile) | 50 or 95 | |
| | 10 | |

30 Year, 0.8% Steel

The following table uses the same following parameters: design Life= 30 years, $P_s=0.8\%$, and $R=95\%$.

Table 49. Inputs for Sensitivity Analysis

| Input | Value | | | Unit |
|---|-----------|----------|------|----------------------|
| Slab thickness | varies | | | inches |
| Design Life (20 or 30) | 30 | | | years |
| Steel content | 0.008 | | | fraction |
| Reinforcing steel bar diameter | 0.875 | | | inches |
| Aggregate type | limestone | | | |
| Shoulder type | Asphalt | Tied | Tied | |
| Stiffness of the shoulder/lane joint | 0.04 | Separate | Mono | |
| Shoulder load transfer efficiency | 5 | 0.77 | 4 | % |
| Total 18 k ESALs - Design Lane | Varies | 40 | 73 | ESALs |
| Annual growth factor | 0 | | | |
| PCC Elastic modulus, 28 days | 4400000 | | | psi |
| PCC Poisson's ratio | 0.15 | | | |
| PCC Coefficient of thermal expansion | 0.0000055 | | | 1/°F |
| PCC Compressive strength, 28 days | 4500 | | | psi |
| PCC Modulus of rupture, 90 days | 750 | | | psi |
| PCC Modulus of rupture, 28 days | 675 | | | psi |
| PCC Top of Slab Strength Reduction Factor | 0.8 | | | |
| PCC Tensile strength, 28 days | 472.5 | | | psi |
| PCC Ultimate drying shrinkage | 0.00078 | | | in/in |
| PCC Thermal diffusivity | 1.22 | | | ft ² /day |
| Cement content | 600 | | | lb/yd ³ |
| Base Elastic modulus | 1300000 | | | psi |
| Base Thickness | 4 | | | inches |
| Base/subbase type | ATB | | | |

| Input | Value | Unit |
|---|---------------------|-------------|
| Subbase friction coefficient | 7.5 | |
| Base load transfer efficiency | 30 | % |
| Construction season | summer | |
| PCC temperature at set time at depth of steel | 106 | °F |
| Relative humidity in the concrete at depth of steel | 85 | % |
| Total stress correction factor | 0.8 | |
| Modulus of subgrade reaction for loading | 50, 100, 200 | psi/in. |
| Modulus of subgrade reaction for curling | 100 | psi/in. |
| Fatigue equation | Zero Maintenance | |
| Reliability | 50 or 95 | |
| Failure criterion (number of punchouts per mile) | 10 | |

APPENDIX C: CONCRETE FATIGUE EQUATIONS

JPCP SENSITIVITY ANALYSIS

The following tables use the following parameters for JPCP: 15 ft slab length, 12 ft slab width, 20-year design life, and 95% reliability. All other values are taken from Chapter 54 of IDOT's *BDE Manual* (2023).

Table 50. JPCP Sensitivity 20 Year Analysis Inputs and Thicknesses-Tied Shoulders, K value = 50 psi/in.

| Poor SSR | | |
|----------|----------|-----------|
| Traffic | Shoulder | Thickness |
| 10 | Tied | 9.87 |
| 35 | Tied | 10.73 |
| 70 | Tied | 11.38 |
| 100 | Tied | 11.41 |

Table 51. JPCP Sensitivity 20 Year Analysis Inputs and Thicknesses-Untied Shoulders, K value = 50 psi/in.

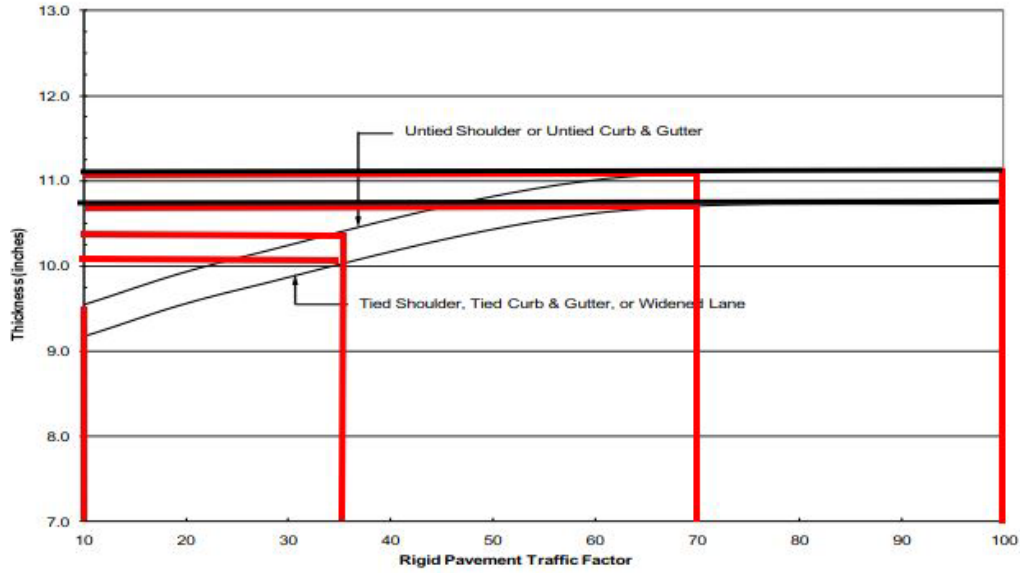
| Poor SSR | | |
|----------|----------|-----------|
| Traffic | Shoulder | Thickness |
| 10 | Untied | 10.13 |
| 35 | Untied | 10.98 |
| 70 | Untied | 11.68 |
| 100 | Untied | 11.70 |

Table 52. JPCP Sensitivity 20 Year Analysis Inputs and Thicknesses-Tied Shoulders, K value = 200 psi/in.

| Granular SSR | | |
|--------------|----------|-----------|
| Traffic | Shoulder | Thickness |
| 10 | Tied | 9.17 |
| 35 | Tied | 10.04 |
| 70 | Tied | 10.71 |
| 100 | Tied | 10.74 |

Table 53. JPCP Sensitivity 20 Year Analysis Inputs and Thicknesses-Untied Shoulders, K value = 200 psi/in.

| Granular SSR | | |
|--------------|----------|-----------|
| Traffic | Shoulder | Thickness |
| 10 | Untied | 9.55 |
| 35 | Untied | 10.42 |
| 70 | Untied | 11.11 |
| 100 | Untied | 11.14 |

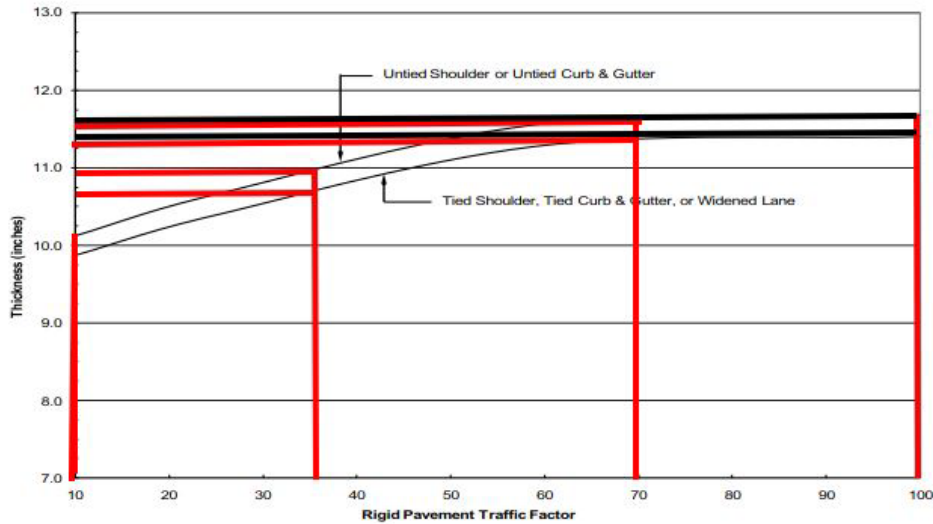


Note: Use of untied shoulder design requires Bureau of Research approval.

**RIGID PAVEMENT DESIGN CHART
(Mechanistic Design: SSR = Granular)**

Figure 57. Graph. Chart for JPCP slab thickness given granular subgrade (K-value= 200 psi/in.).

Source: Chapter 54 of the BDE Manual, IDOT (2023)



Note: Use of untied shoulder design requires Bureau of Research approval.

**RIGID PAVEMENT DESIGN CHART
(Mechanistic Design: SSR = Poor)**

Figure 58. Graph. Chart for JPCP slab thickness given poor subgrade (K-value = 50 psi/in.).

Source: Chapter 54 of the BDE Manual, IDOT (2023)

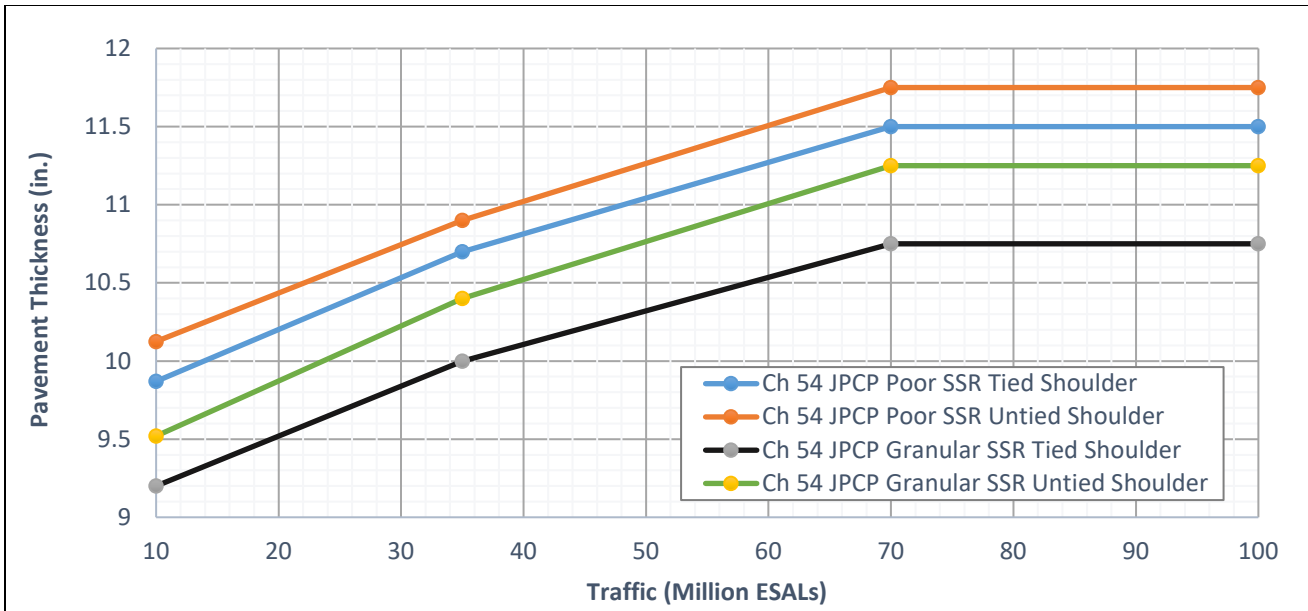


Figure 59. Graph. Sensitivity analysis of JPCP slab thickness.

Source: Chapter 54 of the BDE Manual, IDOT (2023)

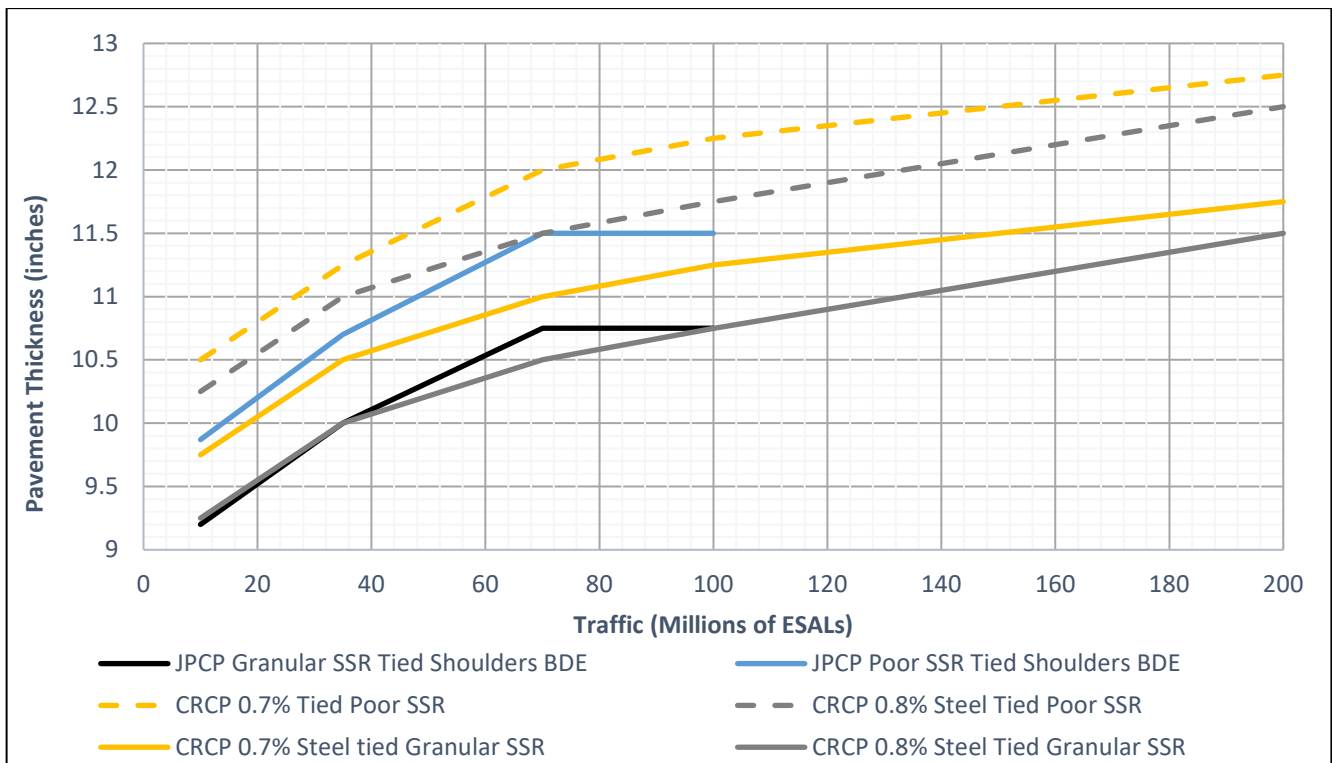


Figure 60. Graph. CRCP vs JPCP slab thickness with tied concrete shoulder.

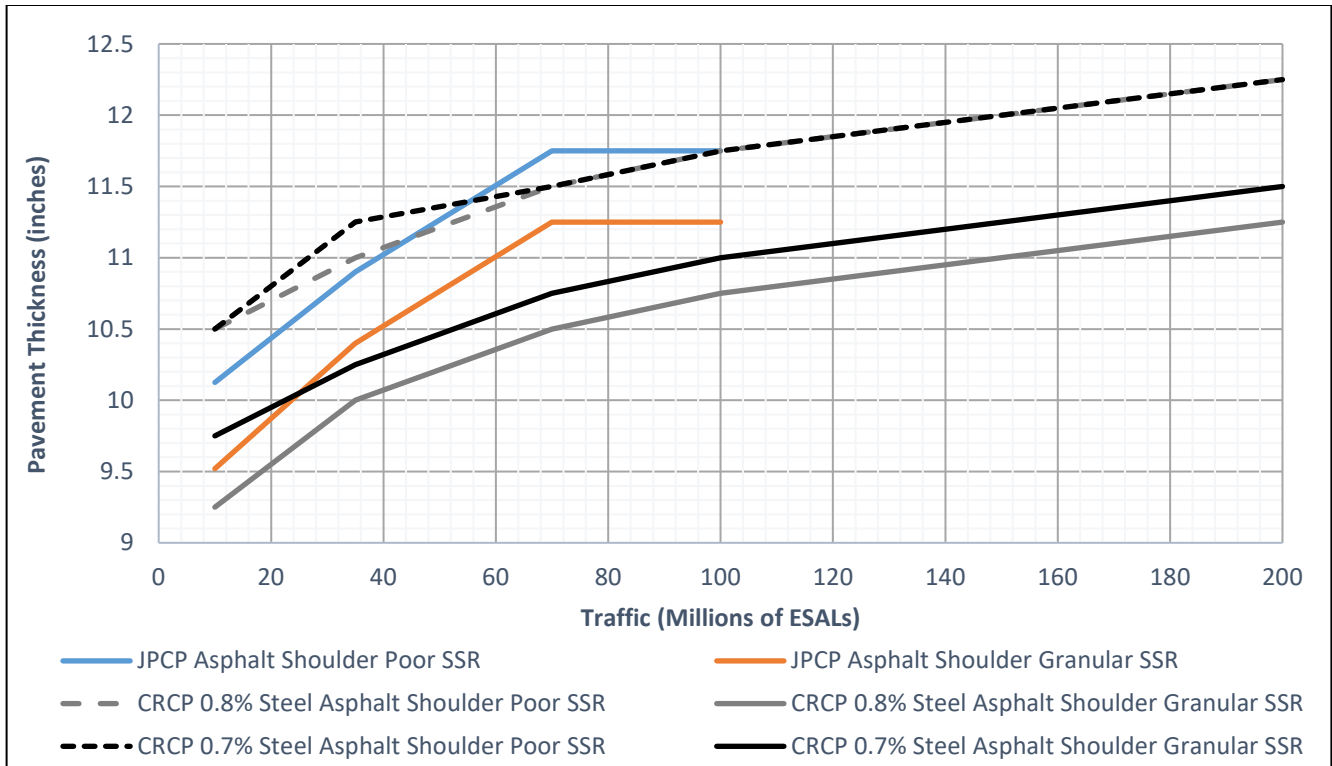


Figure 61. Graph. CRCP vs JPCP slab thickness with asphalt shoulder.

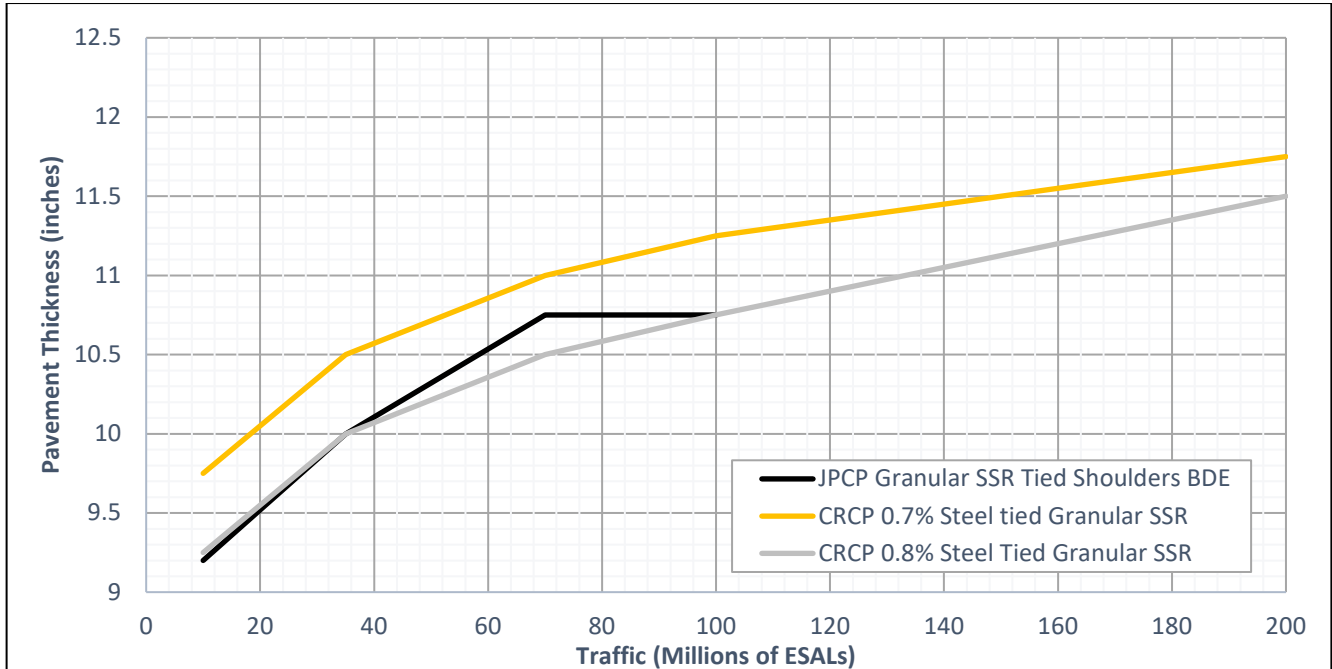


Figure 62. Graph. CRCP vs JPCP slab thickness on granular support with tied shoulder (k-value = 200 psi/in.).

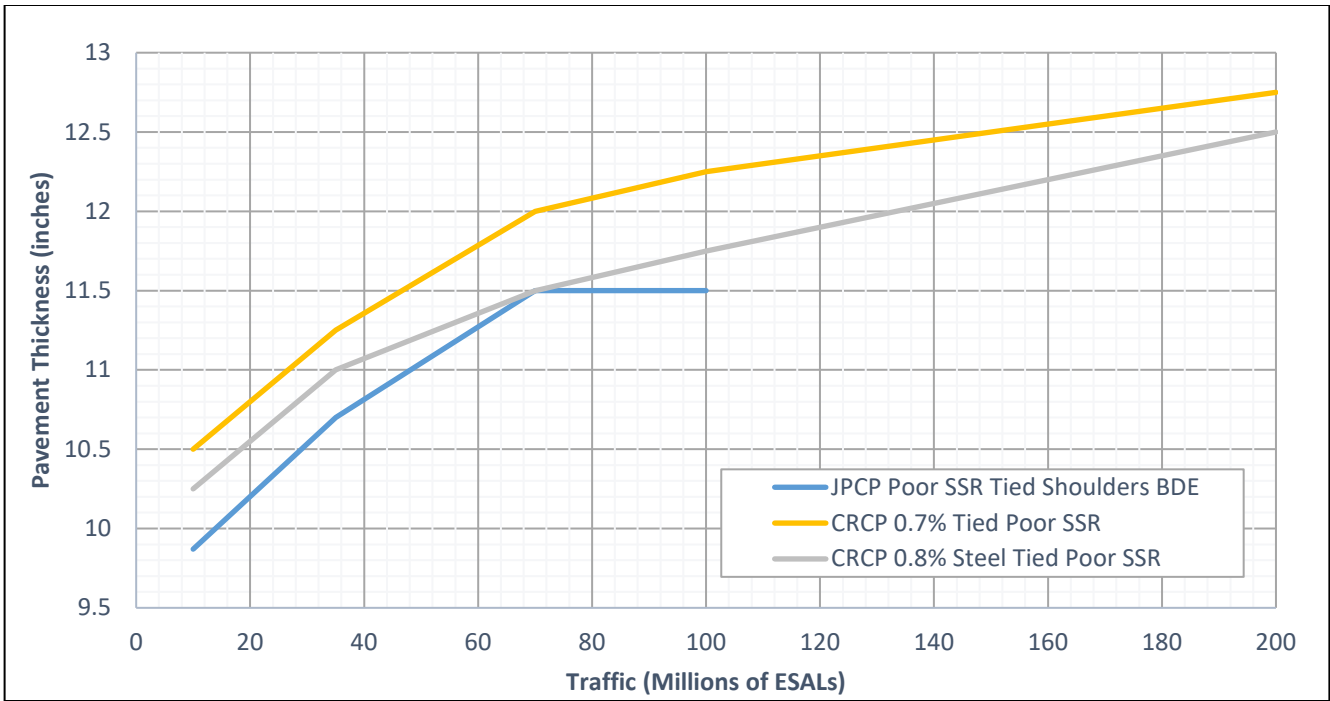


Figure 63. Graph. CRCP vs JPCP slab thickness on poor support with tied shoulder (k-value = 50 psi/in.).

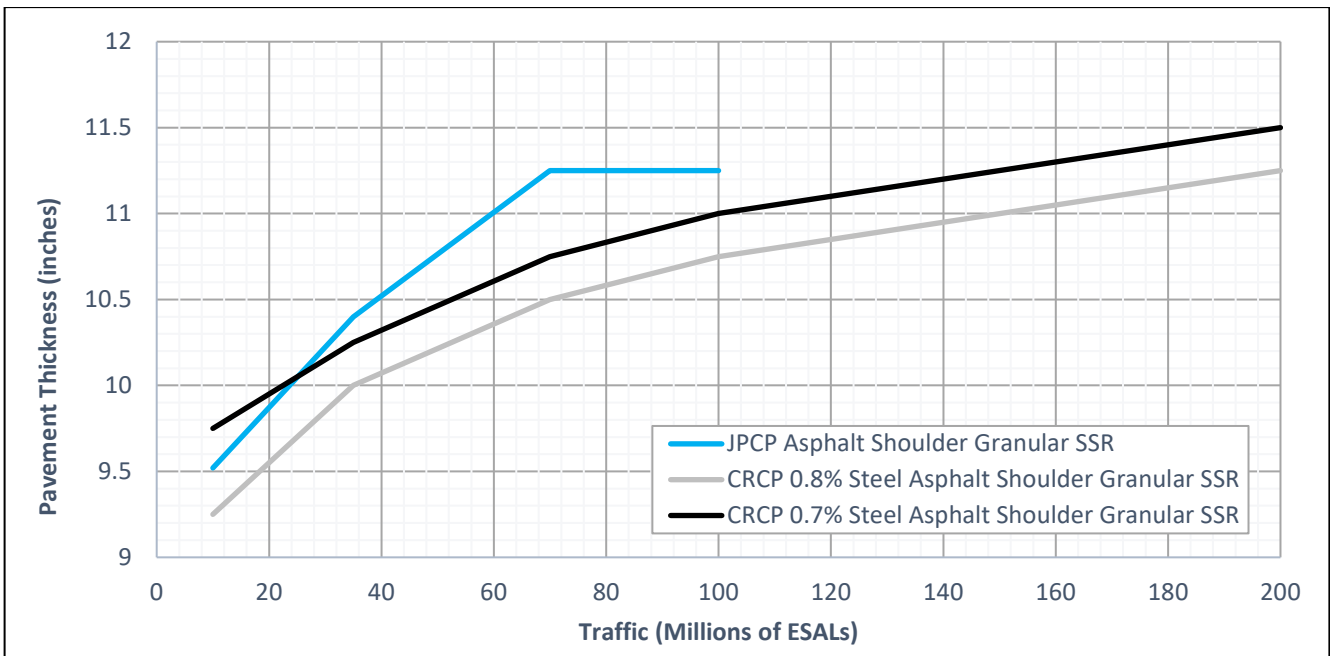


Figure 64. Graph. CRCP vs JPCP slab thickness on granular support with asphalt shoulder (k-value = 200 psi/in.).

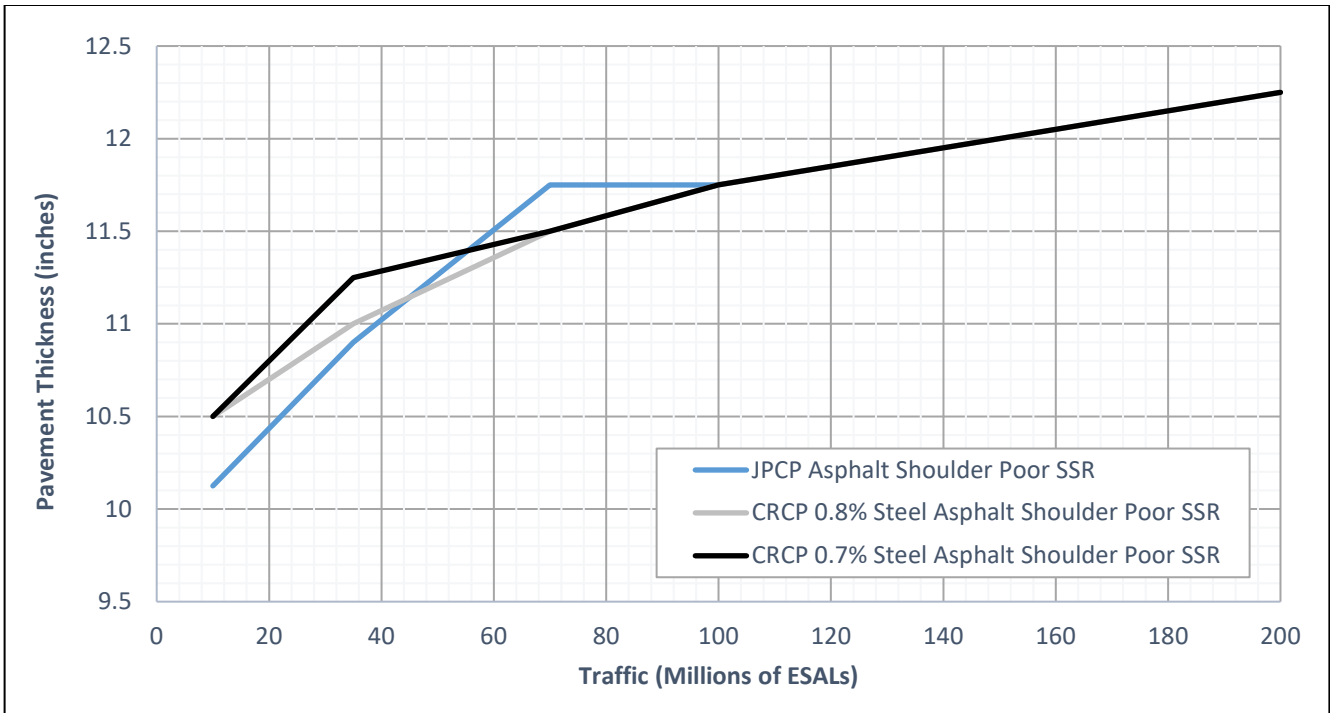


Figure 65. Graph. CRCP vs JPCP slab thickness on poor support with asphalt shoulder (k-value = 50 psi/in.).

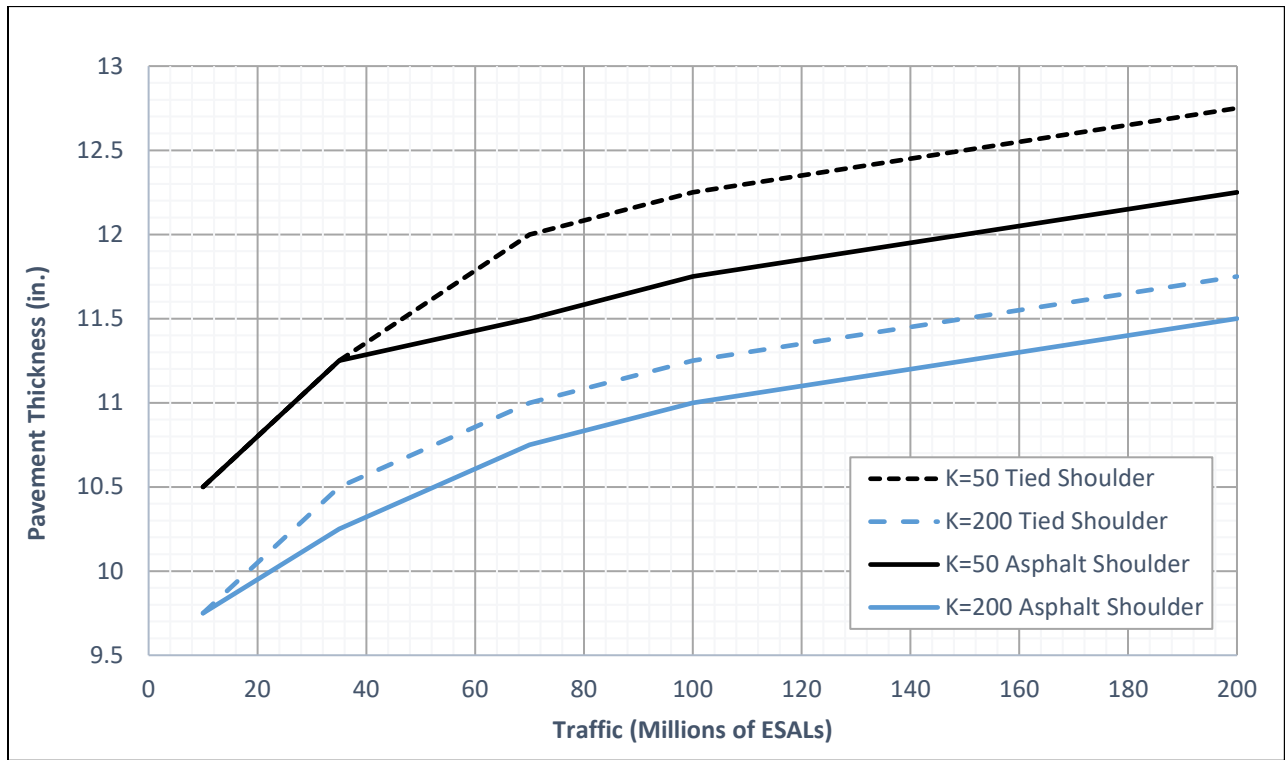


Figure 66. Graph. CRCP sensitivity at 0.8% steel content.

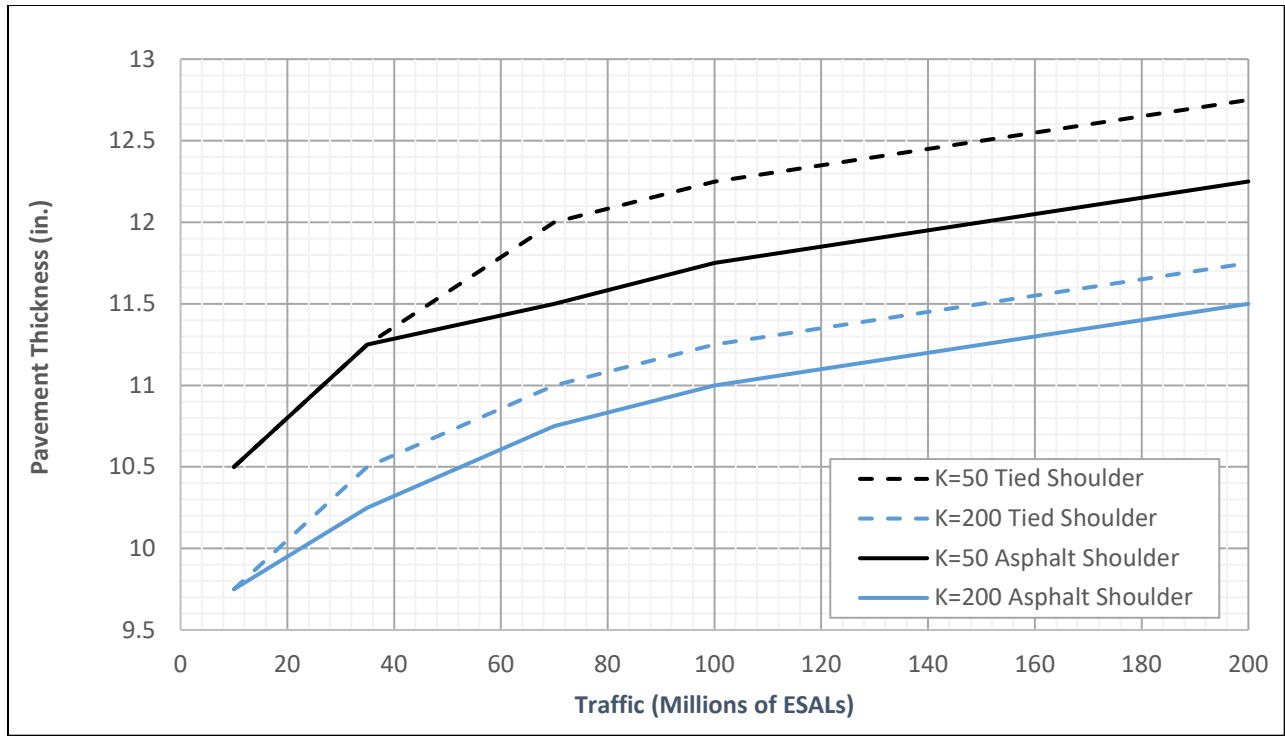


Figure 67. Graph. CRCP sensitivity at 0.7% steel content.

APPENDIX D: UPDATED CRCP DESIGN CHARTS FOR ILLINOIS

Table 54. Thickness Difference between 2009 and Proposed Framework, 20 Years, Asphalt Shoulder

| Design Life = 20 years Shoulder Type = AC | | | | | |
|--|-------------|---------------|---------------------|-------------------------|-------------------------------------|
| k-value, psi | Reliability | Million ESALs | 2009 Thickness, in. | Proposed Thickness, in. | Thickness Difference (old-new), in. |
| 50 | 50 | 10 | 10.00 | 9.75 | 0.25 |
| 50 | 50 | 35 | 11.00 | 10.50 | 0.50 |
| 50 | 50 | 70 | 11.00 | 10.75 | 0.25 |
| 50 | 50 | 200 | 11.50 | 11.25 | 0.25 |
| 50 | 95 | 10 | 11.00 | 10.50 | 0.50 |
| 50 | 95 | 35 | 11.50 | 11.25 | 0.25 |
| 50 | 95 | 70 | 12.00 | 11.50 | 0.50 |
| 50 | 95 | 200 | 12.50 | 12.25 | 0.25 |
| 100 | 50 | 10 | 10.00 | 9.50 | 0.50 |
| 100 | 50 | 35 | 10.50 | 10.00 | 0.50 |
| 100 | 50 | 70 | 10.50 | 10.50 | 0.00 |
| 100 | 50 | 200 | 11.00 | 11.00 | 0.00 |
| 100 | 95 | 10 | 10.50 | 10.25 | 0.25 |
| 100 | 95 | 35 | 11.00 | 10.75 | 0.25 |
| 100 | 95 | 70 | 11.50 | 11.25 | 0.25 |
| 100 | 95 | 200 | 12.00 | 12.00 | 0.00 |
| 200 | 50 | 10 | 9.50 | 9.00 | 0.50 |
| 200 | 50 | 35 | 10.00 | 9.50 | 0.50 |
| 200 | 50 | 70 | 10.00 | 10.00 | 0.00 |
| 200 | 50 | 200 | 11.00 | 10.50 | 0.50 |
| 200 | 95 | 10 | 10.00 | 9.75 | 0.25 |
| 200 | 95 | 35 | 10.50 | 10.25 | 0.25 |
| 200 | 95 | 70 | 11.00 | 10.75 | 0.25 |
| 200 | 95 | 200 | 11.50 | 11.50 | 0.00 |

avg
difference
(inches) 0.28

+: thinner
-: thicker

Table 55. Thickness Difference between 2009 and Proposed Framework, 20 Years, PCC Tied Separate Shoulder

| Design Life = 20 years Shoulder Type = PCC (separate) | | | | | |
|--|-------------|---------------|---------------------|-------------------------|-------------------------------------|
| k-value, psi | Reliability | Million ESALs | 2009 Thickness, in. | Proposed Thickness, in. | Thickness Difference (old-new), in. |
| 50 | 50 | 10 | 10.00 | 9.75 | 0.25 |
| 50 | 50 | 35 | 10.50 | 10.50 | 0.00 |
| 50 | 50 | 70 | 11.00 | 11.00 | 0.00 |
| 50 | 50 | 200 | 11.50 | 11.00 | 0.50 |
| 50 | 95 | 10 | 10.50 | 10.50 | 0.00 |
| 50 | 95 | 35 | 11.50 | 11.25 | 0.25 |
| 50 | 95 | 70 | 12.00 | 12.00 | 0.00 |
| 50 | 95 | 200 | 13.00 | 12.75 | 0.25 |
| 100 | 50 | 10 | 9.50 | 9.50 | 0.00 |
| 100 | 50 | 35 | 10.00 | 10.00 | 0.00 |
| 100 | 50 | 70 | 10.50 | 10.50 | 0.00 |
| 100 | 50 | 200 | 11.00 | 11.25 | -0.25 |
| 100 | 95 | 10 | 10.00 | 10.25 | -0.25 |
| 100 | 95 | 35 | 11.00 | 11.00 | 0.00 |
| 100 | 95 | 70 | 11.50 | 11.50 | 0.00 |
| 100 | 95 | 200 | 12.50 | 12.25 | 0.25 |
| 200 | 50 | 10 | 9.00 | 9.00 | 0.00 |
| 200 | 50 | 35 | 10.00 | 9.50 | 0.50 |
| 200 | 50 | 70 | 10.00 | 10.00 | 0.00 |
| 200 | 50 | 200 | 10.50 | 10.75 | -0.25 |
| 200 | 95 | 10 | 10.00 | 9.75 | 0.25 |
| 200 | 95 | 35 | 10.50 | 10.50 | 0.00 |
| 200 | 95 | 70 | 11.00 | 11.00 | 0.00 |
| 200 | 95 | 200 | 12.00 | 11.75 | 0.25 |

avg
difference
(inches)

0.07
+: thinner
-: thicker

Table 56. Thickness Difference between 2009 and Proposed Framework, 20 Years, Monolithic Shoulder

| Design Life = 20 years Shoulder Type = PCC (monolithic) | | | | | |
|--|-------------|---------------|---------------------|-------------------------|-------------------------------------|
| k-value, psi | Reliability | Million ESALs | 2009 Thickness, in. | Proposed Thickness, in. | Thickness Difference (old-new), in. |
| 50 | 50 | 10 | 10.00 | 9.75 | 0.25 |
| 50 | 50 | 35 | 10.50 | 10.25 | 0.25 |
| 50 | 50 | 70 | 10.50 | 10.50 | 0.00 |
| 50 | 50 | 200 | 11.50 | 11.25 | 0.25 |
| 50 | 95 | 10 | 10.50 | 10.25 | 0.25 |
| 50 | 95 | 35 | 11.00 | 11.00 | 0.00 |
| 50 | 95 | 70 | 11.50 | 11.50 | 0.00 |
| 50 | 95 | 200 | 12.50 | 12.50 | 0.00 |
| 100 | 50 | 10 | 9.50 | 9.25 | 0.25 |
| 100 | 50 | 35 | 10.00 | 9.75 | 0.25 |
| 100 | 50 | 70 | 10.50 | 10.25 | 0.25 |
| 100 | 50 | 200 | 11.00 | 10.75 | 0.25 |
| 100 | 95 | 10 | 10.00 | 9.75 | 0.25 |
| 100 | 95 | 35 | 10.50 | 10.50 | 0.00 |
| 100 | 95 | 70 | 11.00 | 11.00 | 0.00 |
| 100 | 95 | 200 | 12.00 | 12.00 | 0.00 |
| 200 | 50 | 10 | 9.00 | 8.75 | 0.25 |
| 200 | 50 | 35 | 9.50 | 9.25 | 0.25 |
| 200 | 50 | 70 | 9.50 | 9.50 | 0.00 |
| 200 | 50 | 200 | 10.50 | 10.25 | 0.25 |
| 200 | 95 | 10 | 9.50 | 9.25 | 0.25 |
| 200 | 95 | 35 | 10.00 | 10.00 | 0.00 |
| 200 | 95 | 70 | 10.50 | 10.50 | 0.00 |
| 200 | 95 | 200 | 11.50 | 11.25 | 0.25 |

avg
difference
(inches)

0.15
+: thinner
-: thicker

Table 57. Thickness Difference between 2009 and Proposed Framework, 30 Years, Asphalt Shoulder

| Design Life = 30 years Shoulder Type = AC | | | | | |
|--|-------------|---------------|---------------------|-------------------------|-------------------------------------|
| k-value, psi | Reliability | Million ESALs | 2009 Thickness, in. | Proposed Thickness, in. | Thickness Difference (old-new), in. |
| 50 | 50 | 10 | 10.00 | 9.75 | 0.25 |
| 50 | 50 | 35 | 10.50 | 10.25 | 0.25 |
| 50 | 50 | 70 | 11.00 | 10.75 | 0.25 |
| 50 | 50 | 200 | 11.50 | 11.25 | 0.25 |
| 50 | 95 | 10 | 10.50 | 10.50 | 0.00 |
| 50 | 95 | 35 | 11.50 | 11.00 | 0.50 |
| 50 | 95 | 70 | 11.50 | 11.50 | 0.00 |
| 50 | 95 | 200 | 12.50 | 12.25 | 0.25 |
| 100 | 50 | 10 | 9.50 | 9.25 | 0.25 |
| 100 | 50 | 35 | 10.00 | 10.00 | 0.00 |
| 100 | 50 | 70 | 10.50 | 10.25 | 0.25 |
| 100 | 50 | 200 | 11.00 | 11.00 | 0.00 |
| 100 | 95 | 10 | 10.00 | 10.00 | 0.00 |
| 100 | 95 | 35 | 11.00 | 10.75 | 0.25 |
| 100 | 95 | 70 | 11.50 | 11.00 | 0.50 |
| 100 | 95 | 200 | 12.00 | 11.75 | 0.25 |
| 200 | 50 | 10 | 8.50 | 8.75 | -0.25 |
| 200 | 50 | 35 | 9.50 | 9.00 | 0.50 |
| 200 | 50 | 70 | 10.00 | 9.75 | 0.25 |
| 200 | 50 | 200 | 10.50 | 10.25 | 0.25 |
| 200 | 95 | 10 | 9.50 | 9.25 | 0.25 |
| 200 | 95 | 35 | 10.50 | 10.00 | 0.50 |
| 200 | 95 | 70 | 10.50 | 10.50 | 0.00 |
| 200 | 95 | 200 | 11.50 | 11.25 | 0.25 |

avg
difference
(inches) 0.21

+: thinner
-: thicker

Table 58. Thickness Difference between 2009 and Proposed Framework, 30 Years, Tied PCC Separate Shoulder

| Design Life = 30 years | | | | | |
|--------------------------------|-------------|---------------|---------------------|-------------------------|-------------------------------------|
| Shoulder Type = PCC (separate) | | | | | |
| k-value, psi | Reliability | Million ESALs | 2009 Thickness, in. | Proposed Thickness, in. | Thickness Difference (old-new), in. |
| 50 | 50 | 10 | 9.50 | 9.50 | 0.00 |
| 50 | 50 | 35 | 10.50 | 10.25 | 0.25 |
| 50 | 50 | 70 | 10.50 | 10.50 | 0.00 |
| 50 | 50 | 200 | 11.50 | 11.25 | 0.25 |
| 50 | 95 | 10 | 10.50 | 10.25 | 0.25 |
| 50 | 95 | 35 | 11.00 | 11.00 | 0.00 |
| 50 | 95 | 70 | 11.50 | 11.50 | 0.00 |
| 50 | 95 | 200 | 12.50 | 12.50 | 0.00 |
| 100 | 50 | 10 | 9.00 | 9.00 | 0.00 |
| 100 | 50 | 35 | 10.00 | 9.75 | 0.25 |
| 100 | 50 | 70 | 10.50 | 10.00 | 0.50 |
| 100 | 50 | 200 | 11.00 | 10.75 | 0.25 |
| 100 | 95 | 10 | 10.00 | 9.75 | 0.25 |
| 100 | 95 | 35 | 11.00 | 10.50 | 0.50 |
| 100 | 95 | 70 | 11.00 | 11.00 | 0.00 |
| 100 | 95 | 200 | 12.00 | 12.00 | 0.00 |
| 200 | 50 | 10 | 8.50 | 8.50 | 0.00 |
| 200 | 50 | 35 | 9.50 | 9.25 | 0.25 |
| 200 | 50 | 70 | 10.00 | 9.50 | 0.50 |
| 200 | 50 | 200 | 10.50 | 10.25 | 0.25 |
| 200 | 95 | 10 | 9.50 | 9.25 | 0.25 |
| 200 | 95 | 35 | 10.50 | 10.00 | 0.50 |
| 200 | 95 | 70 | 10.50 | 10.50 | 0.00 |
| 200 | 95 | 200 | 11.50 | 11.50 | 0.00 |

avg
difference
(inches) 0.18

+: thinner
-: thicker

Table 59. Thickness Difference between 2009 and Proposed Framework, 30 Years, Monolithic Shoulder

| Design Life = 30 years | | | | | |
|----------------------------------|-------------|---------------|---------------------|-------------------------|-------------------------------------|
| Shoulder Type = PCC (monolithic) | | | | | |
| k-value, psi | Reliability | Million ESALs | 2009 Thickness, in. | Proposed Thickness, in. | Thickness Difference (old-new), in. |
| 50 | 50 | 10 | 9.50 | 9.50 | 0.00 |
| 50 | 50 | 35 | 10.00 | 10.00 | 0.00 |
| 50 | 50 | 70 | 10.50 | 10.50 | 0.00 |
| 50 | 50 | 200 | 11.00 | 11.00 | 0.00 |
| 50 | 95 | 10 | 10.00 | 10.00 | 0.00 |
| 50 | 95 | 35 | 11.00 | 10.75 | 0.25 |
| 50 | 95 | 70 | 11.50 | 11.25 | 0.25 |
| 50 | 95 | 200 | 12.00 | 12.00 | 0.00 |
| 100 | 50 | 10 | 9.00 | 8.75 | 0.25 |
| 100 | 50 | 35 | 9.50 | 9.50 | 0.00 |
| 100 | 50 | 70 | 10.00 | 9.75 | 0.25 |
| 100 | 50 | 200 | 10.50 | 10.50 | 0.00 |
| 100 | 95 | 10 | 9.50 | 9.50 | 0.00 |
| 100 | 95 | 35 | 10.50 | 10.25 | 0.25 |
| 100 | 95 | 70 | 11.00 | 10.75 | 0.25 |
| 100 | 95 | 200 | 11.50 | 11.50 | 0.00 |
| 200 | 50 | 10 | 8.50 | 8.50 | 0.00 |
| 200 | 50 | 35 | 9.00 | 8.75 | 0.25 |
| 200 | 50 | 70 | 9.50 | 9.25 | 0.25 |
| 200 | 50 | 200 | 10.00 | 10.00 | 0.00 |
| 200 | 95 | 10 | 9.00 | 9.00 | 0.00 |
| 200 | 95 | 35 | 10.00 | 9.75 | 0.25 |
| 200 | 95 | 70 | 10.00 | 10.00 | 0.00 |
| 200 | 95 | 200 | 11.00 | 11.00 | 0.00 |

avg difference
(inches)

0.09

+: thinner

-: thicker

APPENDIX E: CRCP PAVEMENT ME DESIGN COMPARISONS

AADTT TO ESAL CORRELATION 20-YEAR TRAFFIC

Table 60. AADTT and ESALs Correlation for 20-Year Traffic Using TTFC1 Distribution

| AADTT | ESALS |
|--------|-------------|
| 1,326 | 10,000,000 |
| 4,643 | 35,000,000 |
| 9,286 | 70,000,000 |
| 13,266 | 100,000,000 |
| 19,898 | 150,000,000 |
| 26,531 | 200,000,000 |
| 33,164 | 250,000,000 |
| 39,797 | 300,000,000 |

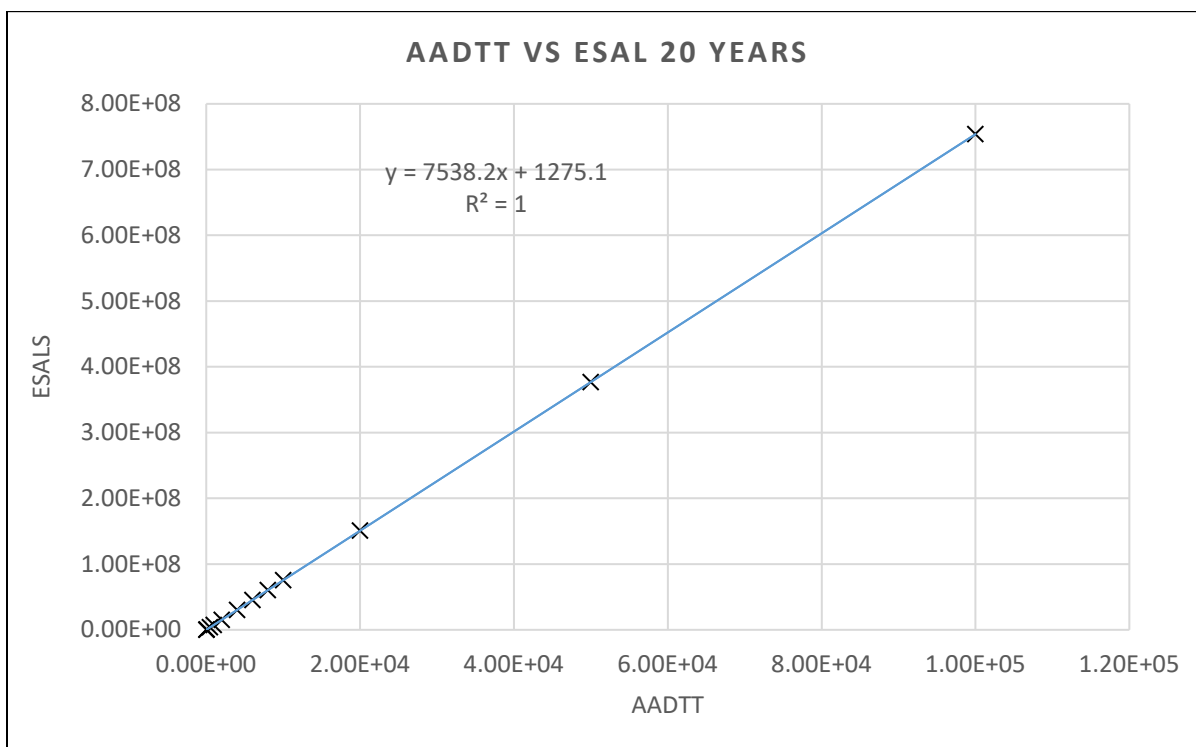


Figure 18. Graph. AADTT vs ESAL correlation, $y = 7,538.2x + 1,275.1$.

AADTT TO ESAL CORRELATION 30-YEAR TRAFFIC

Table 61. AADTT and ESALs Correlation for 30-Year Traffic Using TTFC1 Distribution

| AADTT | ESALS |
|--------|-------------|
| 792 | 10,000,000 |
| 2,772 | 35,000,000 |
| 5,544 | 70,000,000 |
| 7,920 | 100,000,000 |
| 11,879 | 150,000,000 |
| 15,839 | 200,000,000 |
| 19,799 | 250,000,000 |
| 23,759 | 300,000,000 |

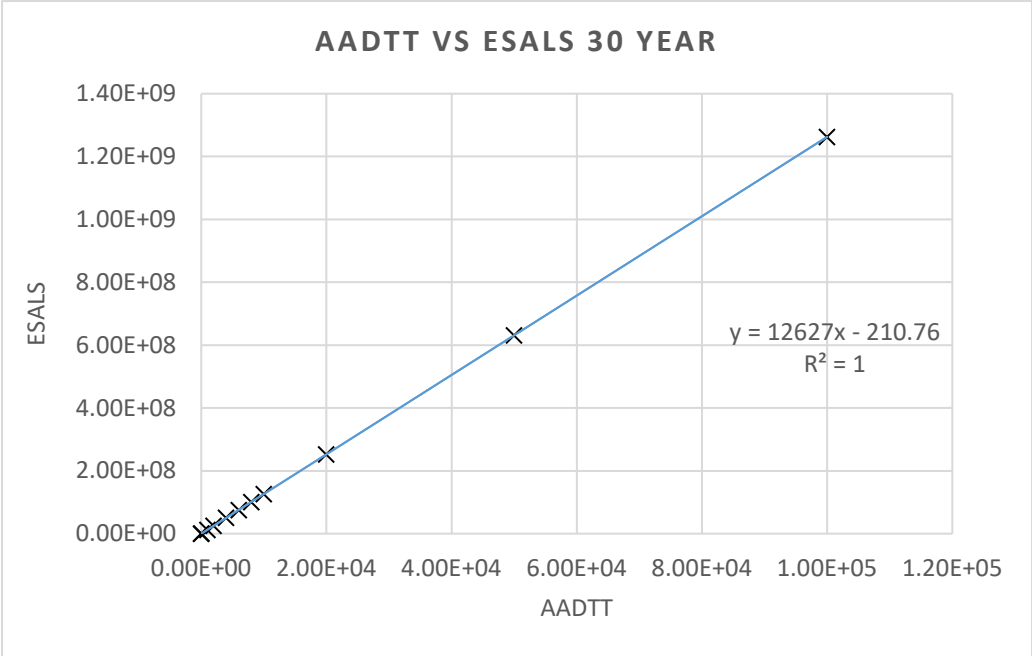


Figure 69. Graph. AADTT vs ESAL correlation 30-year, $y = 12,627x - 210.76$.

Table 62. Comparison of CRCP Slab Thickness between Proposed CRCP Design Framework and AASHTOWare Pavement ME Design, 20-year Asphalt Shoulder

| K-value | Million ESALs | R% | UIUC Thickness, in. | AASHTO Thickness, in. | UIUC-AASHTO, in. |
|---------|---------------|----|---------------------|-----------------------|------------------|
| 50 | 10 | 95 | 10.50 | 8.50 | 2.00 |
| 50 | 35 | 95 | 11.25 | 10.00 | 1.25 |
| 50 | 70 | 95 | 11.50 | 11.00 | 0.50 |
| 50 | 150 | 95 | 12.00 | 12.50 | -0.50 |
| 50 | 300 | 95 | 12.50 | 14.00 | -1.50 |
| 100 | 10 | 95 | 10.25 | 8.50 | 1.75 |
| 100 | 35 | 95 | 10.75 | 10.00 | 0.75 |
| 100 | 70 | 95 | 11.25 | 11.00 | 0.25 |
| 100 | 150 | 95 | 11.75 | 13.00 | -1.25 |
| 100 | 300 | 95 | 12.25 | 14.50 | -2.25 |
| 200 | 10 | 95 | 9.75 | 8.00 | 1.75 |
| 200 | 35 | 95 | 10.25 | 9.50 | 0.75 |
| 200 | 70 | 95 | 10.75 | 11.00 | -0.25 |
| 200 | 150 | 95 | 11.25 | 13.00 | -1.75 |
| 200 | 300 | 95 | 11.75 | 15.00 | -3.25 |

Table 63. Comparison of CRCP Slab Thickness between Proposed CRCP Design Framework and AASHTOWare Pavement ME Design, 30-year Asphalt Shoulder

| K-value | Million ESALs | R% | UIUC Thickness, in. | AASHTO Thickness, in. | UIUC-AASHTO, in. |
|---------|---------------|----|---------------------|-----------------------|------------------|
| 50 | 10 | 95 | 10.50 | 8.50 | 2.00 |
| 50 | 35 | 95 | 11.00 | 10.00 | 1.00 |
| 50 | 70 | 95 | 11.50 | 11.00 | 0.50 |
| 50 | 150 | 95 | 11.75 | 12.50 | -0.75 |
| 50 | 300 | 95 | 12.00 | 14.50 | -2.50 |
| 100 | 10 | 95 | 10.00 | 8.50 | 1.50 |
| 100 | 35 | 95 | 10.75 | 10.00 | 0.75 |
| 100 | 70 | 95 | 11.00 | 11.00 | 0.00 |
| 100 | 150 | 95 | 11.25 | 13.00 | -1.75 |
| 100 | 300 | 95 | 11.75 | 14.50 | -2.75 |
| 200 | 10 | 95 | 9.25 | 8.0 | 1.25 |
| 200 | 35 | 95 | 10.00 | 10.00 | 0.00 |
| 200 | 70 | 95 | 10.50 | 11.50 | -1.00 |
| 200 | 150 | 95 | 10.75 | 13.00 | -2.25 |
| 200 | 300 | 95 | 11.00 | 15.00 | -4.00 |

Table 64. Comparison of CRCP Slab Thickness between Proposed CRCP Design Framework and AASHTOWare Pavement ME Design, 20-year Tied Separate Shoulder

| K-value | Million ESALs | R% | UIUC Thickness, in. | AASHTO Thickness, in. | UIUC-AASHTO, in. |
|---------|---------------|----|---------------------|-----------------------|------------------|
| 50 | 10 | 95 | 10.50 | 8.00 | 2.50 |
| 50 | 35 | 95 | 11.25 | 9.00 | 2.25 |
| 50 | 70 | 95 | 12.00 | 10.50 | 1.50 |
| 50 | 150 | 95 | 12.50 | 12.00 | 0.50 |
| 50 | 300 | 95 | 13.25 | 13.50 | -0.25 |
| 100 | 10 | 95 | 10.25 | 7.50 | 2.75 |
| 100 | 35 | 95 | 11.00 | 9.00 | 2.00 |
| 100 | 70 | 95 | 11.50 | 10.50 | 1.00 |
| 100 | 150 | 95 | 12.00 | 12.00 | 0.00 |
| 100 | 300 | 95 | 12.75 | 14.00 | -1.25 |
| 200 | 10 | 95 | 9.75 | 7.50 | 2.25 |
| 200 | 35 | 95 | 10.50 | 9.00 | 1.50 |
| 200 | 70 | 95 | 11.00 | 10.50 | 0.50 |
| 200 | 150 | 95 | 11.50 | 12.00 | -0.50 |
| 200 | 300 | 95 | 12.25 | 14.00 | -1.75 |

Table 65. Comparison of CRCP Slab Thickness between Proposed CRCP Design Framework and AASHTOWare Pavement ME Design, 30-year Tied Separate Shoulder

| K-value | Million ESALs | R% | UIUC Thickness, in. | AASHTO Thickness, in. | UIUC-AASHTO, in. |
|---------|---------------|----|---------------------|-----------------------|------------------|
| 50 | 10 | 95 | 10.25 | 8.00 | 2.25 |
| 50 | 35 | 95 | 11.00 | 9.00 | 2.00 |
| 50 | 70 | 95 | 11.50 | 10.50 | 1.00 |
| 50 | 150 | 95 | 11.75 | 12.00 | -0.25 |
| 50 | 300 | 95 | 12.25 | 13.50 | -1.25 |
| 100 | 10 | 95 | 9.75 | 7.50 | 2.25 |
| 100 | 35 | 95 | 10.50 | 9.00 | 1.50 |
| 100 | 70 | 95 | 11.00 | 10.50 | 0.50 |
| 100 | 150 | 95 | 11.25 | 12.50 | -1.25 |
| 100 | 300 | 95 | 11.75 | 14.00 | -2.25 |
| 200 | 10 | 95 | 9.25 | 7.50 | 1.75 |
| 200 | 35 | 95 | 10.00 | 9.00 | 1.00 |
| 200 | 70 | 95 | 10.50 | 10.50 | 0.00 |
| 200 | 150 | 95 | 10.75 | 13.00 | -2.25 |
| 200 | 300 | 95 | 11.25 | 14.50 | -3.25 |

Table 66. Comparison of CRCP Slab Thickness between Proposed CRCP Design Framework and AASHTOWare Pavement ME Design, 20-year Monolithic Shoulder

| K-value | Million ESALs | R% | UIUC Thickness, in. | AASHTO Thickness, in. | UIUC-AASHTO, in. |
|---------|---------------|----|---------------------|-----------------------|------------------|
| 50 | 10 | 95 | 10.25 | 7.50 | 2.75 |
| 50 | 35 | 95 | 11.00 | 8.50 | 2.50 |
| 50 | 70 | 95 | 11.50 | 9.50 | 2.00 |
| 50 | 150 | 95 | 12.25 | 11.50 | 0.75 |
| 50 | 300 | 95 | 13.00 | 13.50 | -0.50 |
| 100 | 10 | 95 | 9.75 | 7.50 | 2.25 |
| 100 | 35 | 95 | 10.50 | 8.50 | 2.00 |
| 100 | 70 | 95 | 11.00 | 10.00 | 1.00 |
| 100 | 150 | 95 | 11.75 | 11.50 | 0.25 |
| 100 | 300 | 95 | 12.50 | 13.50 | -1.00 |
| 200 | 10 | 95 | 9.25 | 8.00 | 1.25 |
| 200 | 35 | 95 | 10.00 | 8.50 | 1.50 |
| 200 | 70 | 95 | 10.50 | 10.00 | 0.50 |
| 200 | 150 | 95 | 11.00 | 12.00 | -1.00 |
| 200 | 300 | 95 | 11.75 | 13.50 | -1.75 |

Table 67. Comparison of CRCP Slab Thickness between Proposed CRCP Design Framework and AASHTOWare Pavement ME Design, 30-year Monolithic Shoulder

| K-value | Million ESALs | R% | UIUC Thickness, in. | AASHTO Thickness, in. | UIUC-AASHTO, in. |
|---------|---------------|----|---------------------|-----------------------|------------------|
| 50 | 10 | 95 | 10.00 | 7.50 | 2.50 |
| 50 | 35 | 95 | 10.75 | 8.50 | 2.25 |
| 50 | 70 | 95 | 11.25 | 10.00 | 1.25 |
| 50 | 150 | 95 | 11.50 | 11.50 | 0.00 |
| 50 | 300 | 95 | 11.75 | 13.50 | -1.75 |
| 100 | 10 | 95 | 9.50 | 7.50 | 2.00 |
| 100 | 35 | 95 | 10.25 | 8.50 | 1.75 |
| 100 | 70 | 95 | 10.75 | 10.00 | 0.75 |
| 100 | 150 | 95 | 11.00 | 12.50 | -1.50 |
| 100 | 300 | 95 | 11.25 | 13.50 | -2.25 |
| 200 | 10 | 95 | 9.00 | 7.50 | 1.50 |
| 200 | 35 | 95 | 9.75 | 8.50 | 1.25 |
| 200 | 70 | 95 | 10.00 | 10.00 | 0.00 |
| 200 | 150 | 95 | 10.25 | 13.00 | -2.75 |
| 200 | 300 | 95 | 10.75 | 14.00 | -3.25 |



I ILLINOIS